

**APPROACH PATH CONTROL
FOR
POWERED-LIFT STOL AIRCRAFT**

By D. J. Clymer and C. C. Flora

D6-60222

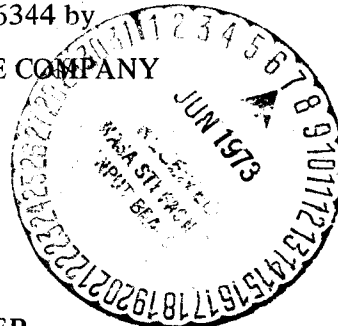
April 1973

(NASA-CR-114574) APPROACH PATH CONTROL N73-24062
FOR POWERED-LIFT STOL AIRCRAFT (Boeing
Commercial Airplane Co., Seattle) 100 p
HC \$7.00 CACL 01C Unclas
G3/02 04004

Prepared under Contract NAS2-6344 by
BOEING COMMERCIAL AIRPLANE COMPANY
Seattle, Washington

for

AMES RESEARCH CENTER
NATIONAL AERONAUTICS AND SPACE ADMINISTRATION



1. Report No. NASA CR-114574	2. Government Accession No.	3. Recipient's Catalog No.	
4. Title and Subtitle APPROACH PATH CONTROL FOR POWERED-LIFT STOL AIRCRAFT		5. Report Date April 1973	
		6. Performing Organization Code	
7. Author(s) D. J. Clymer and C. C. Flora		8. Performing Organization Report No. D6-60222	
		10. Work Unit No.	
9. Performing Organization Name and Address Boeing Commercial Airplane Company P.O. Box 3707 Seattle, Washington 98124		11. Contract or Grant No. NAS2-6344	
		13. Type of Report and Period Covered Contractor Report	
12. Sponsoring Agency Name and Address National Aeronautics and Space Administration Washington, D.C. 20546		14. Sponsoring Agency Code	
		15. Supplementary Notes	
16. Abstract <p>A flight control system concept is defined for approach flightpath control of an augmentor wing (or similar) powered-lift STOL configuration. The proposed STOL control concept produces aircraft transient and steady-state control responses that are familiar to pilots of conventional jet transports, and has potential for good handling qualities ratings in all approach and landing phases. The effects of trailing-edge flap rate limits, real-engine dynamics, and atmospheric turbulence are considered in the study. A general discussion of STOL handling qualities problems and piloting techniques is included.</p>			
17. Key Words (Suggested by Author(s)) STOL handling qualities Stability and control Pilot techniques Flight controls		18. Distribution Statement	
19. Security Classif. (of this report) Unclassified	20. Security Classif. (of this page) Unclassified	21. No. of Pages 95	22. Price*

CONTENTS

	Page
1.0 SUMMARY	1
2.0 INTRODUCTION	3
3.0 SYMBOLS	5
4.0 CONTROL CONCEPT	9
4.1 Characteristics of Powered-Lift STOL	9
4.2 Concept Selection	12
4.3 Pilot Control Technique	21
4.4 System Failure Effects	26
5.0 CONTROL CONCEPT DESCRIPTION	28
5.1 Basic Aircraft Characteristics	28
5.2 System Concept	32
5.3 System Performance	43
6.0 NOISE PROFILES	62
7.0 CONCLUSIONS	65
APPENDIX	66
REFERENCES	95

Preceding page blank

FIGURES

No.		Page
1.	Operational Envelope, Flaps 40	10
2.	Operational Envelope, Flaps 70	11
3.	STOL/CTOL Flightpath Capability	14
4.	Flightpath Angle at Constant Flap Setting	17
5.	Speed-Attitude Variation With Constant Flap Angle	18
6.	Response of Unaugmented Airplane	30
7.	Control System Block Diagram	33
8.	Steady-State Design Map	34
9.	Signal Sensors	37
10.	Effect of α and $\dot{\gamma}$ Feedback	42
11.	Response of Fully Augmented Airplane	46
12.	Glideslope Capture and Tracking Profile	49
13.	Glideslope Tracking in Turbulence	51
14.	Effect of SAS on Turbulence Response	53
15.	Effect of Flap Rate Limit on Glideslope Tracking	54
16.	Effect of Autothrottle Filter on Glideslope Tracking	56
17.	Flare and Go-Around Maneuvers	57
18.	Pilot Closures With Full Augmentation	61
19.	Approach Footprints	63
20.	Takeoff Footprints	64
A-1.	Model 751-103C Augmentor Wing Transport	67
A-2.	Lift Curves, Tail Off ($\delta_{\text{flap}} = 40^\circ$)	69
A-3.	Lift Curves, Tail Off ($\delta_{\text{flap}} = 70^\circ$)	70
A-4.	Drag Characteristics, Tail Off ($\delta_{\text{flap}} = 40^\circ$)	71
A-5.	Drag Characteristics, Tail Off ($\delta_{\text{flap}} = 70^\circ$)	72
A-6.	Pitching Moment, Tail Off ($\delta_{\text{flap}} = 40^\circ$)	73
A-7.	Pitching Moment, Tail Off ($\delta_{\text{flap}} = 70^\circ$)	74
A-8.	Effect of Flap Deflection on Lift	75
A-9.	Effect of Flap Deflection on Drag	76
A-10.	Effect of Flap Deflection on Pitching Moment	77
A-11.	CL_{max} ($\delta_{\text{flap}} = 40^\circ$ and 70°)	78
A-12.	α_{wing} at CL_{max} ($\delta_{\text{flap}} = 40^\circ$ and 70°)	79
A-13.	Horizontal Lift Curve	80
A-14.	Downwash—Augmentor Wing ($\delta_{\text{flap}} = 40^\circ$)	81

FIGURES (Concluded)

No.		Page
A-15.	Downwash–Augmentor Wing ($\delta_{\text{flap}} = 70^\circ$)	82
A-16.	Engine Model Step Response	86
A-17.	Engine Model Schematic	87
A-18.	Engine Characteristics	88
A-19.	Engine Model Rate Limits	90
A-20.	Pilot Model Logic	91
A-21.	Pilot Model Block Diagram	93

TABLES

No.		Page
1.	Powered-Lift Longitudinal Control Concepts	15
2.	Summary of Handling Qualities (Ref. 6)	20
3.	Control System Gains	40
A-1.	Configuration Constants	66

APPROACH PATH CONTROL FOR POWERED-LIFT STOL AIRCRAFT

By D. J. Clymer and C. C. Flora
Boeing Commercial Airplane Company
Seattle, Washington

1.0 SUMMARY

The objective of this study was to define a flight control system concept for approach flightpath control of an augmentor wing (or similar) powered-lift STOL configuration. The control system was to have potential for good handling qualities that must characterize a next-generation transport aircraft. Wherever possible, system requirements such as flap rate and deflection limits were to be identified to allow update of aircraft weight and cost estimates. Noise profiles were to be constructed for single- and two-slope approaches to determine if any significant noise gains could be made.

Review of available simulator and flight test results led to the conclusion that at present, a control system concept that encourages conventional pilot technique appears to have the greatest potential for attainment of good handling qualities in all phases of the approach and landing maneuver. Work done to date on control systems that encourage unconventional pilot techniques has indicated deficiencies in performance, particularly in the flare maneuver. It is thought that these deficiencies may result in part from the higher pilot workload levels associated with increased number of controller inputs required.

The proposed STOL control concept produces aircraft transient and steady-state responses that are familiar to pilots of conventional jet transports. This is achieved by synchronizing power and flap commands so that the major power-lift aerodynamic coupling is removed. The major distinguishing design feature of this control system is that the trailing-edge flap system becomes an active controlled element (active flap). An unpiloted computer study using a representative augmentor wing configuration was conducted to define the effects of major data nonlinearities, actuator rate limits, and real-engine dynamics on the design of the active-flap control system. Atmospheric turbulence was included and a pilot model for glideslope capture and tracking was developed. It was found that flap system rate capabilities of 10 to 15 deg/sec are required, and the dynamic response of conventional jet engines appears to be adequate. Aircraft motion sensor requirements can be satisfied with conventional equipment. This system appears to offer potential for ride qualities improvement in turbulence. There is no inherent negative limit on the glideslopes that can be negotiated, provided the appropriate L/D can be incorporated to permit operation at acceptable power and flap settings.

Controller configurations and control surface usage are compatible with both STOL and CTOL operation, and mode selection is straightforward.

Results of noise calculations indicate that for the augmentor wing configuration, there is no significant noise gain to be made by going to two-slope, steep approaches. This conclusion is based on analysis of 80 PNdB and higher noise profiles, and on the assumption that the basic aircraft noise levels are attenuated to 89 PNdB at the 500-ft sideline and that transition maneuvers are made at altitudes of 500 ft or higher.

2.0 INTRODUCTION

Powered-lift STOL aircraft configurations have potential for alleviating the congestion in today's air transportation system. The unique low-speed flight capability of these vehicles allows them to operate with greatly reduced field lengths, thereby allowing utilization of presently unused air and ground space. The logical evolution of this concept could lead to a new short-haul transportation system with facilities located close to population centers for traveler convenience. Existing major air terminals would continue to function as components of a long-haul transportation system. The physical separation of these two systems has the potential capability to greatly reduce air and ground congestion, thus providing for expanded passenger service.

The powered-lift STOL concept has three unique characteristics that influence the design of the longitudinal control system in low-speed flight.

- Operation on the back side of the drag curve
- Strong interaction between the thrust and lift
- Low $N_{z\alpha}$ for flightpath control

These characteristics make the powered-lift STOL very different from today's conventional jet transport in the areas of speed and longitudinal flightpath control. The longitudinal response of the basic STOL vehicle to throttle and column inputs has characteristics in common with both VTOL and CTOL vehicles. With respect to piloting techniques, the STOL flight envelope can be considered an intermediate area between VTOL and CTOL, and new approaches to control and handling qualities problems must be taken. To a fair extent, the selection of a control system concept will depend upon the designer's preconception of whether "conventional" airplane flying qualities are required.

There are many operational factors that influence this choice of emphasis. For example, if the STOL pilots are expected to be drawn largely from a population with conventional jet transport experience, it seems likely that the system designer should try to design control systems that emphasize CTOL controller characteristics because these systems would appear to offer a significant advantage in pilot transition training. If, on the other hand, pilot transition training were not considered a key issue, the system designer might tend toward control concepts with more unusual controller characteristics if these systems could be shown to offer advantages in simplicity and safety. There is a spectrum of control systems that can be envisioned and it is expected that ultimately, vehicles with satisfactory (though quite different) handling qualities could be developed using many different approaches.

This report presents a flight control system concept that permits conventional pilot technique to be used for powered-lift STOL flight. The system offers potential for good handling qualities ratings, appropriate for a next-generation family of aircraft. Essentially conventional longitudinal controller characteristics are provided, which should greatly reduce the requirement for special pilot transition training.

3.0 SYMBOLS

AR	aspect ratio b^2/S
b	wingspan, ft
C, \bar{c}	wing MAC, ft
C_D	drag coefficient
C_J	blowing momentum coefficient, gross blowing thrust/ qS
C_L	aircraft net lift coefficient
$C_{L_{max}}$	maximum wing-body lift coefficient at C_J
$C_{L_{wb}}$	wing-body lift coefficient
C_{L_α}	wing-body lift curve slope at C_J
C_{LC_J}	$\partial C_L / \partial C_J$ at constant α
$C_{m_{0.25c}}$	wing-body pitching moment coefficient about 0.25c reference point
CWS	control wheel steering
C_x	stability axis longitudinal force coefficient
$C_{x_{C_J}}$	$\partial C_x / \partial C_J$ at constant α
H_w/C	height of wing above ground plane in fractions of MAC
h	altitude, ft
\dot{h}_{baro}	barometric altitude rate, ft/sec
i_w	wing incidence angle

$K_{\theta \delta}$	gain of unaugmented θ / δ_e transfer function
L/D	lift-drag ratio
\dot{M}	engine mass flow rate, slugs/sec
N_x	longitudinal load factor, g
N_z	vertical load factor, g
$N_z \alpha$	$\partial N_z / \partial \alpha$
Q_B	body axis pitch rate, deg/sec
q	dynamic pressure, $1/2 \rho V^2$, lb/ft ²
q/q _∞	in ground effect calculation, the ratio of dynamic pressure with ground constraint to free-stream value
RMS	root mean square $\left\{ \frac{1}{T} \int_0^T [f(t)]^2 dt \right\}^{1/2}$
S, S _w	wing reference area
U _E	earth-referenced speed, ft/sec
u _g	turbulence component along X body axis, ft/sec
V, V _A	true airspeed, kt or ft/sec
V _{Ag}	velocity of head or tail wind with respect to ground
V _S	stall speed, kt or ft/sec
\bar{V}	tail volume coefficient, $\frac{S_H \ell_H}{S \bar{c}}$
w _g	turbulence component normal to X body axis, ft/sec
α_F	fuselage angle of attack, (α_{w-i_w})

α_{\max}	maximum wing angle of attack at C_J
α_w	wing angle of attack
γ	flightpath angle (airmass referenced)
γ_E	glidepath angle (earth referenced)
ΔCol	column deflection, in.
$\Delta \theta / \Delta \gamma$	steady-state ratio of fuselage attitude change to flightpath angle change in a maneuver
δ_{col}	control column deflection
δ_e	elevator deflection to stabilizer chord plane
δ_{flap}	wing trailing-edge flap deflection
δ_{stab}	stabilizer deflection relative to X body axis
δ_{th}	throttle command, %
ϵ	downwash angle at stabilizer chord plane
θ	aircraft pitch attitude with respect to earth axes
θ/δ_e	aircraft pitch attitude to elevator transfer function
$\sigma_{u, w}$	root mean square of horizontal and vertical turbulence velocities, ft/sec
τ	time constant, sec
Subscripts	
app	approach
co	crossover

GE	refers to conditions in ground effect
IC	initial condition, referring to the value of a system variable at time of control system engagement
o	value of system variable at trim
SS	steady state
∞	refers to conditions out of ground effect

4.0 CONTROL CONCEPT

The choice of pilot control technique is a fundamental decision that must be made in the design of a powered-lift STOL flight control system. The decision has significant implications for aircraft systems design. The control system concept presented in this report allows conventional airplane piloting techniques to be employed. This section outlines the reasons for this choice.

4.1 CHARACTERISTICS OF POWERED-LIFT STOL

Powered-lift STOL aircraft have three inherent characteristics that affect the design of the longitudinal flight control system. First, high C_L/AR ratios cause operation well on the back side of the drag curve, which requires simultaneous closure of pitch attitude and thrust control loops for flightpath control. Second, propulsive lift interaction causes the throttle to be a good N_z controller but a poor N_x controller. Third, the basic $N_{z\alpha}$ is low, and therefore pitch attitude tends to be ineffective for control of normal load factor. These characteristics combine to cause unusual transient and steady-state speed and flightpath control characteristics.

It should be noted that the term "powered lift" as used in this document is intended to describe vehicles that develop propulsive lift primarily through utilizing favorable interaction between engine exhaust and wing circulation (AW, IBF, EBF, USB). Configurations that develop propulsive lift primarily through simple deflection of engine gross thrust (deflected thrust) have not been included in this category.

The STOL flight envelope bridges the gap between VTOL and CTOL. The STOL response to longitudinal control may vary from a VTOL-type response to a CTOL-type response, depending on the magnitude of the powered-lift effects. For example, advancing the throttles in a CTOL airplane produces primarily a forward acceleration (N_x), whereas in some STOL aircraft, advancing throttles produces primarily an upward acceleration (N_z).

Figures 1 and 2 show the trimmed operational envelopes for a conventional augmentor wing configuration at two flap settings. For convenience, these figures have lines of constant power setting, wing angle of attack (α_w), and fuselage attitude (θ). A description of the configuration will be found in the appendix. These steady-state characteristics are generally representative of a broad range of powered-lift STOL configurations.

Figures 1 and 2 show that at the nominal approach speed of 80 kt the aircraft is on the back side of the drag curve ($\partial\gamma/\partial V$ is positive). It is also apparent that changes in flightpath angle at

Notes: $\delta_{flap} = 40^\circ$
 $h = 1000$ ft
 Trim with $cg = 0.47 \bar{c}$

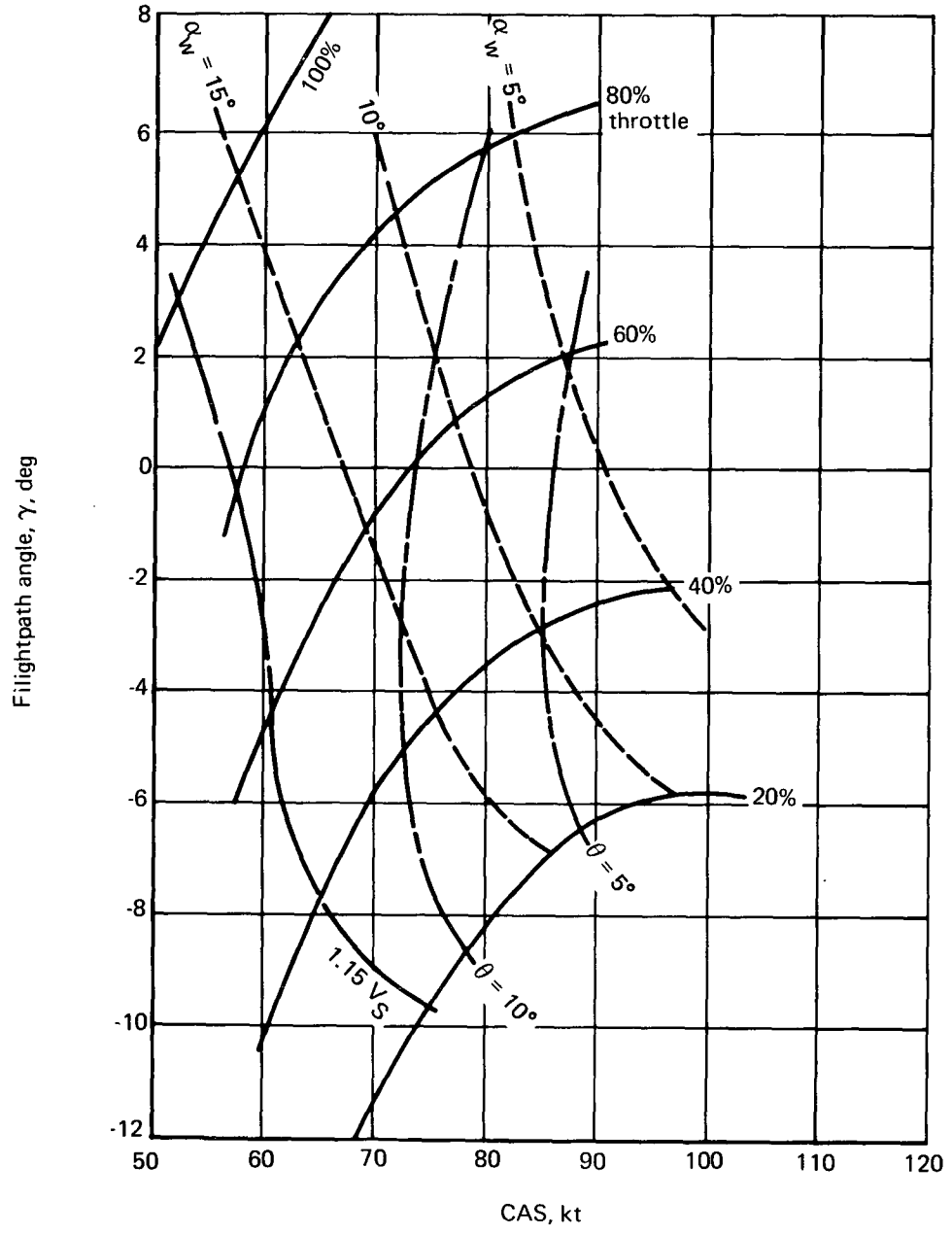


FIGURE 1.—OPERATIONAL ENVELOPE, FLAPS 40

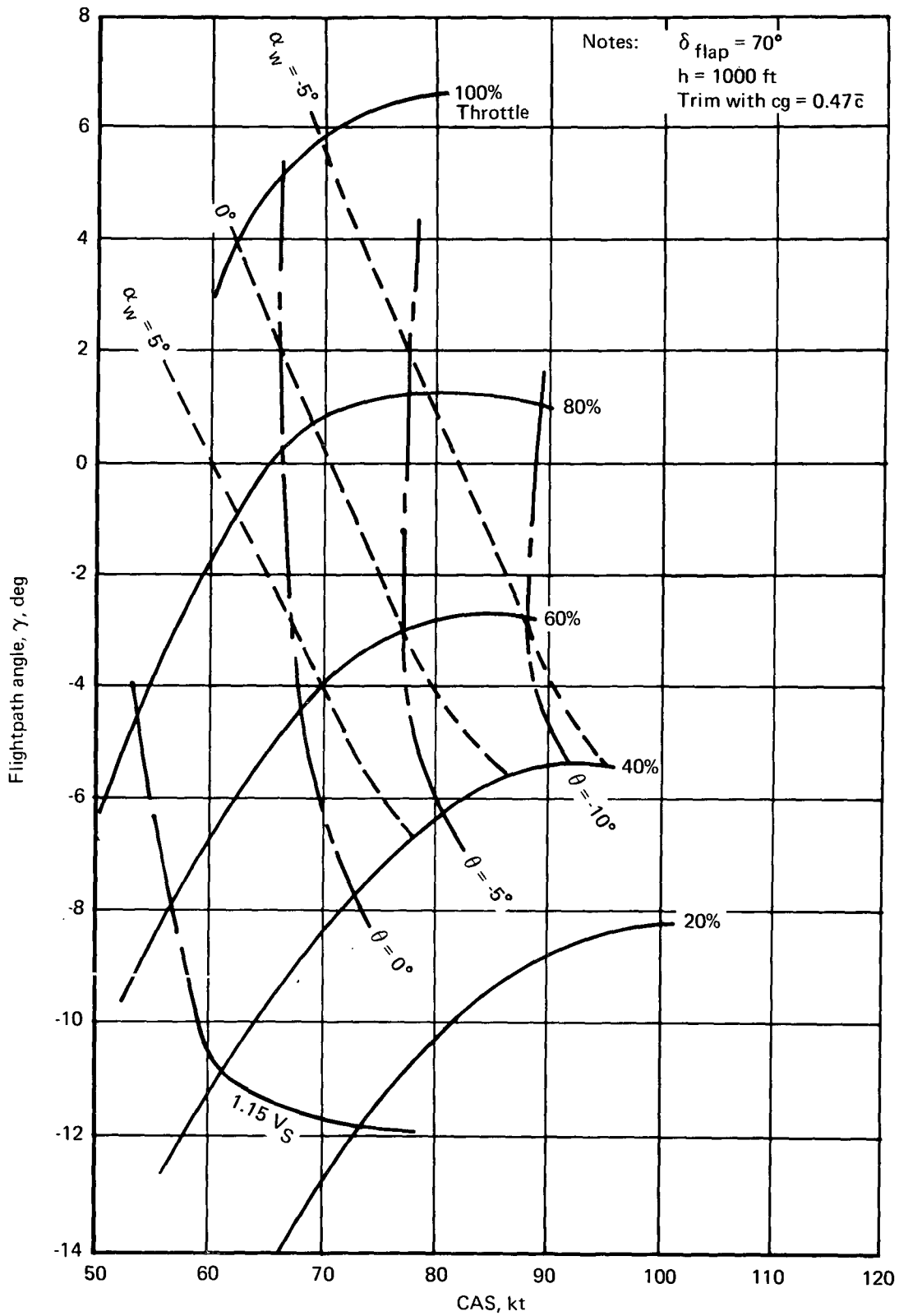


FIGURE 2.—OPERATIONAL ENVELOPE, FLAPS 70

constant airspeed and flap angle are made at essentially constant fuselage attitude and varying angle of attack. This steady-state attitude-flightpath response is opposite to that of a conventional jet transport configuration, where there is negligible interaction between power and lift.

In addition, certain transient response characteristics of powered-lift STOL configurations differ significantly from those of CTOL aircraft. For STOL aircraft, attitude response to column tends to be sluggish and strongly coupled with the phugoid mode, and flightpath response to attitude changes is slow. These effects are illustrated in section 5.1.

These basic differences in longitudinal control characteristics between STOL and CTOL configurations give rise to fundamental questions about control system concepts and piloting techniques required for STOL.

It has been amply demonstrated (ref. 1) that powered-lift configurations, with no longitudinal augmentation, can be flown safely by experienced pilots. It has also been determined that significant improvements in STOL handling qualities can be made by incorporating pitch axis stability augmentation system (SAS) functions, although flare control remains difficult. But it is probable that STOL configurations that have typically unconventional speed and flightpath responses to column and throttle may require significant additional pilot checkout training for pilot populations having experience in conventional jet transports (ref. 2). On the other hand, it is possible to design more complex STOL flight control systems that provide more conventional control responses and probably require a minimum of pilot checkout training. Thus, the choice of control system involves consideration of many operational factors, not all of which can be properly evaluated at this time.

It seems likely that a good pitch axis inner-loop or attitude SAS is probably a minimum requirement for a powered-lift STOL aircraft. For commercial transport applications, it may also be desirable to provide additional SAS functions (such as autospeed, direct lift control (DLC), power-lift decoupling) for more conventional column and throttle responses. The following two sections discuss various STOL control concepts and explain the relative advantages and disadvantages of the concept selected in this study.

4.2 CONCEPT SELECTION

To facilitate discussion of various powered-lift STOL longitudinal control concepts, it is useful to classify the concepts according to the role of the wing trailing-edge flap system. In this context, an active-flap system is defined as one where the flap system is an automatically controlled element. A passive-flap system is one where the flaps are occasionally adjusted by the pilot in a

scheduled manner. With either concept the throttles might be actively and/or passively controlled. Figure 3 shows representative lift versus propulsive force polars for conventional and powered-lift STOL aircraft. It is apparent that the STOL vehicle cannot cover the same range of flightpath angles as the CTOL aircraft at fixed flap angle. Thus, the active-flap concept can be considered a natural outgrowth of the powered-lift concept.

Table 1 lists a variety of STOL longitudinal control concepts with respect to flap concept, augmentation level, dominant control characteristic, and probable performance level. Inner-loop augmentation refers to modification of attitude control characteristics; outer-loop augmentation refers to modification of speed and altitude control using functions such as direct lift control, autospeed control, glidepath hold, and so on. Control characteristic refers to the dominant short-term response to deflections of the column or throttles. All configurations are assumed to be initially on the back side of the drag curve. This table is not intended to be exhaustive; many additional concepts can be envisioned.

The passive-flap systems (table 1A,B,C) are characterized by strong power-lift coupling. Throttle inputs produce large N_z and small N_x . This response is typical of powered-lift STOL, but would be considered unconventional by pilots familiar with CTOL aircraft. As indicated in table 1A, unaugmented STOL configurations, although safe for test pilots, are probably not acceptable for commercial applications because of poor inner-loop control and the coupled speed- N_z response to column or throttle inputs.

The performance potential of passive-flap systems with various degrees of augmentation (table 1B,C) is presently unknown. Parametric studies of systems with good inner-loop characteristics (refs. 4 and 5) suggest good flightpath control performance may be obtained for certain aerodynamic configurations. Flare, however, remains a problem (ref. 4). The system with inner- and outer-loop augmentation (table 1C) was not fully developed due to time limitations. The pilots complained of sluggish speed control and poor flare consistency (see table 2B).

Additional work on these passive-flap systems remains to be done. At present, a passive-flap system totally acceptable for commercial STOL applications has not been defined. It is likely that passive-flap systems will require additional pilot checkout training because of their unconventional throttle and column responses.

The active-flap system defined in table 1D was evaluated in the reference 6 piloted simulation, and it produced good handling qualities in all phases of the approach, flare, and touchdown maneuvers (see table 2A). Wing trailing-edge flaps and engine throttles are synchronized to produce power-lift decoupling, effective autospeed control, and conventional transient and steady-state column control characteristics. A glideslope-hold function was also provided.

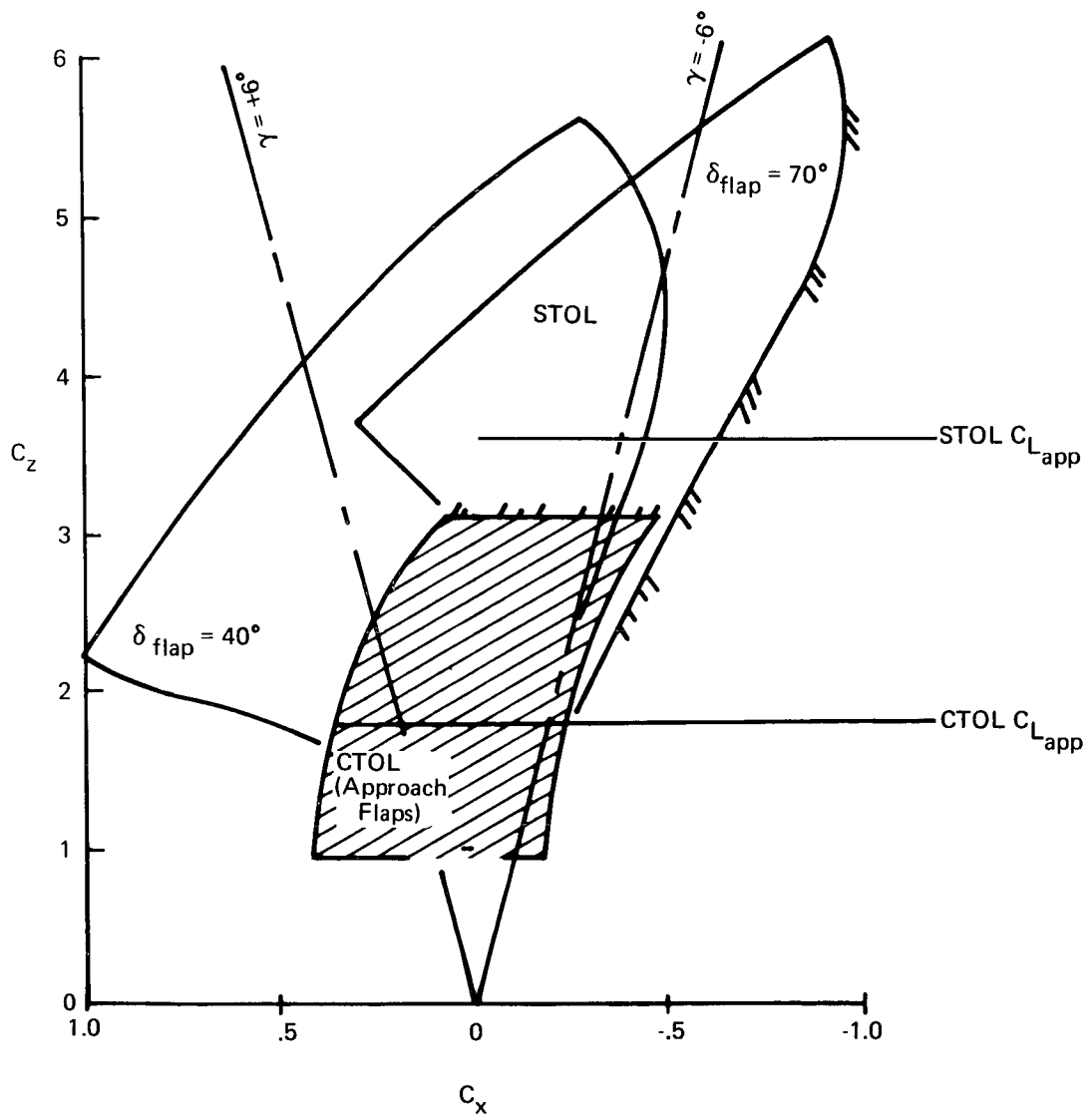


FIGURE 3.—STOL/CTOL FLIGHTPATH CAPABILITY

TABLE 1.—POWERED-LIFT LONGITUDINAL CONTROL CONCEPTS

Concept	Level of augmentation	Controller characteristic		Comment
		Column	Throttle	
PASSIVE FLAP	A. UNAUGMENTED	Loose attitude control	Coupled power-lift (unconventional)	Coupled speed— N_z response to column or throttle. Probably unacceptable for next-generation commercial STOL (refs. 1, 3, 4).
	B. INNER LOOP	Good attitude control and phugoid suppression (ref. 4)	↓	Potential dependent on specific configuration parameters (refs. 4, 5). Flare may be problem (ref. 4).
	C. INNER LOOP OUTER LOOP ($\gamma, \dot{\gamma} \rightarrow$ Engines) ($\Delta V \rightarrow$ Elevator)	↓	↓	Partially decoupled speed— N_z response to column or throttle. Sluggish speed response and poor flare control (ref. 6) Potential unknown.
ACTIVE FLAP	D. INNER LOOP OUTER LOOP (γ CWS with autospeed control through synchronized actuation of throttle and flaps; ref. 6)	Good control of attitude, N_z , and glidepath	Uncoupled power-lift (conventional) speed controlled by autospeed	Good pilot ratings in all approach, flare and touchdown phases. Flight director not required. Minimum pilot transition training required.
	E. INNER LOOP OUTER LOOP (Autospeed control achieved by simultaneous actuation of spoilers and flaps; ref. 7) Flightpath controlled by throttles.	Good control of attitude	Coupled power-lift (unconventional) Good control of N_z and glidepath	Good pilot ratings possible in approach. Flight director required for good flare and touchdown (ref. 7). Significant pilot transition training may be required.

The active-flap system defined in table 1E had a passive throttle function and produced autospeed control by simultaneous actuation of spoilers and wing flaps. The inherent power-lift coupling was retained and the throttle was primarily used to control N_z and glidepath. The column was used for attitude control. This configuration was difficult to flare, and it was necessary to provide a special flight director function (flare director) to produce acceptable flare performance. This difficulty appears to be characteristic of control systems where there is strong power-lift coupling and flare is initiated with throttle. See section 4.3.4 for further discussion.

Some important distinctions can be drawn between the various systems of table 1 by considering the aircraft steady-state pitch attitude relationships.

Figure 4 shows the variation of trim fuselage attitude with flightpath angle for the representative augmentor wing transport configuration at the nominal 80-kt approach speed. This figure is related directly to figures 1 and 2. For flightpath angle change maneuvers at constant flap angle, systems A, B, C, and E of table 1 produce a steady-state altitude ratio, $\Delta\theta/\Delta\gamma$, of essentially zero. As discussed in section 4.3, this characteristic is unconventional; for the conventional jet transport, $\Delta\theta/\Delta\gamma \cong 1.0$.

Figure 4 also shows a line for $\Delta\theta/\Delta\gamma = 1.0$, constructed through a nominal flap setting of 40° for level flight. System D of table 1 produces this conventional $\Delta\theta/\Delta\gamma = 1.0$ ratio because it synchronizes flaps and throttles, as explained in section 5.2. This relationship is important for systems where flightpath angle changes are initiated through column inputs because the initial and steady-state responses are compatible.

Figure 5 shows the variation of trim fuselage attitude with speed for the representative augmentor wing transport in level flight. A representative slope for a conventional transport is also shown. Systems A, B, and C of table 1 produce slopes, $\Delta\theta/\Delta V$, that are nearly twice those of conventional aircraft. The flap angle management with speed change task would appear to add significantly to pilot workload for systems A, B, and C.

System D of table 1 provides automatic management of flap angle with speed change because the autospeed control is mechanized through the active-flap system. The attitude and flightpath hold functions further reduce pilot workload during speed change maneuvers. A zero speed-attitude gradient is shown in figure 5 for illustration, although as explained in section 5.2.1, this system is capable of producing a wide range of attitude-speed gradients. System E of table 1 also has potential for automatic flap management with speed change because its autospeed function is mechanized through the active-flap system.

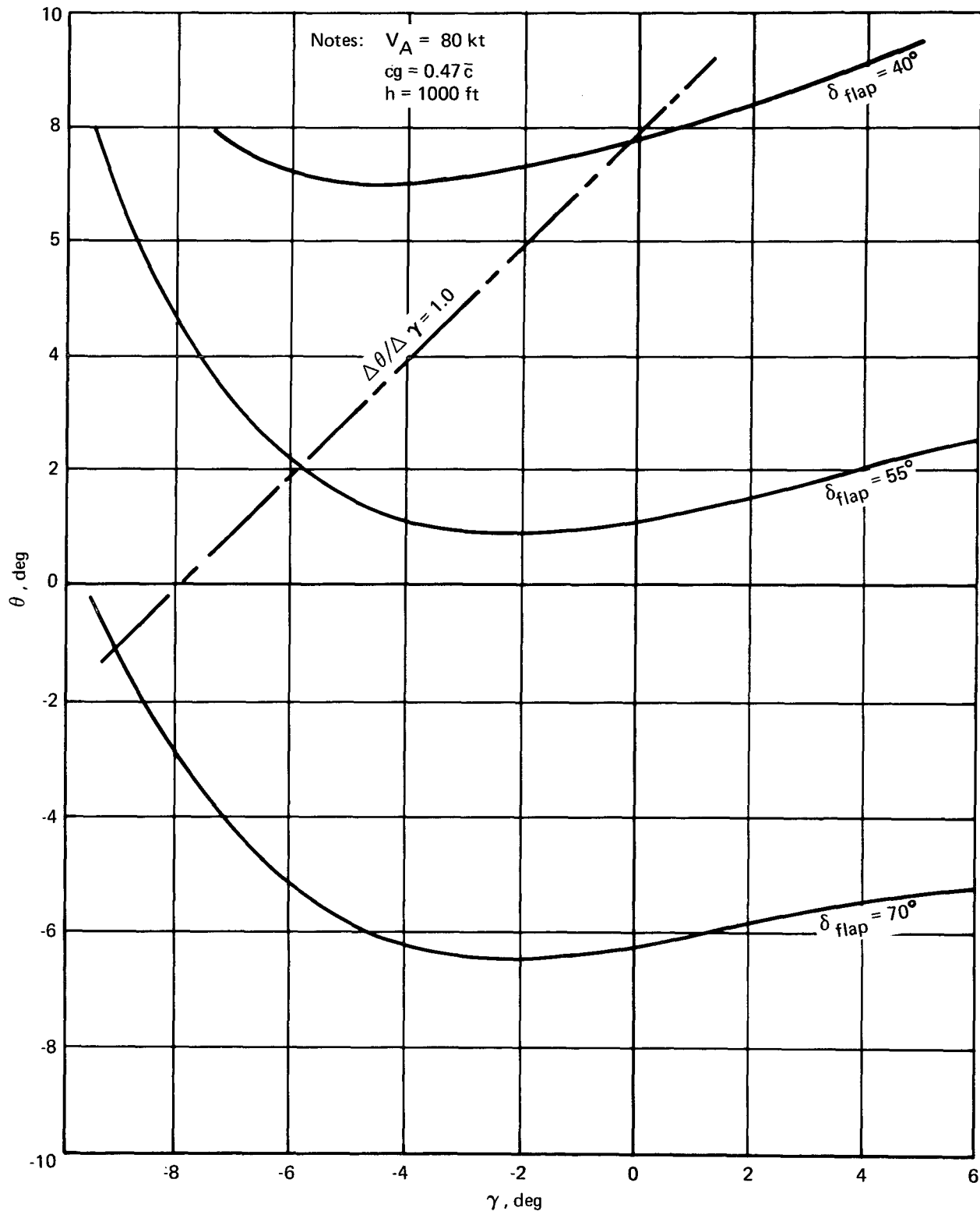


FIGURE 4.—FLIGHTPATH ANGLE AT CONSTANT FLAP SETTING

Notes: $\gamma = 0$
 $cg = 0.47 \bar{c}$
 $h = 1000 \text{ ft}$

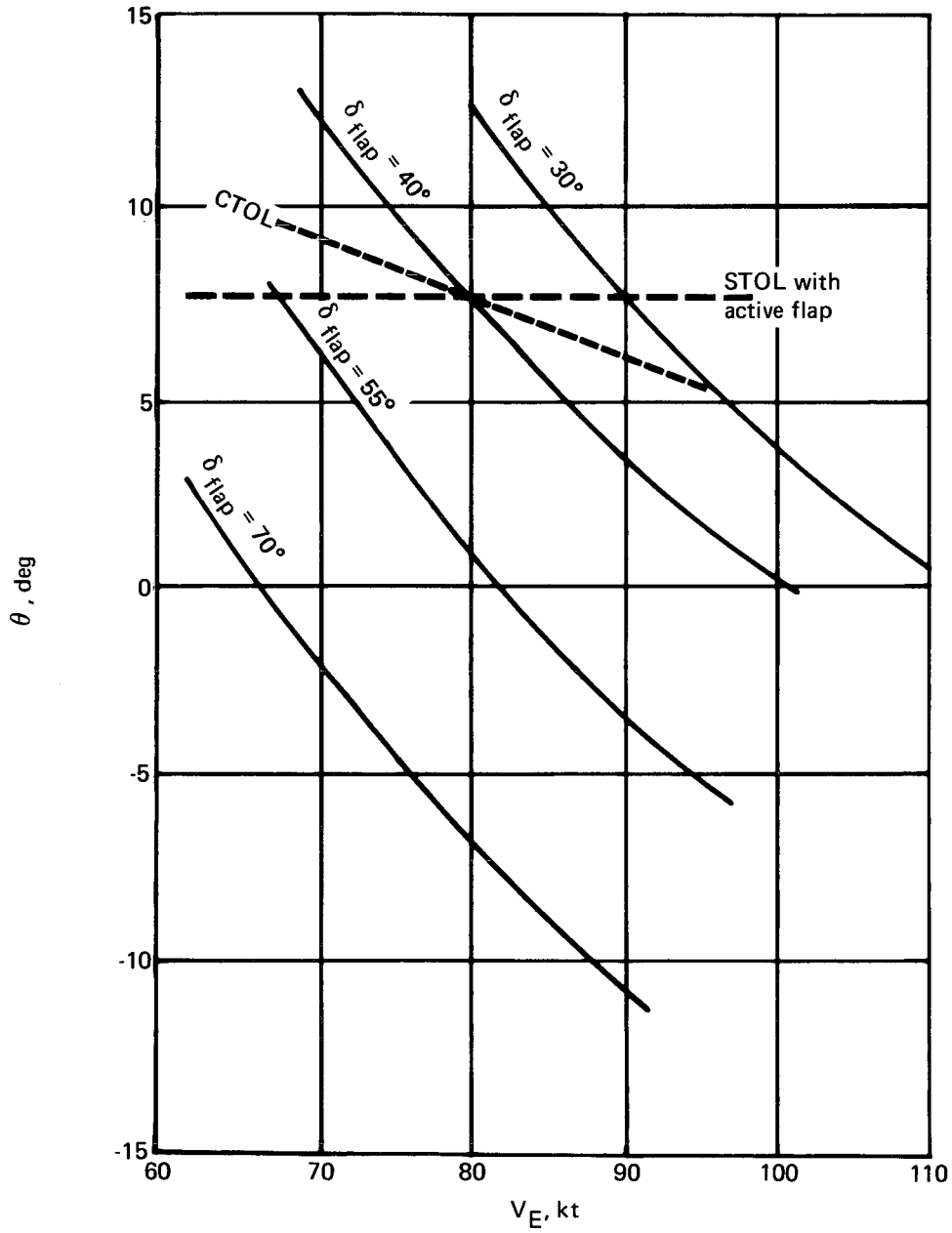


FIGURE 5.—SPEED-ATTITUDE VARIATION WITH CONSTANT FLAP ANGLE

Table 2A summarizes the characteristics of the active-flap control concept evaluated in the reference 6 study (table 1D). The pilot enthusiasm is evident. Table 2 also shows evaluations of passive-flap systems evaluated in the reference 6 study as points of comparison. The passive-flap systems clearly require additional work.

The STOL flight control system concept corresponding to system D of table 1 was selected for this study. This system produces transient and steady-state control responses that are similar to those of conventional jet transports. This system was selected because:

- Repeated Boeing simulator studies, using a pilot population with jet transport experience, have indicated wide acceptance for this system in all approach, flare, and landing phases.
- The selected concept provides essentially conventional column response and functions, and should require a minimum of pilot training for transition checkout.

The following control system functions are provided:

- An autospeed function where operation is on the back side of the drag curve
- Column proportional plus integral feed-forward into a DLC system to augment the inherently low $N_{z\alpha}$, sharpen the altitude response to column, and control the steady-state $\Delta\theta/\Delta\gamma$
- Pitch axis SAS for positive attitude control
- Automatic flap management to reduce pilot workload and establish a desirable steady-state $\Delta\theta/\Delta V$ response

In addition, if handling qualities are desired that exceed today's jet transport but are compatible with next-generation aircraft, it is desirable to add:

- A γ control wheel steering (γ CWS) function

This full control wheel steering concept was selected because it has the potential for superior pilot ratings at small additional complexity.

TABLE 2.—SUMMARY OF HANDLING QUALITIES (REF. 6)

SAS	Pilot technique	Control system paths	Comments
A. γ CWS with active flap and auto-speed	No. 1 Conventional jet transport technique: Column $\rightarrow \theta \rightarrow h$ Throttle $\rightarrow V$	$\delta_{col}, V_{cmd}, \alpha, \dot{\gamma}, \Delta V \rightarrow$ Engines $\delta_{col}, V_{cmd}, \alpha, \dot{\gamma}, \Delta V \rightarrow$ Flap $\delta_{col}, Q, \theta \rightarrow$ Elevator	Easy-to-fly pilot ratings: 1.5 \rightarrow 3 No pilot retraining required. Problem areas: <ul style="list-style-type: none"> ● Active flap system required. ● Quick thrust and flap response required to achieve N_z response necessary for STOL.
B. Basic controls with passive flap and autospeed	No. 2 Unconventional: Column $\rightarrow \theta \rightarrow V$ Throttle $\rightarrow h$	$\delta_{th}, \gamma, \dot{\gamma} \rightarrow$ Engines $\delta_{col}, Q, \theta, \Delta V \rightarrow$ Elevator	Handling qualities require improvement for normal airline operation. Pilot ratings: 3 \rightarrow 8 Problem areas: <ul style="list-style-type: none"> ● Requires pilot retraining ● Sluggish speed control ● Difficult to flare consistently
C. Unaugmented	No. 2 Unconventional: Column $\rightarrow \theta \rightarrow V$ Throttle $\rightarrow h$	$\delta_{th} \rightarrow$ Engines $\delta_{col} \rightarrow$ Elevator	Handling qualities unacceptable for routine operations Pilot ratings: 4.5 \rightarrow 8 Problem areas same as SAS B except more severe. In addition: <ul style="list-style-type: none"> ● Poor pitch damping ● Strong thrust/pitch interaction

4.3 PILOT CONTROL TECHNIQUE

This section discusses aspects of pilot technique that relate to approach landing operations of powered-lift STOL aircraft. The discussion is generalized and is not meant to be exhaustive. It is intended to focus attention to some of the basic problem areas of STOL handling qualities and system design.

Two basic STOL control concept groupings are contrasted:

1. Those systems where power-lift coupling is retained, and the throttle produces the primary short-term N_z response (as noted in table 1, these may have either passive- or active-flap systems).
2. Those systems where power and lift are decoupled and the column provides the primary short-term N_z response. This corresponds to the selected control system concept (table 1D).

It is hoped that this discussion will clarify the reasons for the good performance of the selected control system concept, and will point out areas where additional work might be useful in developing different concepts.

4.3.1 Pilot Control Logic

The basic pilot task is to control the airplane airspeed vector in a three-dimensional space. Typically, airspeed and glidepath control are longitudinal tasks, and heading control is a lateral-directional task.

For the longitudinal tasks, the primary controllers are the column and the throttles. There are a variety of possible control logic loops available to the pilot, and the choice is a function of aircraft characteristics and pilot training.

The control task has basically two aspects (ref. 5). There are trim change maneuvers that are made in essentially open-loop fashion (gross altitude correction, for example) where aircraft long-term response is important, and there are closed-loop regulatory maneuvers (about a selected trim point) where aircraft short-term response is most important.

The response of flightpath and speed will generally be compatible with one of the following piloting techniques:

- *Technique 1*—Pitch rate/attitude are used to control load factor/flightpath angle. The throttle is used to control airspeed.
- *Technique 2*—Pitch attitude is used to control airspeed. The throttle is used to control load factor/flightpath angle.

In practice, pilots use a coordinated combination of these techniques and alter their control modes in an adaptive manner. For example, in a conventional jet aircraft, short-term corrections may tend to be made with technique 1, while long-term corrections may more closely resemble technique 2. However, these definitions are useful in identifying the basic cross-check logic used by the pilot when faced with tasks such as landing approach and flare.

There is some disagreement among pilots regarding the definition of control logic they use to control an airplane (see ref. 8, for example). In general, it can probably be assumed that for short-term corrections a jet transport pilot uses technique 1 for cruise; technique 1 and/or 2 for approach, depending on wind conditions and level of aircraft speed stability; and technique 1 for flare. Technique 2 appears to be most familiar to pilots who are accustomed to flying on the back side of the drag curve where $\partial\gamma/\partial V > 0$ (ref. 9).

The unaugmented powered-lift STOL configuration would seem to be well suited to the technique 2 mode of control because these configurations are typically on the back side of the drag curve and because there is a strong interaction between power and lift. The throttle is a good N_z controller but a poor N_x controller. This technique has in fact been used successfully in both simulation and flight test studies of powered-lift STOL configurations (see refs. 1, 3, 4, 6, and 7, for example).

Regardless of the piloting technique employed, it is a fundamental control requirement that column or throttle commands produce essentially distinct short-term speed or load factor response. If, for example, the throttles are to be considered the primary controller of N_z and flightpath, the speed response to throttle input (if any) must be well separated from the load factor response in magnitude and bandwidth. In addition, all control responses must be free from poorly damped dynamic components that distract the pilot from performance of his basic control tasks.

Unaugmented powered-lift STOL configurations violate this fundamental control requirement. For these configurations, the short-period and phugoid responses tend to be tightly coupled and poorly damped so that individual column and throttle inputs produce essentially undifferentiated

responses with poorly damped dynamic components. A very significant contribution of the reference 4 study is the suggested technique of using a rate-command attitude-hold SAS to achieve essential phugoid suppression. This removes the lightly damped oscillatory component from the throttle and column responses and makes it possible to select (at least in a parametric study) configuration parameters that will provide good glideslope control.

With respect to piloting technique, it is interesting to note that in the reference 4 study, technique 2 was emphasized. In the reference 10 study, which used essentially the same aircraft simulation and pitch axis augmentation as the reference 4 study but incorporated an autospeed control function, technique 1 was emphasized for flightpath control. This is compatible with the established pilot preference for technique 2 when on the back side of the drag curve. The autospeed function of reference 10 probably produced effective front side operation. In any event, the question of control technique is complex, and simple rules probably cannot be formulated.

The control concept that is selected in this document provides well-differentiated, well-damped responses to column and speed commands and has a tight autospeed function, as demonstrated in section 5. It is compatible with pilot technique 1, and broad pilot acceptance has been shown for similar systems in reference 6 and Boeing in-house studies.

4.3.2 Closed-Loop Tasks

The pilot must control the aircraft velocity vector in a three-dimensional space. In a conventional airplane, the two vector angles (γ, ψ) usually are tracked using column and wheel inputs, and the vector magnitude (V) is controlled in essentially open-loop or discontinuous fashion using the throttle inputs. Pilot workload and performance in this conventional mode of operation provide the basis of comparison for pilot rating of various transport configurations for a pilot population with jet transport experience.

A jet transport typically operates slightly on the front side of the drag curve in the approach configuration. For aircraft that operate on the back side of the drag curve, the piloting task is more difficult because conventional control of flightpath angle (γ) will cause a speed divergence, and speed must also be controlled in a closed-loop fashion. The pilot must now close three loops using three separate controllers. The deterioration of pilot rating that accompanies back side operation reflects this increase in workload due to the additional active pilot control task.

It appears that if powered-lift STOL aircraft are to have pilot workload, safety, and acceptance levels equivalent to those of today's conventional jet transports, the pilot task is going to have to be limited to not more than two closed-loop tasks (heading and glideslope) using not more than two related control functions (wheel and column). Additional pilot tasks must be open-loop tasks that

are performed in a discontinuous or scheduled manner. This consideration probably dictates the need for some form of autospeed control for powered-lift STOL aircraft. It also raises questions about pilot workload with systems that use throttles to control load factor because flightpath control and heading control (wheel) require separate controllers.

The selected control system concept uses controller functions that are similar to those of a conventional jet transport. Column and wheel functions are used to control glideslope and heading; airspeed is controlled by an autospeed function.

4.3.3 Trim Change Tasks

The discussion of pilot technique has so far been primarily concerned with the short-term corrections that a pilot makes during terminal area tracking maneuvers. The aircraft steady-state response to these short-term inputs ($\Delta\theta/\Delta\gamma$; $\Delta\theta/\Delta V$) is also important to the pilot in trim change tasks. The steady-state response should generally be compatible with the short-term piloting technique.

When a jet transport pilot initiates a flightpath change at constant speed using technique 1, he commands a change in pitch attitude (short-term correction) that produces the load factor change required to bend the flightpath. A more or less discrete power change is made (long-term correction) to achieve equilibrium on the new path. When equilibrium on the new path has been achieved, the angle of attack essentially returns to its initial value, and in the steady state, change in pitch attitude equals the change in flightpath angle, $\Delta\theta/\Delta\gamma = 1.0$. Thus, the conventional jet transport flies where it is pointed.

Powered-lift STOL configurations are characterized by a strong thrust-lift interaction. When a flightpath angle change is made, the steady-state angle of attack is also changed because there is a new trim power setting, and $\Delta\theta/\Delta\gamma \ll 1.0$. This relationship is shown in figure 4 for the representative augmentor wing transport configuration at 80 kt. For maneuvers at constant flap angle, steady-state $\Delta\theta/\Delta\gamma$ is nonlinear, is always much less than 1.0, and may be negative. When technique 2 is being used for short-term conditions, small positive values of $\Delta\theta/\Delta\gamma$ are probably acceptable (perhaps desirable), but negative values are undesirable because the pilot would prefer to pull the nose up when adding power (refs. 4 and 7).

If technique 1 is being used for short-term corrections, this steady-state characteristic is particularly confusing because in this mode the pilot associates attitude with flightpath angle, and the steady state is not compatible with the initial response.

Figure 4 shows a line for $\Delta\theta/\Delta\gamma = 1.0$. It is apparent that flap angle must be made a variable if the steady-state maneuver response of the powered-lift STOL is to match that of the conventional aircraft and technique 1 is to be used. As explained in section 5, the selected control concept has $\Delta\theta/\Delta\gamma$ of approximately unity, although the exact value is adjustable.

Another steady-state parameter that is important to the pilot is the steady-state change in fuselage attitude with speed at constant flightpath angle, $\Delta\theta/\Delta V$. This parameter is particularly important if technique 2 is being used because the pilot associates speed changes with attitude. The initial and steady-state values should be in the same direction. In addition, large values of $\Delta\theta/\Delta V$ are undesirable if they cause the pilot to lose sight of the runway, cause passenger discomfort, or exceed a geometry limit on touchdown.

Figure 5 shows the variation of trim fuselage attitude with speed for a typical augmentor wing transport in level flight. A representative slope for a conventional jet transport is also shown. Powered-lift STOL aircraft with passive-flap systems characteristically have slopes more than twice as high as those of conventional aircraft. Regardless of the piloting technique employed, it is apparent that flap angle management with speed changes will tend to be a high workload item for the pilot. This function should be automated.

The selected control system concept provides automatic flap angle management in speed change maneuvers, as explained in section 5.2.1. This should greatly reduce pilot workload in the approach phase.

4.3.4 Flare

Certain powered-lift STOL configurations appear to be difficult to flare (refs. 4, 6, and 7). These configurations encouraged the combined use of throttles and pitch attitude for flare, and the touchdown performance (precision and sink rate) was inconsistent. All the evaluations were conducted in piloted simulation with wind tunnel or theoretical ground effect estimates. Flight data are not presently available for these systems.

It is also known that at least one powered-lift STOL configuration, the Breguet 941, has acceptable flare characteristics (refs. 2 and 3). This aircraft was flared primarily with column inputs. These evaluations were made in a flight test program. This configuration was reported to have a favorable ground effect.

Interpretation of these results for the two flare techniques is complicated by the following factors:

- The ground effects in the simulations are of unknown validity and are probably more adverse than actual flight. Favorable ground effect is very beneficial in a flare maneuver.
- The simulator is probably not capable of producing visual and motion cues that reproduce exactly the real flight environment.

With these reservations, some tentative conclusions can be drawn.

Reference 4 has pointed out that pilot comments indicate the extreme difficulty of performing a two-control flare (column and throttles) because of the short duration of the maneuver. The pilots expressed a strong desire for a single controller with which to perform the flare. This observation is compatible with the two sets of test data quoted above, and is also compatible with the way conventional aircraft are flared. Reference 7 also points out that flightpath response to control is probably more critical for flare than approach, and special attention must be given to aircraft and engine dynamics for flare.

The following additional comments also seem appropriate. Since the flare is ideally an energy exchange maneuver (reduced flightpath potential energy is reflected in an airspeed decrease with throttle setting constant or reduced), it is clear that flare with throttles (energy increase) requires precise power management if objectionable airspeed increases are to be avoided during flare and touchdown. This area will require careful attention in the design of systems where the throttle is the primary N_z /flightpath controller. The inclusion of a tight autospeed function should be beneficial. Also, some appropriate cues (flare director) and perhaps a throttle feel system would allow the pilot to make more precise throttle inputs during flare. Additional work must be done in this area.

The selected control system is flared with column inputs (technique 1) and produces good flare load factor response through simultaneous flap and engine actuation. Airspeed is held constant by a tight autospeed function. The flare characteristics of this system were well received by pilots in the reference 6 study (see table 2). A flare director is not required.

4.4 SYSTEM FAILURE EFFECTS

The question of redundancy requirements for the selected control system remains to be answered. Since this control system concept alters the basic characteristics of the unaugmented aircraft, the question arises as to the impact of system failures that cause the augmented aircraft to suddenly revert back to the cross-coupled, unaugmented configuration. Before this question can be completely resolved, additional piloted simulator studies will be required to determine the level of pilot performance possible under these conditions. There are two possibilities:

- Techniques 1 and 2 may not be strongly incompatible (see sec. 4.3). Most pilots are familiar with technique 2 because it is the basic technique for flying on the back side of the drag curve. A pilot learns or is at least made aware of this technique in his basic training. Under these conditions, there might be no unusual flight control system redundancy requirements.
- If the transition in technique exceeds the capabilities of the average pilot, then a “hard SAS” concept would be required. This would probably require some minimum control SAS function such as autothrottle and/or engine-flap interconnect.

In any event, some level of fail-operational capability will be required. It may, however, be possible to allow a graduated failure sequence in which angle-of-attack feedback paths have lower reliability than pitch axis and autospeed SAS functions, for example.

5.0 CONTROL CONCEPT DESCRIPTION

A control system concept is defined that allows a powered-lift STOL aircraft to be flown using conventional pilot technique. This concept was evaluated during the reference 6 simulator study and was found to provide good handling qualities in all phases of the approach and landing mission in both still air and turbulence.

The essential distinguishing feature of this STOL control concept is the active role of the trailing-edge flap and throttle systems. This active-flap concept allows the decoupling of power and lift so that energy management functions can be performed with essentially conventional aircraft attitude and controller relationships. Although developed for an augmentor wing data set, the concept is directly applicable to any powered-lift concept with suitable gain adjustments and selection of the appropriate trailing-edge flap segment. There are no inherent limits to the glideslope angles that can be negotiated other than those imposed by the basic L/D characteristics of the airframe. Controller configurations and control surface usage are compatible with both STOL and CTOL operation.

As with conventional aircraft, this control concept produces changes in fuselage attitude approximately equal to the change in flightpath angle. The effect of steep approaches on passenger comfort has not been evaluated.

5.1 BASIC AIRCRAFT CHARACTERISTICS

The control system concept that is described in this section was developed for an augmentor wing STOL transport configuration with the following characteristics:

Weight—200 000 lb

Wing loading—78 lb/sq ft

Approach speed—80 kt

Field length—2000 ft

Number of engines—4

The mathematical model included all important longitudinal aerodynamic and system nonlinearities, including a representative turbofan engine model with lags and ram drag effects, downwash computation with ground plane, and control actuator rate limits. A description of the airplane model will be found in the appendix. It should be noted that this augmentor wing

configuration is representative of a wide range of powered-lift STOL concepts, and with minor modification the control system concept is equally applicable to all powered-lift STOL configurations.

Figures 1 and 2 show the STOL operational envelopes for the augmentor wing configuration for 40° and 70° flap settings. Boundaries of 1.15 V_S are shown for reference. At the nominal approach speed of 80 kt and the approach power settings used in this study, the aircraft is on the back side of the drag curve.

The unaugmented longitudinal dynamic response of this configuration is characterized by essentially critically damped short-period roots and neutrally damped phugoid roots. There is small frequency separation between phugoid and short-period roots, and poor root placement with respect to numerator zeros, so that either column or throttle inputs excite both modes. This is characteristic of many STOL configurations. These characteristics are reflected by the following representative augmentor wing transfer functions for a speed of 80 kt. The effect of trim condition is small.

$$\left. \begin{array}{l} \delta_{\text{flap}} = 40^\circ \\ \gamma_0 = 0^\circ \end{array} \right\} \frac{\theta}{\delta_e} = \frac{K_{\theta\delta} (S^2 + 0.61S + 0.162)}{(S + 0.883)(S + 0.264)(S^2 + 0.0065S + 0.0465)}$$

$$\left. \begin{array}{l} \delta_{\text{flap}} = 70^\circ \\ \gamma_0 = -8^\circ \end{array} \right\} \frac{\theta}{\delta_e} = \frac{K_{\theta\delta} (S^2 + 0.45S + 0.10)}{(S^2 + 1.06S + 0.318)(S^2 - 0.0136S + 0.0548)}$$

Figure 6 shows time responses to column and throttle steps for the unaugmented aircraft. These responses are characterized by strongly coupled speed and flightpath responses occurring at the essentially undamped phugoid frequency. Uncompensated throttle or column inputs produce similar and basically useless coupled responses. To produce the desired aircraft motions, the pilot must make coordinated column and throttle inputs (control crossfeed). The pilot ratings of 6 to 8 in table 2C reflect the difficulty of this task.

Two basic functions of the STOL control and augmentation system are to restore the basic separation of the column and throttle functions that are characteristic of conventional airplanes and to suppress poorly damped dynamic response components.

Notes: $V = 80 \text{ kt}$
 $\gamma_o = -6^\circ$
 $\delta_{\text{flap}} = 70^\circ$
 $\text{cg} = 0.47 \bar{c}$

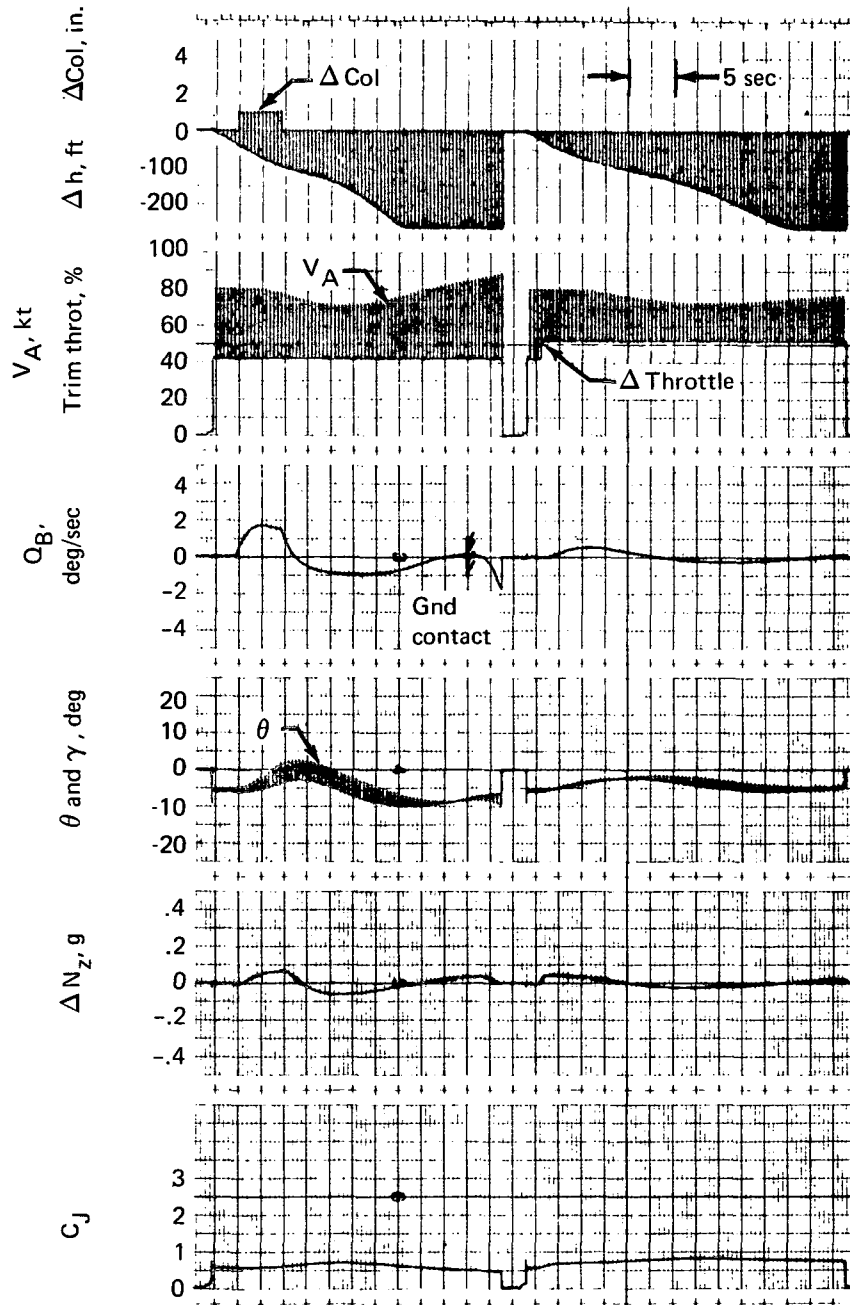


FIGURE 6.—RESPONSE OF UNAUGMENTED AIRPLANE

Notes:

$V = 80 \text{ kt}$

$\gamma_0 = -6^\circ$

$\delta_{\text{flap}} = 70^\circ$

$\text{cg} = 0.47\bar{c}$

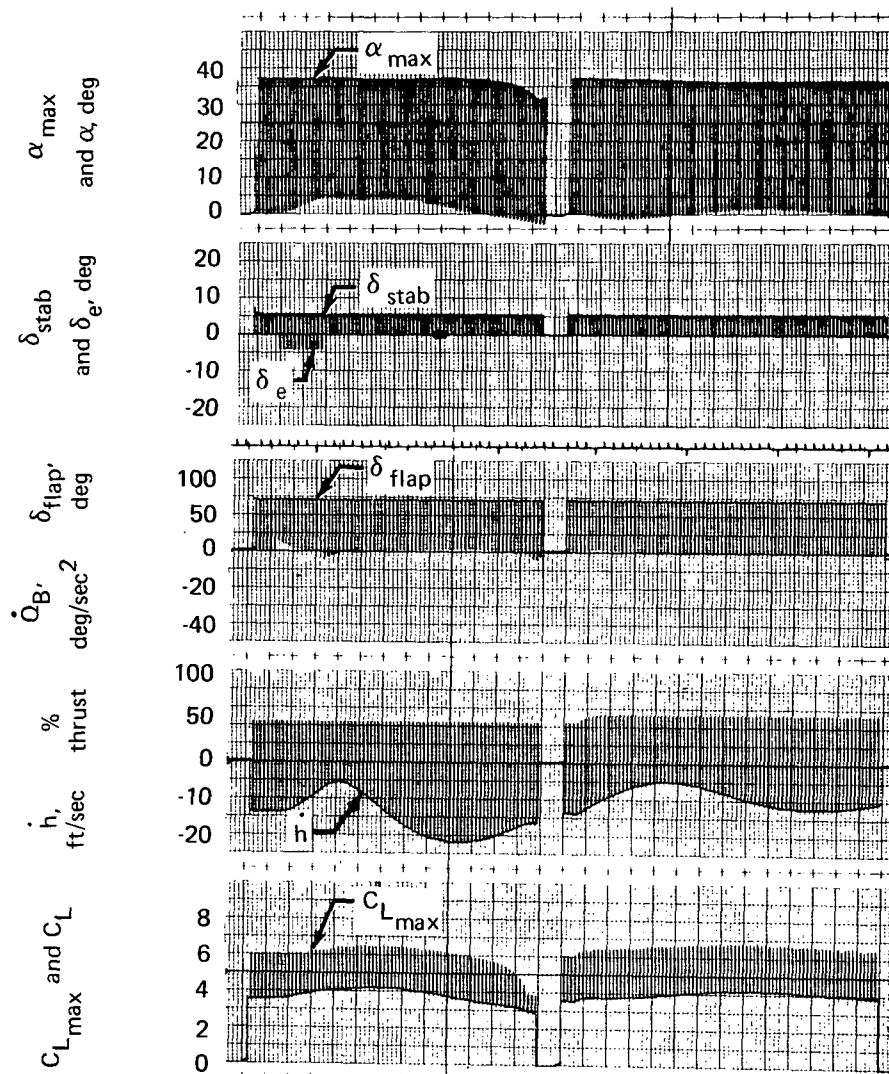


FIGURE 6.—CONCLUDED

5.2 SYSTEM CONCEPT

As stated in section 4.2, the chosen STOL control system concept produces jet transient and steady-state control responses similar to those of a conventional jet transport and is compatible with pilot control technique 1 (see sec. 4.3 for definition). The following functions are provided:

- Autospeed
- Pitch rate command, attitude hold
- Quickening of load factor response to column
- Flightpath control wheel steering (γ CWS)
- Automatic flap management

The system offers potential for good pilot ratings in all phases of the approach and landing maneuver.

The underlying principles are to feed back key attitude and speed holding parameters (θ , α , V) into the most sensitive channels (elevator, flaps, throttles) and to provide suitable controller feed-forward paths to permit pilot selection of the operating point.

Figure 7 shows the conceptual control system block diagram in which the essential feed-forward and feedback paths are delineated. Basically, the pilot selects aircraft pitch attitude (θ) by making an appropriate column input, and the angle-of-attack (α) feedback path forces the maneuver to progress at constant α so that $\Delta\theta = \Delta\gamma$ (because $\gamma = \theta - \alpha$). The autospeed function automatically holds speed at the selected value. The α and speed (V) feedbacks are fed into both throttles and flaps to decouple the responses. The additional γ and column paths into throttle and flap basically control the load factor response time, flightpath overshoot, and steady-state $\Delta\theta/\Delta\gamma$ response. These details will be explained in following paragraphs.

5.2.1 System Design Map

The operation of the control system can be readily understood by referring to figure 8. This figure is a design map for a speed of 80 kt that shows steady-state flightpath angle as a function of trimmed angle of attack for a range of flap deflections. Also shown are lines of constant power, pitch attitude (θ), and stall margin ($\alpha_{\max} - 15^\circ$). This constant speed map is valid because the autospeed function has an integral circuit that holds airspeed constant in flightpath change maneuvers.

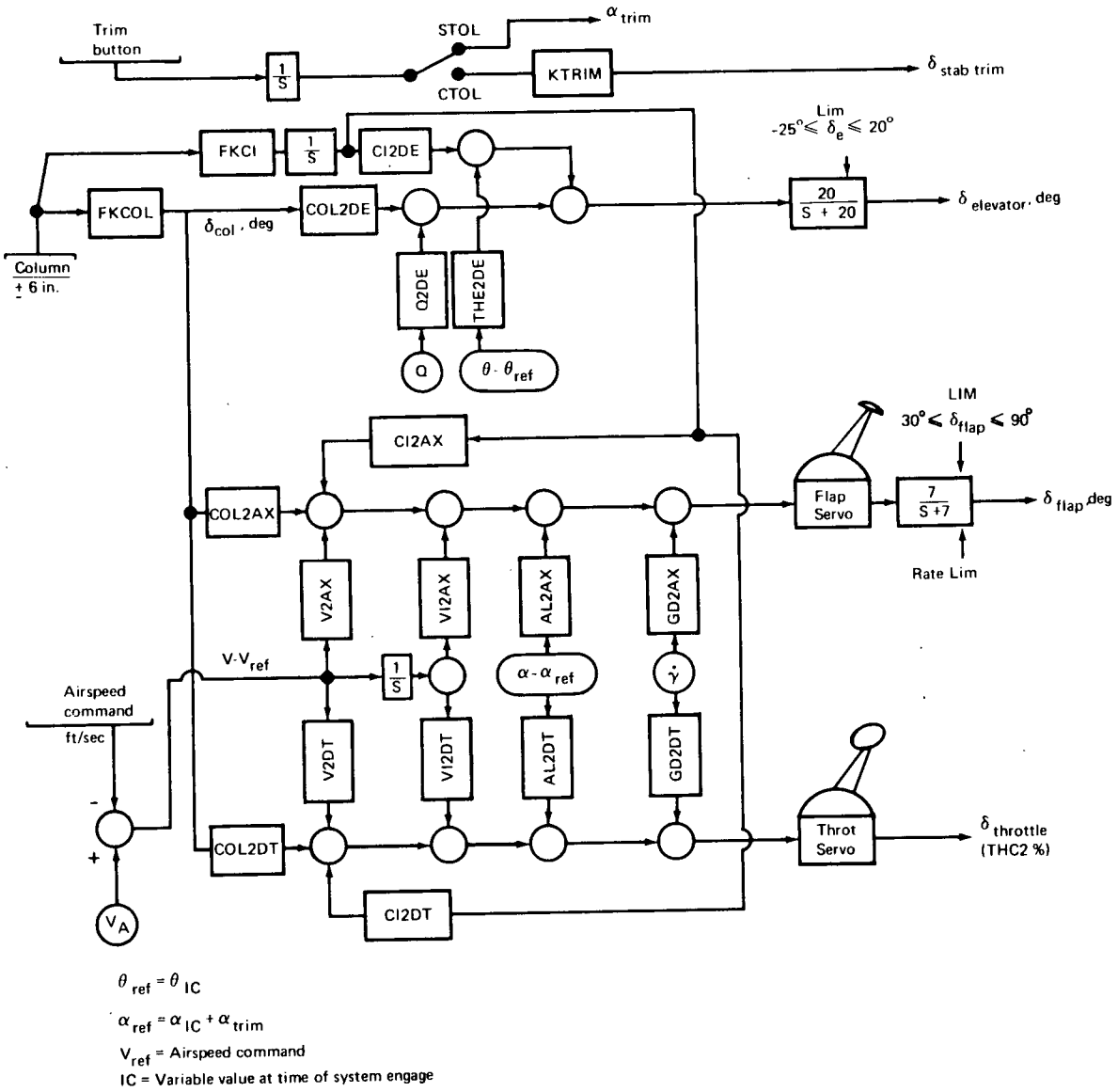


FIGURE 7.—CONTROL SYSTEM BLOCK DIAGRAM

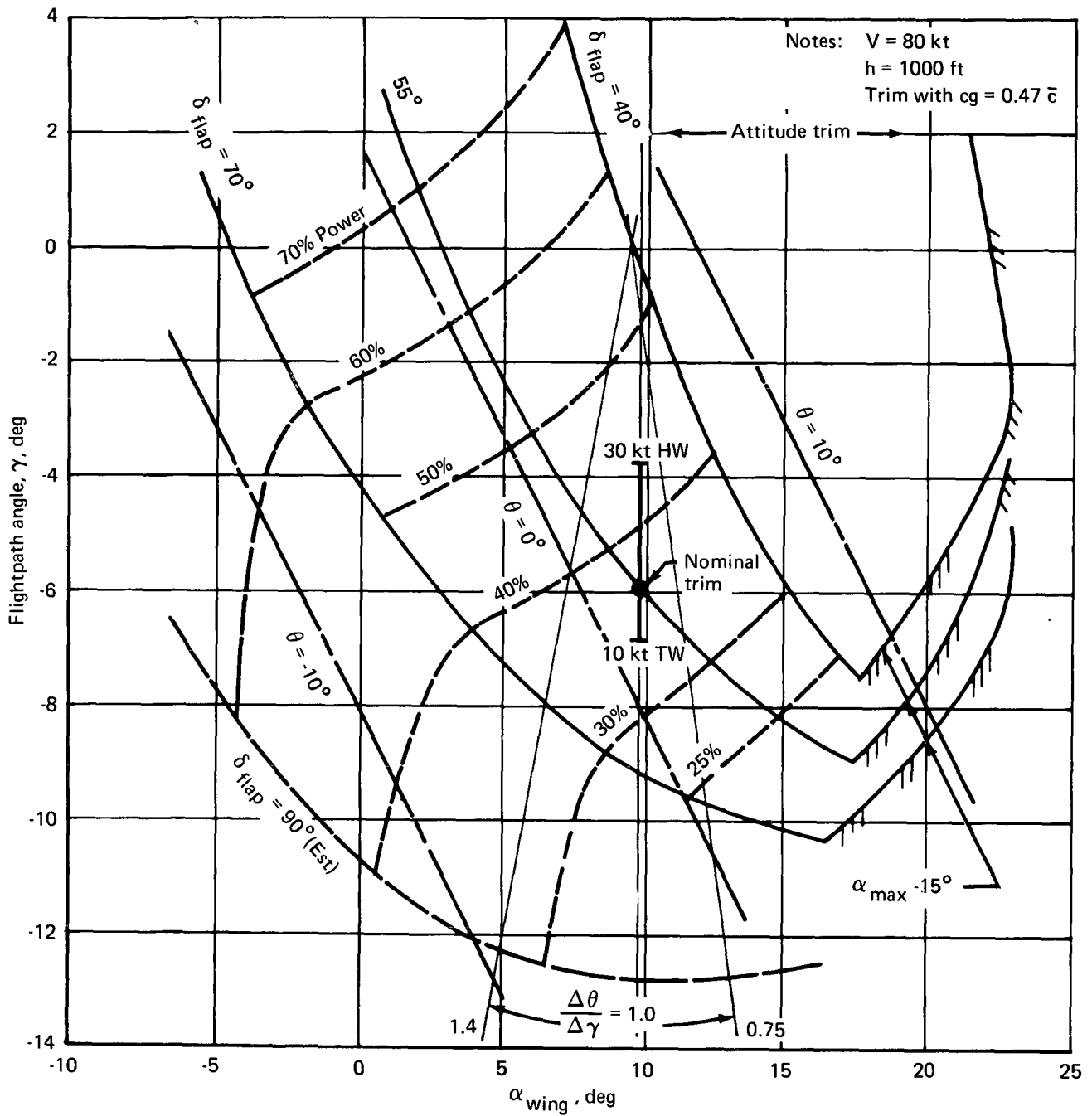


FIGURE 8.—STEADY-STATE DESIGN MAP

The design map can be used to judge the system performance in head and tail winds by noting that:

$$\gamma \cong \left(1 + \frac{V_{Ag}}{V_A}\right) \gamma_E$$

For example, figure 8 shows the range in γ corresponding to a 10-kt tailwind and 30-kt headwind with glidepath angle held at the nominal -6° value.

A key feature of the STOL flight control system is its ability to provide a fixed (and adjustable) value of steady-state pitch attitude change to flightpath angle change ratio, $\Delta\theta/\Delta\gamma$. As discussed in section 4.3.3, this parameter is of basic importance for technique 1 systems where the pilot associates pitch attitude with short-term flightpath angle changes. Figure 8 shows lines of constant $\Delta\theta/\Delta\gamma$ for the range $0.75 \leq \Delta\theta/\Delta\gamma \leq 1.4$, which is believed to bracket the range for good technique 1 handling qualities acceptance. A value of $\Delta\theta/\Delta\gamma = 1.0$ was selected for this study.

Figure 8 shows that once the trim angle of attack for level flight has been selected by the pilot, the relationship between flightpath angle, flap deflection, and power setting is uniquely defined by the control system throughout the achievable range of flightpath angles. Thus, to capture flightpath gradient the pilot simply pushes over to the desired γ (rate of descent) and then neutralizes the column. The control system captures the selected flightpath and selects the appropriate flap and power setting for $\Delta\theta/\Delta\gamma = 1.0$. The autospeed function holds speed at the selected value. Similarly, to initiate a flare or go-around, the pilot pulls on the column until the desired rate of sink or climb is achieved. All terminal maneuvers require only column and wheel inputs, which greatly reduces pilot workload.

The choice of trim angle of attack for level flight must be based on a compromise of fuselage pitch attitude balanced against maximum and minimum flightpath angles desired, and maintenance of a safe angle-of-attack margin from stall ($\alpha_{max} - 15^\circ$). The trim α_w value of 9.8° was selected for this study because it provides a realistic compromise of these factors. Flightpaths of -9° can be achieved at flaps 70 (a γ maneuver margin of over 3° steeper is available by letting flaps go to 90° in the transient). Climb capability of more than 700 ft/min is available at the engine-out (75%) power level.

The system schematic diagram (fig. 7) shows a proposed alpha trim feature that is activated when the STOL control system mode is selected. In this mode the trim button provides a bias signal that indexes the reference angle-of-attack level (α_{ref}). This arrangement seems logical because it gives the pilot direct control over the angle-of-attack margin, which is of primary importance in STOL terminal maneuvers. In the CTOL control system mode, the trim button would control

stabilizer incidence as usual. In the STOL mode, stabilizer incidence could be scheduled, along with reference pitch attitude, as a function of the airspeed select setting. This incidence programming would keep the elevator essentially faired to preserve maneuver authority.

As mentioned in section 4.2, automatic control of flap deflection with speed change is a natural function of the recommended STOL flight control system. This can be readily seen by referring to figure 5 and noting that the proposed system has attitude (θ) and flightpath (γ) hold and autospeed functions. When speed is changed at constant θ and γ , the flap deflection is automatically defined. It is important to notice that the relationship is not rigidly fixed, however. If, for example, it were desired to have some nonzero gradient of pitch attitude with speed, the pilot could select the desired gradient with the α trim. It would also be a simple matter to program the desired attitude reference bias signal as a function of autothrottle speed command setting. There are many possibilities and, regardless of the combination selected, the proposed STOL flight control system offers potential for reduced pilot workload due to automatic management of flap setting during speed-change maneuvers.

5.2.2 Signal Sensors

This section presents a possible system of aircraft motion sensors for use with the STOL control system shown in figure 7. Many possible signal sources can be conceived, particularly for a future STOL system incorporating digital terminal area navigation equipment such as STOLAND. However, this proposed sensor system uses essentially conventional signal sources. The use of INS data is desirable but probably not essential. The primary concern is to provide practical measurement and effective isolation of turbulence effects. Structural mode filtering is not considered because it is configuration oriented and beyond the scope of this study.

The STOL control system as shown in figure 7 is complete and well suited to computer representation. In translating it into flight hardware, however, certain sensor signals must be redefined because they are either mathematical variables such as $\dot{\gamma}$, which are not directly measurable, or they are sensitive to turbulence such as V_A and α and must be filtered.

Figure 9 shows a signal sensor scheme that uses conventionally measured signals and shows how these can be combined and filtered to produce the clean sensor inputs required for the figure 7 schematic. A basic consideration is the derivation of the angle-of-attack signal source. It is possible to measure this signal directly with an α vane, but this scheme is sensitive to turbulence effects and produces glideslope errors for operation with head and tail winds. As an alternative, it was decided to derive an earth-oriented glidepath angle variable, γ_E , using complementary filtered barometric altitude rate and aircraft normal acceleration signals.

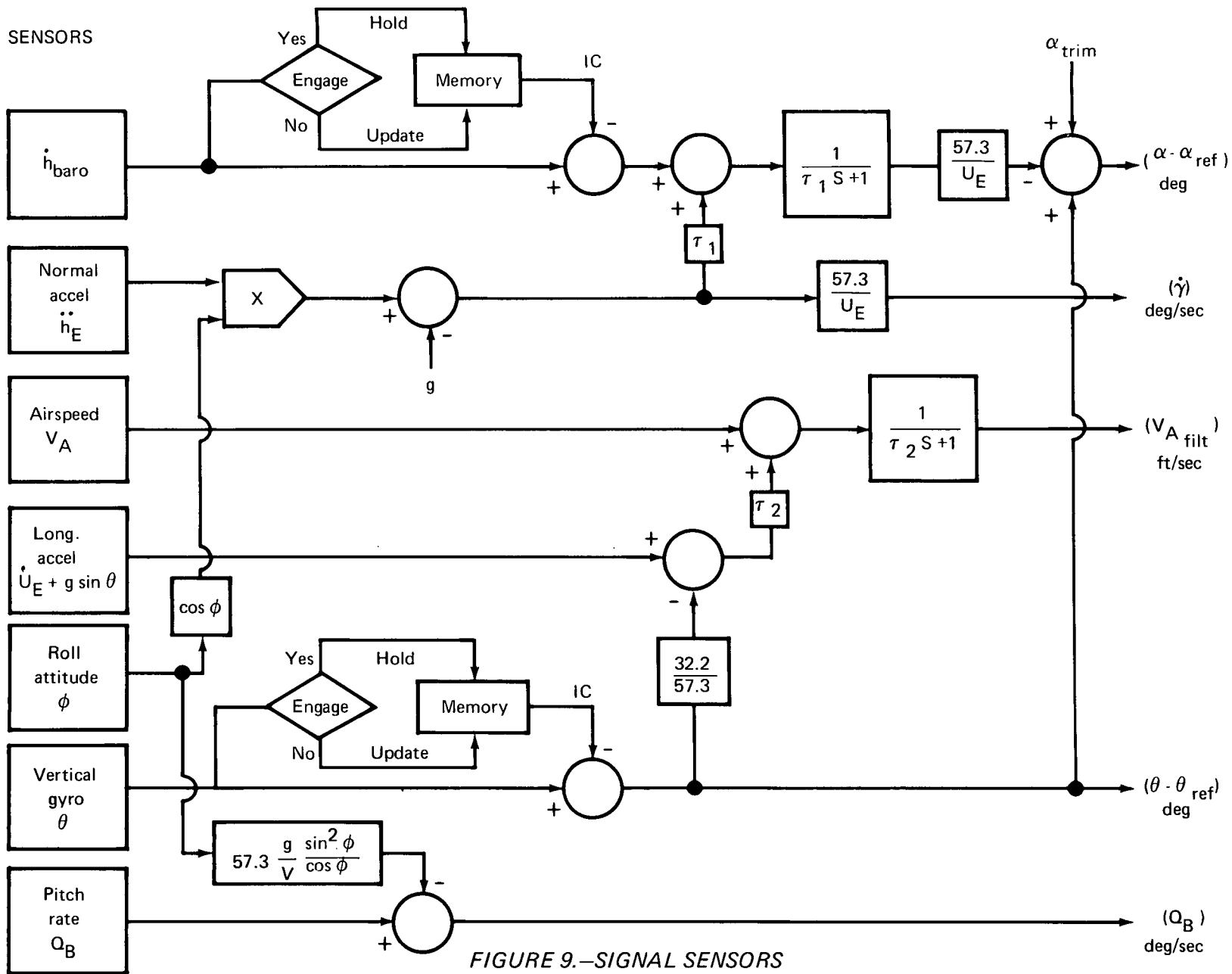


FIGURE 9.—SIGNAL SENSORS

$$\gamma_E = \frac{\dot{h}}{U_E}$$

$$\dot{\gamma}_E \cong \frac{\ddot{h}}{U_E}$$

where U_E is the earth-referenced velocity from the INS system. Complementary filtering is recommended to reduce any turbulence effects on barometric altitude rate due to static pressure fluctuations.

The effective angle of attack is then derived by:

$$(\alpha - \alpha_{\text{ref}}) = (\theta - \theta_{\text{IC}}) - (\gamma_E - \gamma_{\text{IC}}) + \alpha_{\text{trim}}$$

The initial condition circuits are also shown in figure 9. These circuits are activated when the STOL control mode is selected.

It is necessary to provide filtering of the airspeed signal, V_A , because of turbulence-related noise in the pitot and static pressure systems. The derived airspeed signal is formed by complementary filtering of the pitot system signal with the aircraft longitudinal acceleration. As shown in section 5.3.3, a filter time constant, τ_2 , of 3 to 4 sec is adequate.

The pitch attitude and pitch rate signal paths are conventional.

The signal sensor arrangement of figure 9 was simulated in this present study and was used to produce all the time responses of section 5.3. Atmospheric turbulence effects were included in the airspeed sensor signal, but were not included in the barometric altitude rate signal because reliable modeling of the static pressure disturbance was not available.

For operation in head or tail winds, the proposed sensor system causes the aircraft to maintain its glidepath (aim point) while holding constant airspeed. This is believed to be the most desirable arrangement for terminal area maneuvers.

5.2.3 Gain Path Functions

This section identifies the primary functions of the various gain paths in figure 7, and presents numerical gain values for satisfactory control of the augmentor wing aircraft presented in this document.

As outlined in section 5.2, the basic approach to the STOL control system design problem was to identify suitable feed-forward and feedback gains to provide the desired system dynamic and steady-state response. This process was accomplished by a directed trial-and-error process using time responses to controller step inputs. In general, the system is insensitive to changes in gain values and is free from difficult gain interactions, so the gain selection process proceeded rapidly.

Because system dynamics are straightforward, root locus methods were not required for synthesis of the STOL control system. The cause and method of correction for any undesirable dynamic characteristic were usually obvious (excessive autothrottle integral gain causes unacceptable loss of damping and speed overshoot, for example).

Table 3 lists the appropriate gains for the STOL control system defined in figure 7. The computer names for the gain functions have been retained because these names immediately identify the associated sensor signal and its destination within the system. Thus, THE2DE is “theta to delta elevator” and so forth. The appropriate units are also indicated in the table.

The following discussion of system gains will be based on figure 7. Referring to the top of the figure, the pitch control system is a conventional rate-command, attitude-hold circuit. The column integral feed-forward path generates the attitude command signal to null the attitude feedback signal, and the gain magnitude establishes attitude rate. The column proportional feed-forward path develops a rate signal to null the attitude rate feedback. These two paths in combination establish the net attitude rate response. The primary function of the column proportional feed-forward and pitch rate feedback circuits is to control the overshoot in pitch attitude capture.

The lower portion of figure 7 shows that the speed, angle of attack, and flightpath rate variables are all fed back to parallel flap and power paths. This synchronized use of the flap and power functions provides decoupling of the power and lift functions that characterize powered-lift STOL aerodynamics. For example, the speed feedback gains (autospeed) are proportioned to give essentially pure flightpath acceleration (C_x) in response to an airspeed error signal. The gain ratio can be developed from the aircraft C_L - C_x polar, for the condition $\Delta C_L = 0$, and is given by:

$$\frac{V2AX}{V2DT} \cong \begin{array}{c} -\frac{\partial C_L}{\partial C_J} \\ \frac{\partial C_L}{\partial \delta_{flap}} \end{array} \left| \begin{array}{l} \alpha, \delta_{flap} \\ \alpha, C_J \end{array} \right. \frac{\partial C_J}{\partial \% \text{ Throttle}}$$

The individual gain magnitudes are selected to give the desired tightness of speed control and acceptable system stability. As will be discussed in section 5.3.2, the system response to commanded speed change is rapid with negligible overshoot. Although not required for this aircraft, a speed error or power setting to elevator path could be provided for configurations with large power-induced pitching moments.

TABLE 3.—CONTROL SYSTEM GAINS

Gain	Units	Value
FKCOL	deg/in.	2.3
FKC I	$\frac{\text{deg/sec}}{(\text{in.})}$	4.1
COL2DE	deg/deg	-1.0
CI2DE	deg/deg	-1.0
Q2DE	$\frac{\text{deg}}{\text{deg/sec}}$	4.0
THE2DE	deg/deg	4.0
COL2AX	deg/deg	2.8
CI2AX	deg/deg	0.175
COL2DT	$\frac{\% \text{ Thrust}}{\text{deg}}$	12.0
CI2DT	$\frac{\% \text{ Thrust}}{\text{deg}}$	0.75
V2AX	$\frac{\text{deg}}{\text{ft/sec}}$	3.0
V2DT	$\frac{\% \text{ Thrust}}{\text{ft/sec}}$	-1.56
VI2AX	deg/ft	0.4
VI2DT	$\frac{\% \text{ Thrust}}{\text{ft}}$	-0.18
AL2AX	deg/deg	2.5
AL2DT	$\frac{\% \text{ Thrust}}{\text{deg}}$	11.2
CD2AX	$\frac{\text{deg}}{\text{deg/sec}}$	-3.4
CD2DT	$\frac{\% \text{ Thrust}}{\text{deg/sec}}$	-14.0

Similarly, the gain ratios for the angle of attack and flightpath rate functions are chosen to give essentially vertical (ΔC_L) response to these error signals.

The primary function of the angle of attack (α) and flightpath rate ($\dot{\gamma}$) feedback paths is to provide the γ control wheel steering (γ CWS) mode of operation (α and θ hold is equivalent to flightpath hold). The $\dot{\gamma}$ feedback path basically controls the overshoot of flightpath angle capture. This effect is demonstrated in figure 10, which shows the time response to a 1-in. column step for various combinations of α and $\dot{\gamma}$ feedback. For all cases shown, the basic paths (θ , Q, V feedback and column feed forward) are held at the optimum values defined in table 3.

Figure 10 shows the crisp capture characteristics of the full CWS system. It is interesting to note that with the α and $\dot{\gamma}$ feedback paths open, system response is poor but possibly acceptable. This configuration might represent an acceptable state of partial system failure.

The angle-of-attack feedback also controls the droop in speed command maneuvers.

The column proportional feed-forward gains (COL2AX, COL2DT) shown in figure 7 provide adjustment of the load factor response time constant, τ_{N_z} . The following table illustrates the range of responses that can be obtained.

COL2AX	COL2DT	τ_{N_z} , sec
0	0	2.5
2.1	9	1.2
2.8	12	0.3

In this table, the equivalent load factor response time constant, τ_{N_z} , is defined as the time required for the load factor to reach 63% of its peak value following a column step input. Values less than 1.0 sec are considered to be required for good technique 1 system operation.

The column integral feed-forward paths (CI2AX, CI2DT) in figure 7 provide direct control over the steady-state $\Delta\theta/\Delta\gamma$ ratio. The following table shows the range of responses that can be developed.

CI2AX	CI2DT	$(\Delta\theta/\Delta\gamma)_{SS}$
0	0	1.4
0.175	0.75	1.0
0.35	1.5	0.79
0.7	3.0	0.6

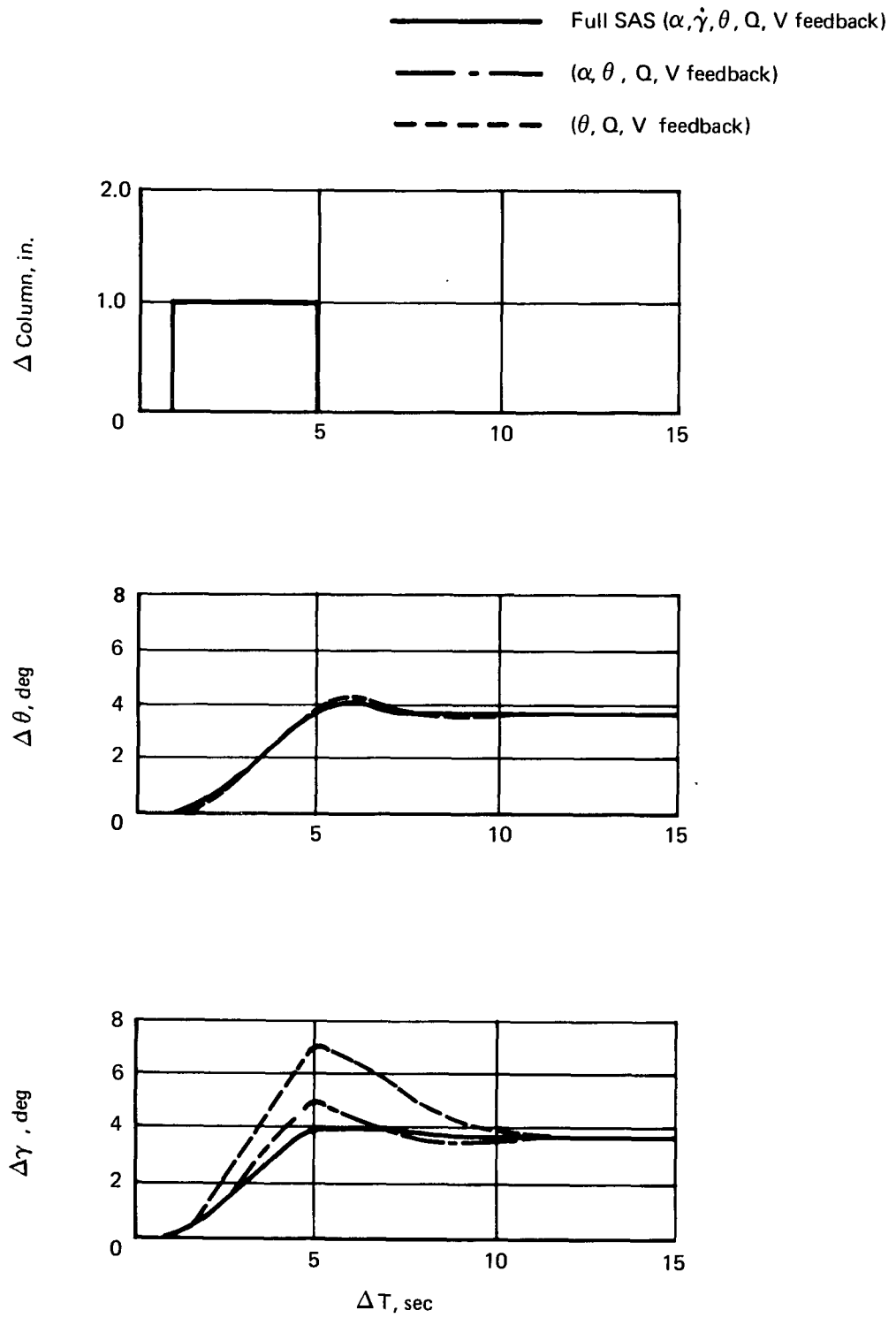


FIGURE 10.—EFFECT OF α AND $\dot{\gamma}$ FEEDBACK

It should be noted that the steady-state ratio is basically fixed by the V2AX and V2DT velocity gains, which are dictated by autothrottle performance considerations. The CI2AX and CI2DT gain paths are added to provide direct control of $(\Delta\theta/\Delta\gamma)_{SS}$. The angle-of-attack feedback paths AL2AX and AL2DT do not directly influence $(\Delta\theta/\Delta\gamma)_{SS}$. They do, however, force it toward unity and reduce the effect of data nonlinearities and external disturbances.

The basic column feed-forward gains, FKCI and FKCOL, establish the column sensitivity. For the reference 6 study, a nominal value of 0.1 g/in. was selected for the 80-kt approach condition.

The STOL control system is generally insensitive to gain levels and aerodynamic data nonlinearities. Gain scheduling was not required over the range of flightpath angles $-12^\circ \leq \gamma \leq 8^\circ$ and approach speeds of 80 to 90 kt considered in this study.

5.3 SYSTEM PERFORMANCE

The performance of the STOL flight control system is demonstrated. It is shown that the response of the augmented aircraft is well damped and essentially decoupled with respect to power-lift effects. The column provides effective control over attitude and load factor for technique 1 control, and a tight autospeed function is provided to mask the effect of operation on the back side of the drag curve. The system provides compliance with the design criteria presented in this section. This STOL control system was rated good by the pilots for all terminal flight phases in the reference 6 simulation study, as summarized in table 2.

The results of flightpath capture and tracking maneuvers in turbulence using a pilot model show that the rate capability of the active-flap system must be approximately 15 deg/sec. The accompanying dynamic response characteristics of existing turbojet engines appear to be adequate for this control system concept.

The proposed STOL control system provides good flare and go-around capability in which only column inputs are required by the pilot.

The flightpath capability of the STOL control system is limited only by the basic aerodynamic L/D characteristics of the associated airplane.

5.3.1 Criteria

The following criteria will be used as a guide to demonstrate the general acceptability of the proposed STOL control system. The list is not intended to be exhaustive. Basically, it contains

items that reflect important control-related factors such as management of power and flaps in maneuvers to provide load factor capability and maintain stall angle margin. The integrity of the basic aerodynamic design is not of direct interest in this study.

1. Flightpath Control

Starting in level flight, it shall be possible, without encountering stall, to capture a flightpath 2° steeper than the desired flightpath. For a system with an autothrottle function, it will be assumed that the speed command is correctly set and the speed error shall be equal to the system droop.

For this study configuration, the steepest contemplated flightpath, including an increment of 2° steeper for maneuver margin (ref. 11), will be assumed to correspond to $\delta_{\text{flap}} \leq 70^\circ$. Any additional flap capability, $70^\circ \leq \delta_{\text{flap}} \leq 90^\circ$, will provide additional margin for the transient effects of turbulence. Maintenance of proper stall margins will be demonstrated by recording the appropriate C_L and α values.

2. Load Factor Capability

- a. The maximum load factor available from a maximum effort column input shall be greater than 0.5 g.
- b. The equivalent load factor time constant in response to a column step input, τ_{N_z} , shall be approximately 1.0 sec or less.

3. Margin From Stall

- a. At all trim points, the angle of attack shall be at least 15° less than the maximum for that particular power setting, $\alpha \leq (\alpha_{\text{max}} - 15^\circ)$. This is to provide protection for 20-kt vertical gusts at 80-kt approach speed.
- b. During maneuvers, the peak transient angle of attack shall be at least 7° less than the maximum available at the instantaneous power setting.

4. Go-Around

The altitude loss following a go-around control input from the final segment glideslope (-6°) shall be less than 50 ft.

5. Flare

Starting from a flare height of 50 ft (cg height), it shall be possible to flare to less than 300 ft/min touchdown using a peak load factor of 0.2 g. Ground effects shall be included.

The combination of 50-ft flare height and 0.2 g load factor was derived from the results of the reference 6 study.

6. Speed Margin (ref. 11)

$$V_{app} \geq 1.15 V_{min}$$

This is basically a SAS-off margin, but is included in this study to serve as a point of reference and to show compatibility with reversion to SAS-off operation.

5.3.2 Response to Speed and Column Commands

Figure 11 shows the response of the augmented aircraft to speed and column commands. The aircraft is initially trimmed in level flight at 80 kt with a 40° initial flap deflection and a trim wing angle of attack $\alpha_{w_0} = 9.8^\circ$ ($\alpha_{F_0} = 7.8^\circ$).

The first run on figure 11 shows the response to a 10-kt speed step command. The speed response is fast and precise. The pitch attitude (θ) and flightpath angle (γ) traces are essentially constant throughout the maneuver, showing the effective decoupling achieved by the STOL control system. The engine output thrust trace shows the initial thrust increase required to accelerate to higher speed and the reduced steady-state level that typifies operation on the back side of the drag curve. The flap deflection trace shows how the flaps automatically deflect to maintain essentially constant load factor level. The stall margin is essentially constant throughout the maneuver.

The second trace on figure 11 shows the response to a 1-in. column pushover and release maneuver with a 5-sec duration. The pitch attitude and flightpath angle traces show the crispness with which the control system captures and holds the selected flightpath angle, and the accuracy with which $\Delta\theta/\Delta\gamma = 1.0$ is held for the duration of the maneuver. The speed trace reflects tight speed control during this constant-speed maneuver. The power and flap deflection traces show the automatic synchronized adjustment of these parameters that is predicted by the system design map (fig. 8) for $\Delta\theta/\Delta\gamma = 1.0$. The stall margins remain essentially constant throughout the maneuver, which is typical of this system. The load factor trace is crisp, reflecting the rapid load factor buildup $\tau_{N_z} \ll 1.0$ sec. Column sensitivity is 0.1 g/in. Criteria 2a and 2b are satisfied.

Notes: $V = 80$ kt
 $\gamma_0 = 0$
 $\delta_{flap} = 40^\circ$
 $cg = 0.47 \bar{c}$

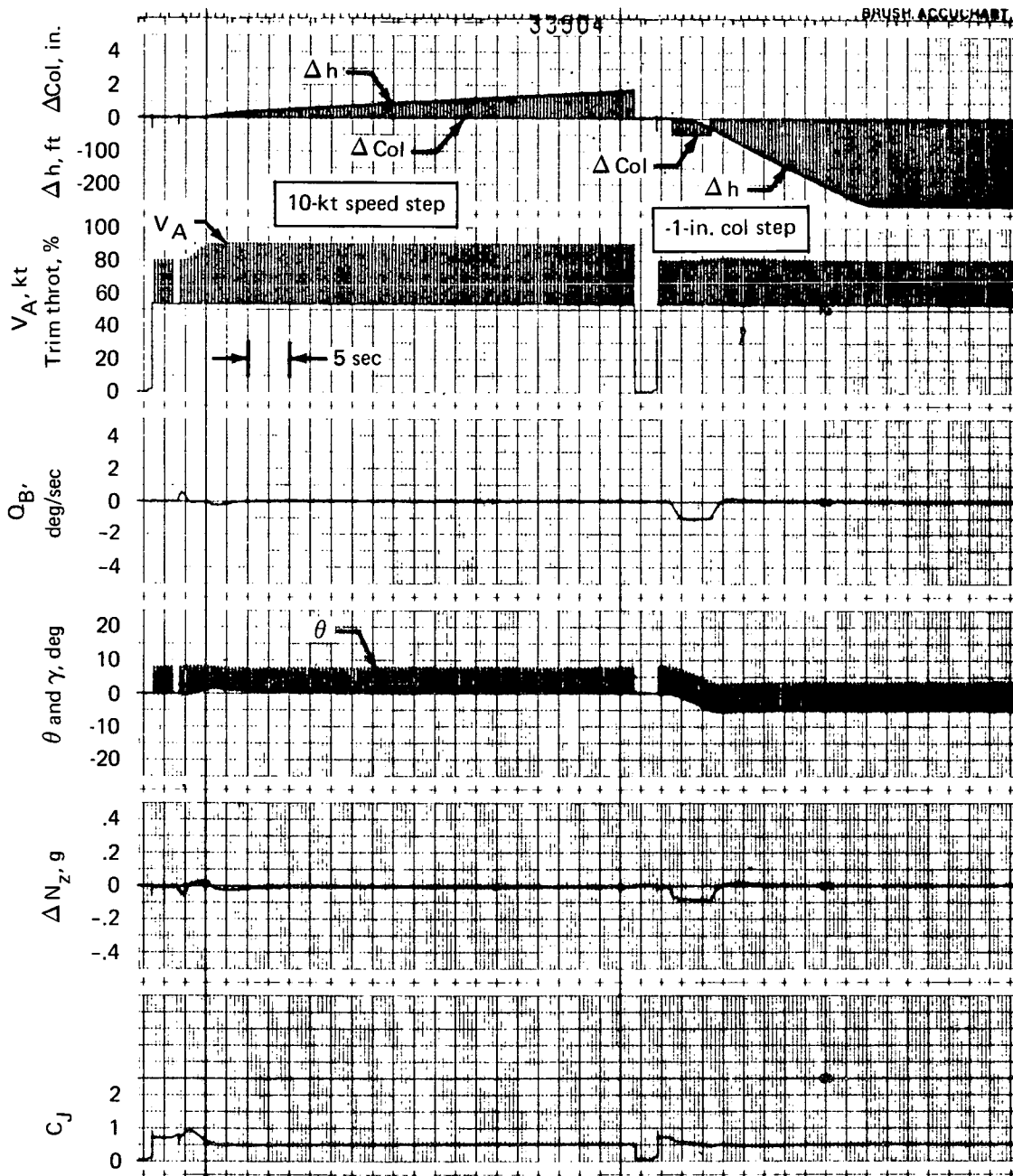


FIGURE 11.—RESPONSE OF FULLY AUGMENTED AIRPLANE

Notes: $V = 80$ kt
 $\gamma_o = 0$
 $\delta_{flap} = 40^\circ$
 $cg = 0.47 \bar{c}$

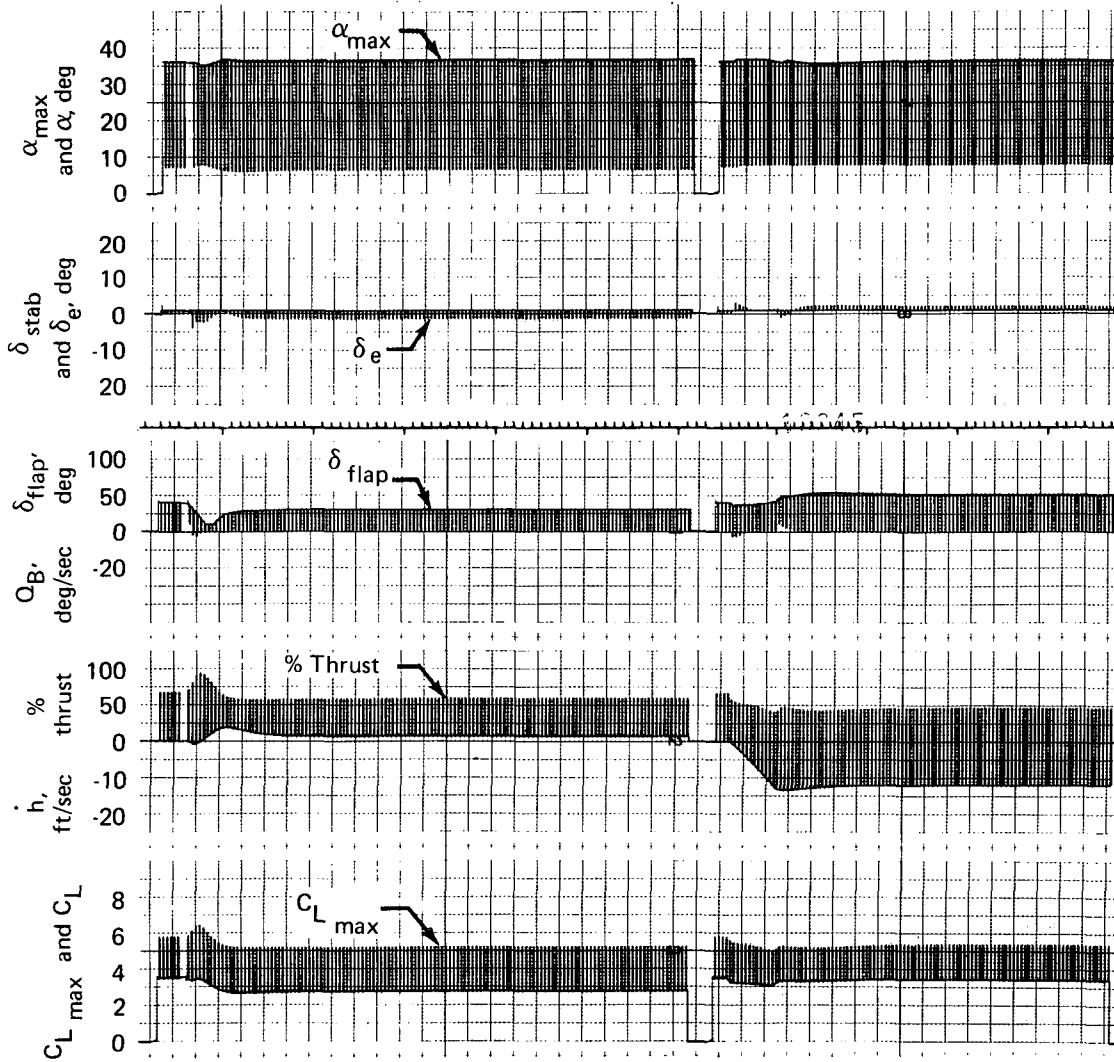


FIGURE 11.—CONCLUDED

It can be seen that the STOL control system produces essential decoupling of power and lift-change functions and ensures that all aircraft motions are well damped. It restores the basic attitude and altitude change function to the column and provides a tight autospeed function to mask the effect of operation on the back side of the drag curve.

The speed-change response of figure 11 (first run) shows essentially constant pitch attitude with a 10-kt commanded speed increase from 80 to 90 kt. It can be seen that the flaps automatically retract from 40° to 30° during the maneuver, which is predicted by figure 5. Thus, automatic flap management with speed change is an inherent feature of this STOL control system, as discussed in section 5.2.1. If something other than zero pitch attitude gradient with speed were desired, it is a simple matter to program a pitch attitude command signal as a function of speed command setting.

The small load factor disturbance shown in the first trace of figure 11 is the result of the step speed command. For more realistic speed ramp inputs, this load factor disturbance disappears.

5.3.3 Flightpath Capture and Track

An essential aspect of this STOL control system evaluation was to judge system performance under conditions of closed-loop operation in turbulence. To achieve this goal, a pilot model was developed to capture and track arbitrary glidepaths constructed of linear segments and angles. This pilot model is described in block diagram form in the appendix. Basically, the model consists of a series of logic blocks that are progressively selected by appropriate gate functions that determine aircraft position with respect to the desired path.

Figure 12 shows a series of flightpath responses with the pilot model tracking a simple flightpath profile consisting of an initial altitude hold segment at 1000-ft altitude, followed by capture and track of a -6° flightpath. The turbulence level is $\sigma_u = \sigma_w = 7$ ft/sec and the approach speed is 80 kt. As can be seen from the response envelope, the pilot model provides tight capture and tracking in this severe turbulence environment. Steady winds were not represented in the simulation.

A typical run is initiated with the model holding constant altitude by feeding back altitude error plus rate into the column. Speed is held by the control system autospeed function.

When the aircraft comes within a predetermined distance of the -6° flightpath, the logic gates switch to a -1 deg/sec pushover maneuver, which is held for 4.5 sec, bringing the aircraft into proximity with the -6° flightpath.

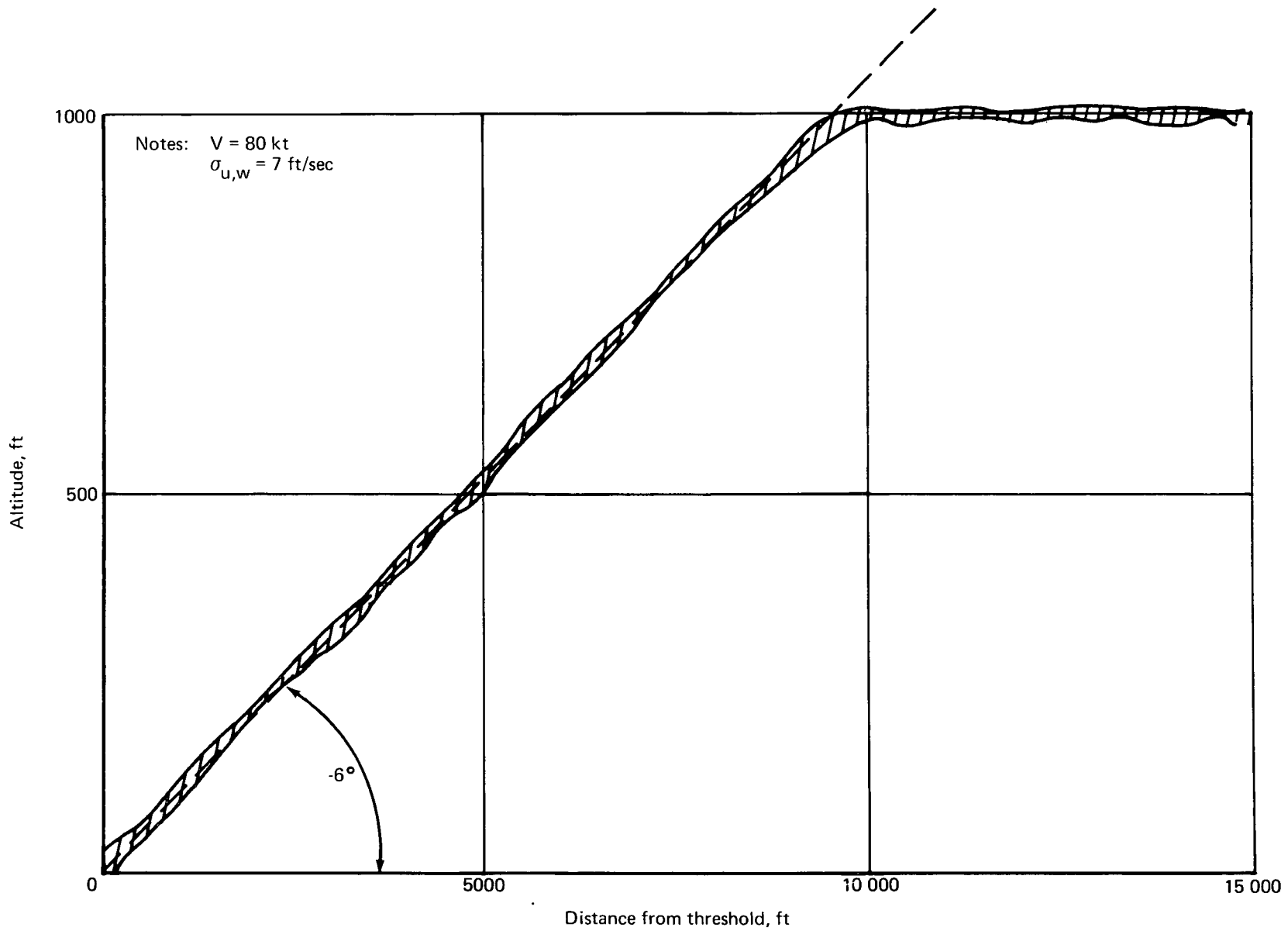


FIGURE 12.—GLIDESLOPE CAPTURE AND TRACKING PROFILE

Following this, the logic gates select a second track mode in which altitude error plus biased rate from the desired flightpath are fed back to the column. This mode is held until ground contact, at which time the computation is automatically ended. The flare is not represented.

Figure 13 shows a time history of a typical flightpath capture and track maneuver that illustrates the feature just discussed. It is emphasized that the RMS 7 ft/sec turbulence level used in this study is believed to be a severe level. The altitude hold, flightpath capture, and flightpath track phases of the maneuver can easily be identified from the Δ column and Δ h traces at the top of the figure.

The performance of the control system in this severe turbulence environment can be judged by referring to the attitude (θ), flightpath angle (γ), and airspeed traces. Tight control is maintained at all times during the maneuver. It should be noted that the flap deflection, engine thrust, and elevator deflection traces do not contain high-frequency turbulence components. This is due to natural filtering effects of the airframe plus additional complementary sensor filtering, as discussed in section 5.2.2. Throughout the maneuver, adequate stall (α and C_L) margins are maintained and criterion 3b is satisfied.

Figure 14 shows a comparison of the normal load factor traces for the augmented and SAS-off conditions for level flight in RMS 7 ft/sec turbulence. The RMS load factor levels computed for the run duration are also noted. It is apparent that the STOL control system attenuates the normal load factor response to turbulence at the lower frequencies. The high-frequency components are equal since the flaps and engines are not allowed to respond at higher frequencies. Thus, the STOL control system offers significant ride qualities improvement over the unaugmented configuration.

A study was conducted, using the flightpath capture and tracking model, to determine the critical flap system rate requirement and the time constant required for the complementary filter in the autothrottle speed circuit. In this study, four strips of random turbulence were selected that had computed RMS levels, over the problem duration, essentially equal to the reference level of 7 ft/sec. These four strips were indexed so that they could be repeated sequentially, with every fifth run repeating the sequence. In running these parametric studies, each configuration was subjected to the same four random turbulence strips. This precaution was taken to ensure that the studies were not biased in some unknown manner by the nonhomogeneous nature of the random turbulence field. Throughout these studies, the engine dynamic response was representative of a modern turbojet. The engine model response is given in the appendix.

Figure 15 shows the results of a series of flightpath tracking runs in which the flap system rate limit was progressively reduced from 30 to 5 deg/sec. Key flightpath and system parameters were monitored, and RMS values were computed during the run duration. These key RMS parameters include:

Notes: $V = 80$ kt
 $cg = 0.47 \bar{c}$
 $\sigma_u = \sigma_w = 7$ ft/sec
 $h_o = 1000$ ft

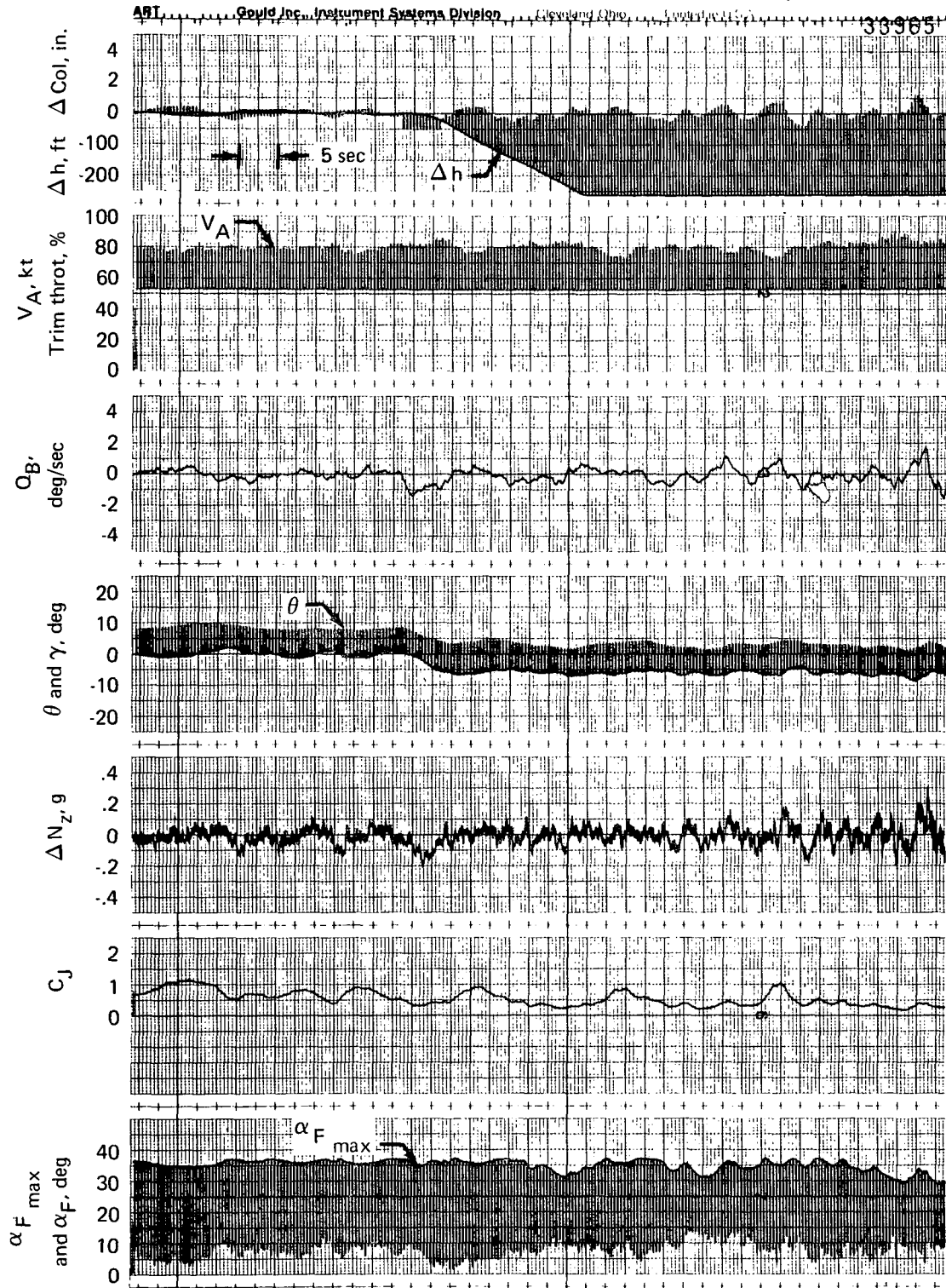


FIGURE 13.—GLIDESLOPE TRACKING IN TURBULENCE



Notes: $V = 80$ kt
 $cg = 0.47 \bar{c}$
 $\sigma_u = \sigma_w = 7$ ft/sec
 $h_o = 1000$ ft

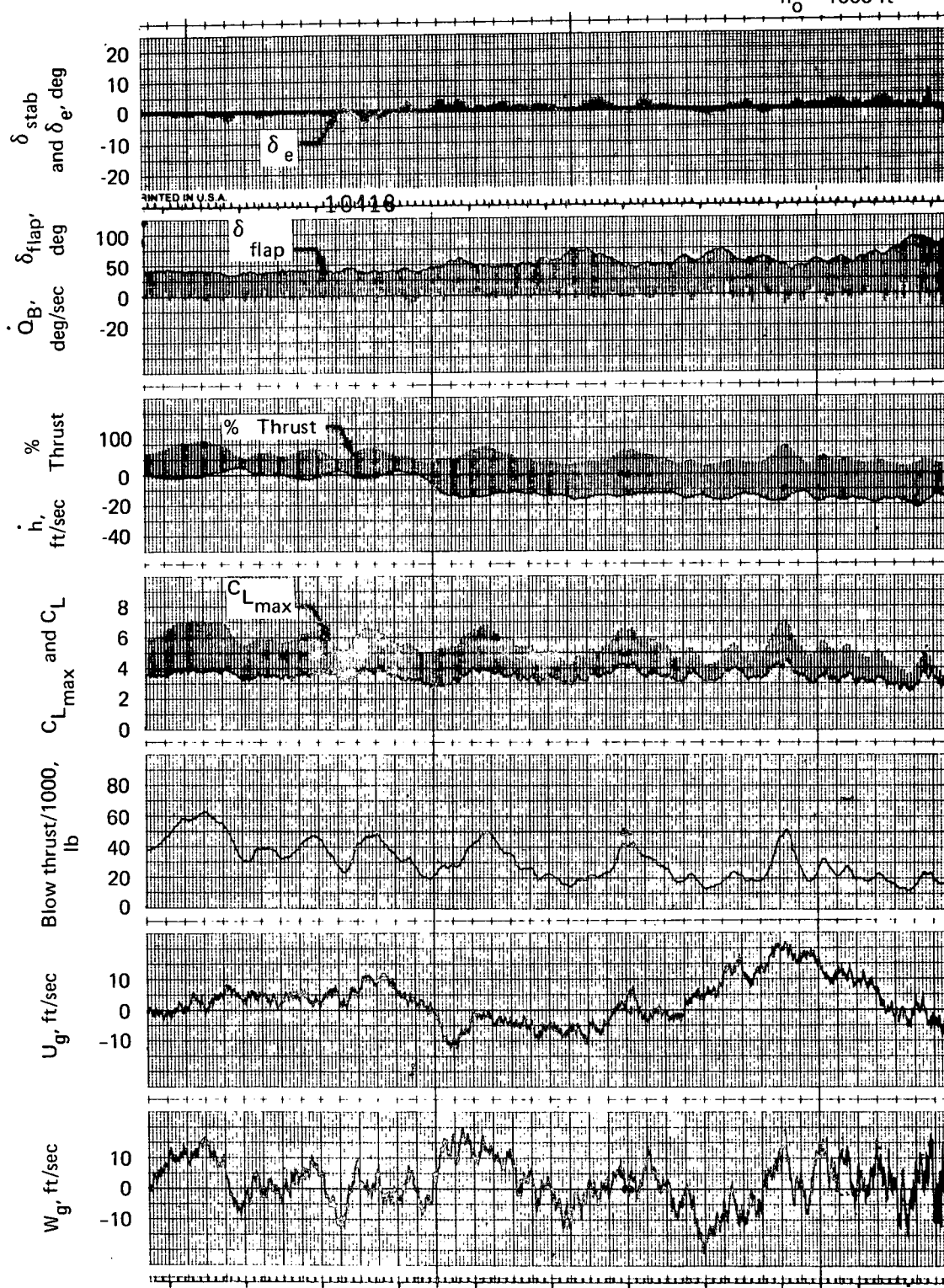


FIGURE 13.—CONCLUDED

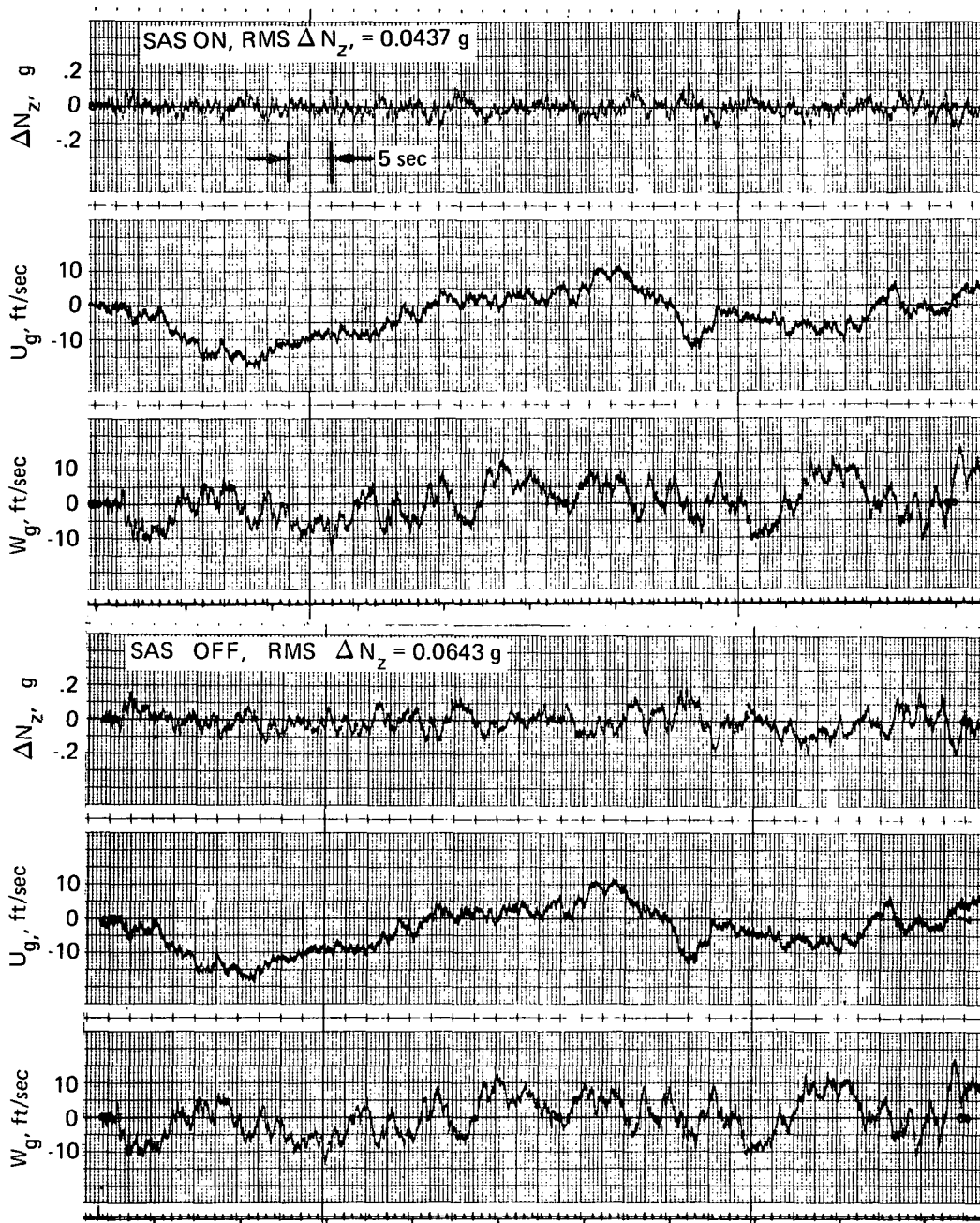


FIGURE 14.—EFFECT OF SAS ON TURBULENCE RESPONSE

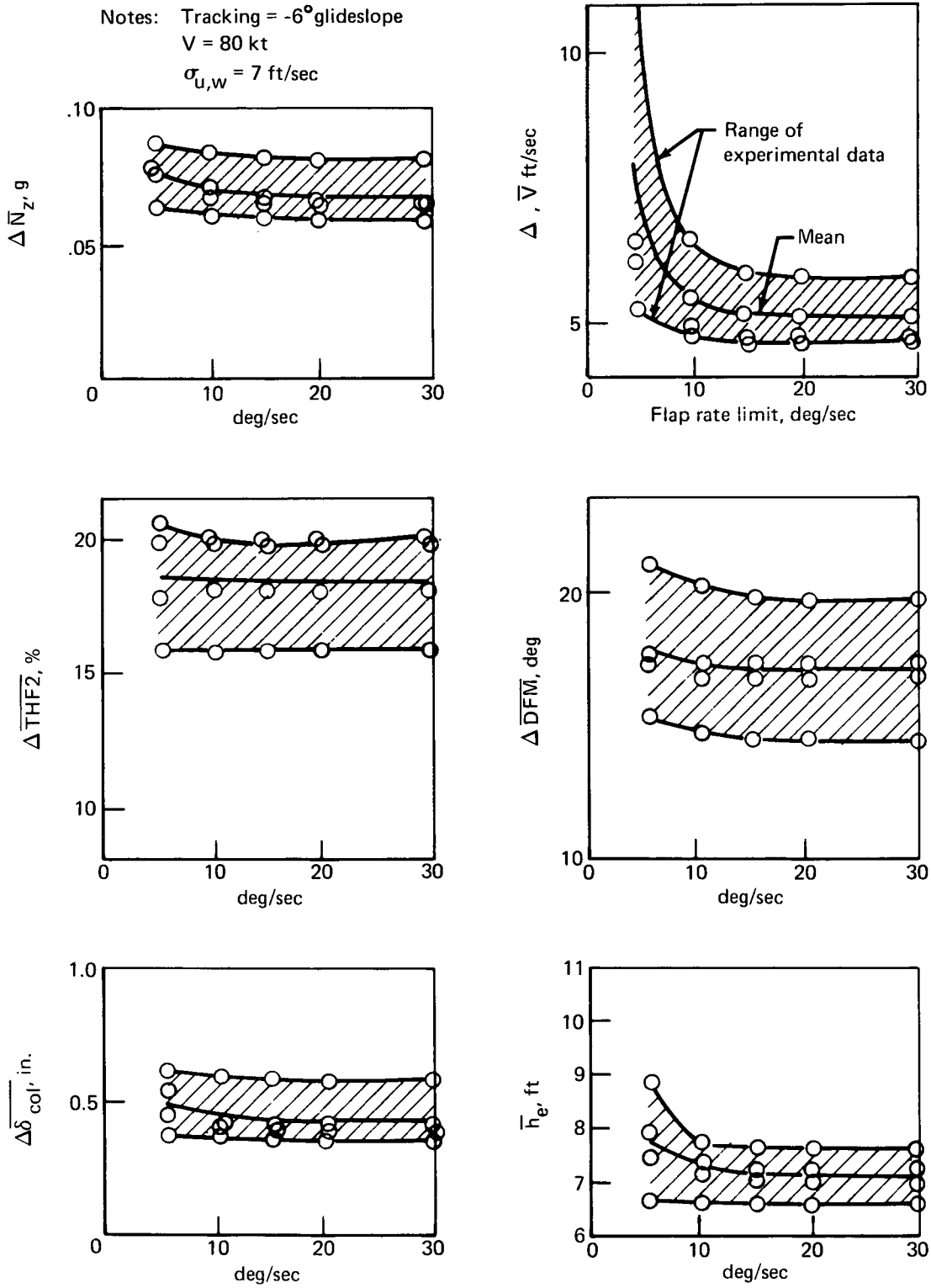


FIGURE 15.—EFFECT OF FLAP RATE LIMIT ON GLIDESLOPE TRACKING

Normal load factor (\overline{N}_z)

Airspeed error ($\Delta \overline{V}$)

Engine thrust deviation ($\Delta \overline{THF}_2$)

Flap activity ($\Delta \overline{DFM}$)

Column activity ($\Delta \overline{\delta}_{col}$)

Glideslope error (\overline{h}_e)

The figure shows the points for each of the four turbulence strips. The solid curve is an average trend faired through the centroid of these points. It can be seen that a flap system rate limit of 15 deg/sec should provide adequate system performance. This result is compatible with flap rates observed during the reference 6 piloted work.

Figure 16 shows a similar study to determine the critical time constant for the complementary filter, τ_2 , in the autothrottle speed circuit. It appears that a value of 3 to 4 sec is adequate.

As explained in section 5.2.2, the effect of atmospheric turbulence was not represented in the barometric altitude rate signal. It is assumed that a value of 3 to 4 sec for the filter time constant, τ_1 , would be a reasonable value, however.

5.3.4 Flare and Go-Around

Figure 17 shows time histories of flare and go-around maneuvers. These maneuvers were flown from the strip recorders using a sidearm controller that was interfaced with the computer through appropriate digital-to-analog conversion. In performing these maneuvers, the airplane was initially trimmed in level flight at 200-ft altitude and 80-kt airspeed. The aircraft was then pushed over to capture a -6° flightpath. When the 50-ft flare altitude was reached, an aft column input was made until the desired touchdown sink rate of approximately 3 ft/sec was achieved. The aircraft was then flown to touchdown at this sink rate. The effect of ground proximity on lift, drag, and pitching moment is included in this simulation. The reduction in maximum angle of attack (α_{max}) and lift coefficient ($C_{L_{max}}$) due to ground proximity can be clearly seen in figure 17. The method of ground effect representation is outlined in the appendix.

The first run on figure 17 shows a 0.1 g flare initiated at an altitude of 50 ft. At the point of flare initiation, the sink rate is approximately 15 ft/sec (900 ft/min). This sink rate is quickly arrested, and touchdown occurs at the desired 3 ft/sec.

Notes: Tracking = -6° glideslope
 $V = 80$ kt
 $\sigma_{u, w} = 7$ ft/sec
 Flap rate lim = 15 deg/sec

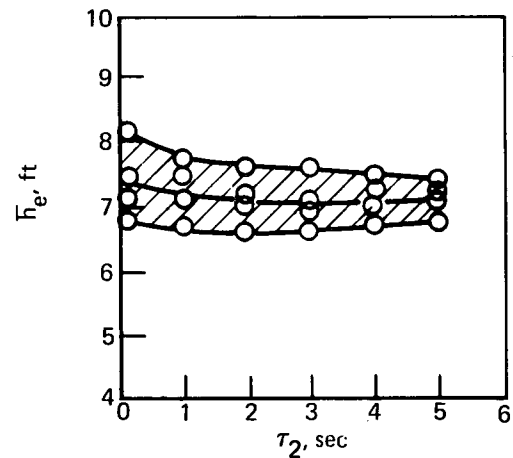
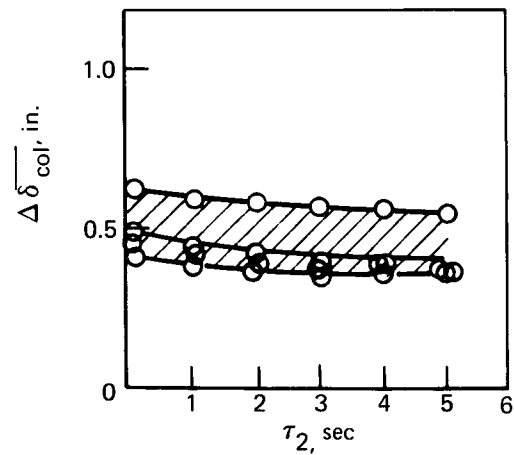
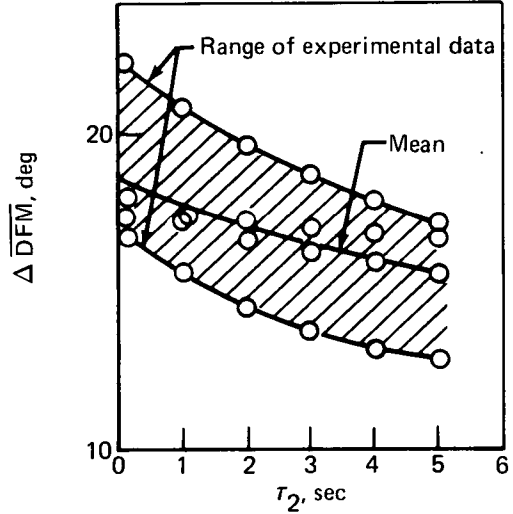
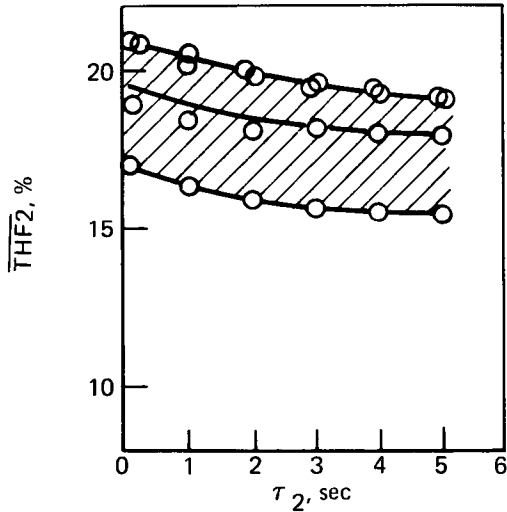
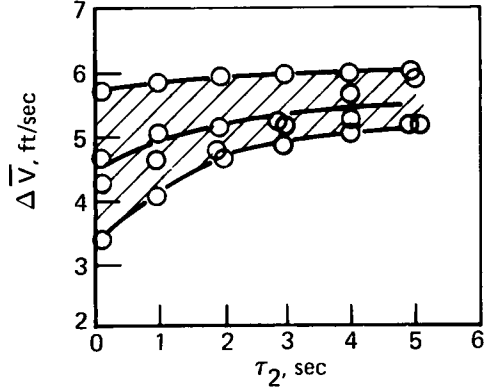
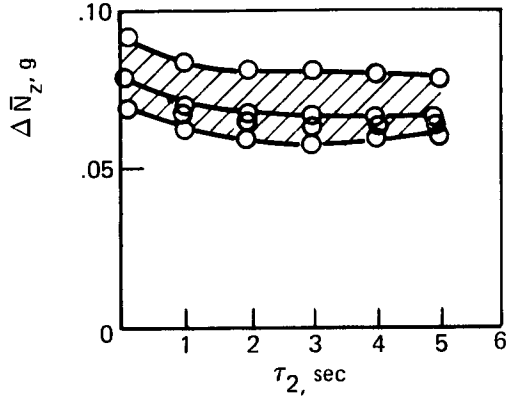
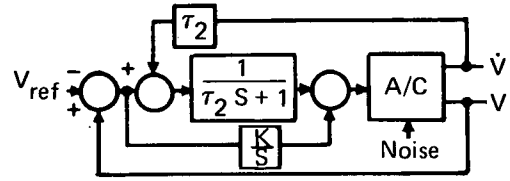


FIGURE 16.—EFFECT OF AUTOTHROTTLE FILTER ON GLIDESLOPE TRACKING

Notes: $V = 80$ kt
 $\gamma_o = 0$
 $\delta_{flap} = 40^\circ$
 $cg = 0.47 \bar{c}$
 $h_o = 200$ ft

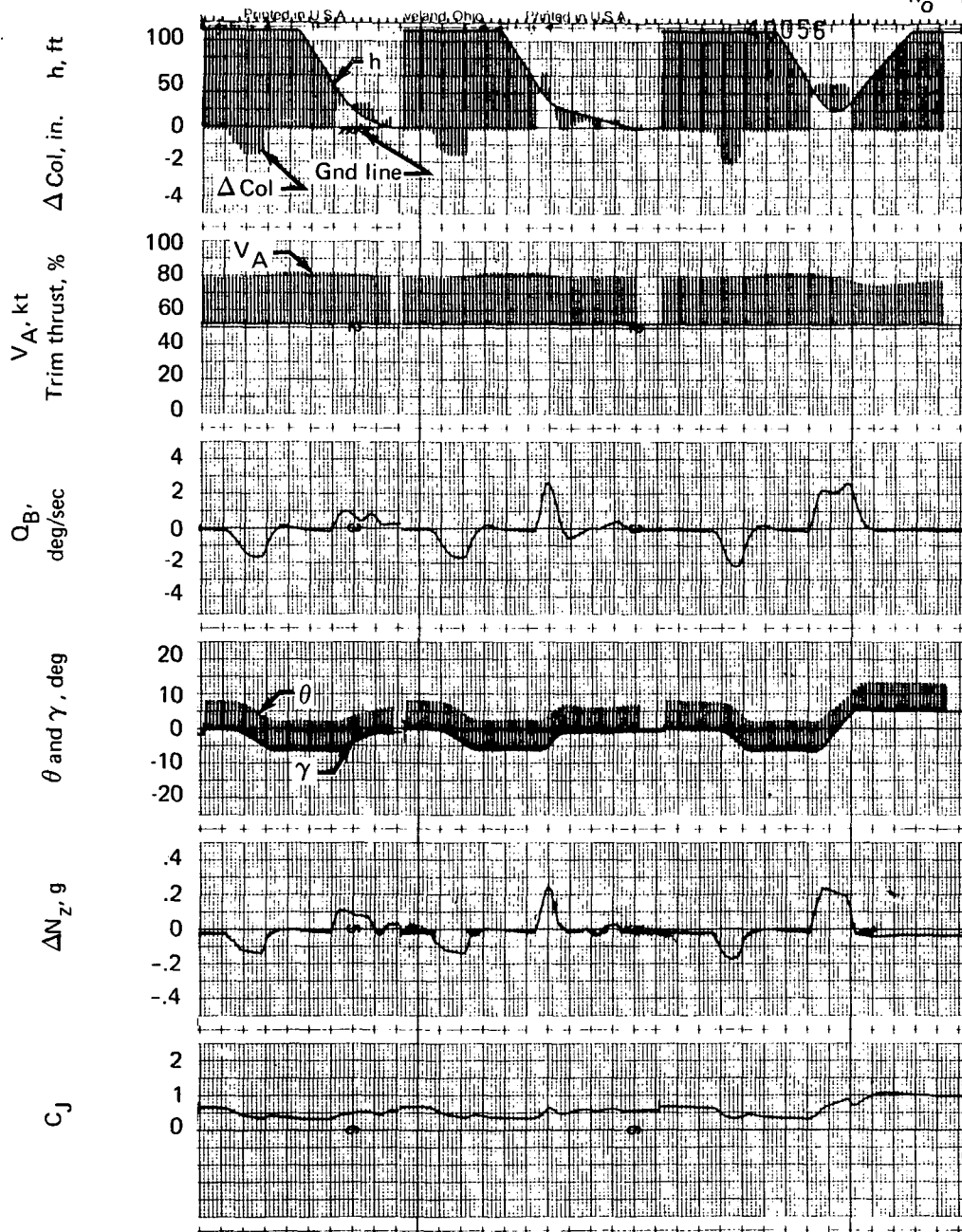


FIGURE 17.—FLARE AND GO-AROUND MANEUVERS

Notes: $V = 80$ kt
 $\gamma_o = 0$
 $\delta_{flap} = 40^\circ$
 $cg = 0.47 \bar{c}$
 $h_o = 200$ ft

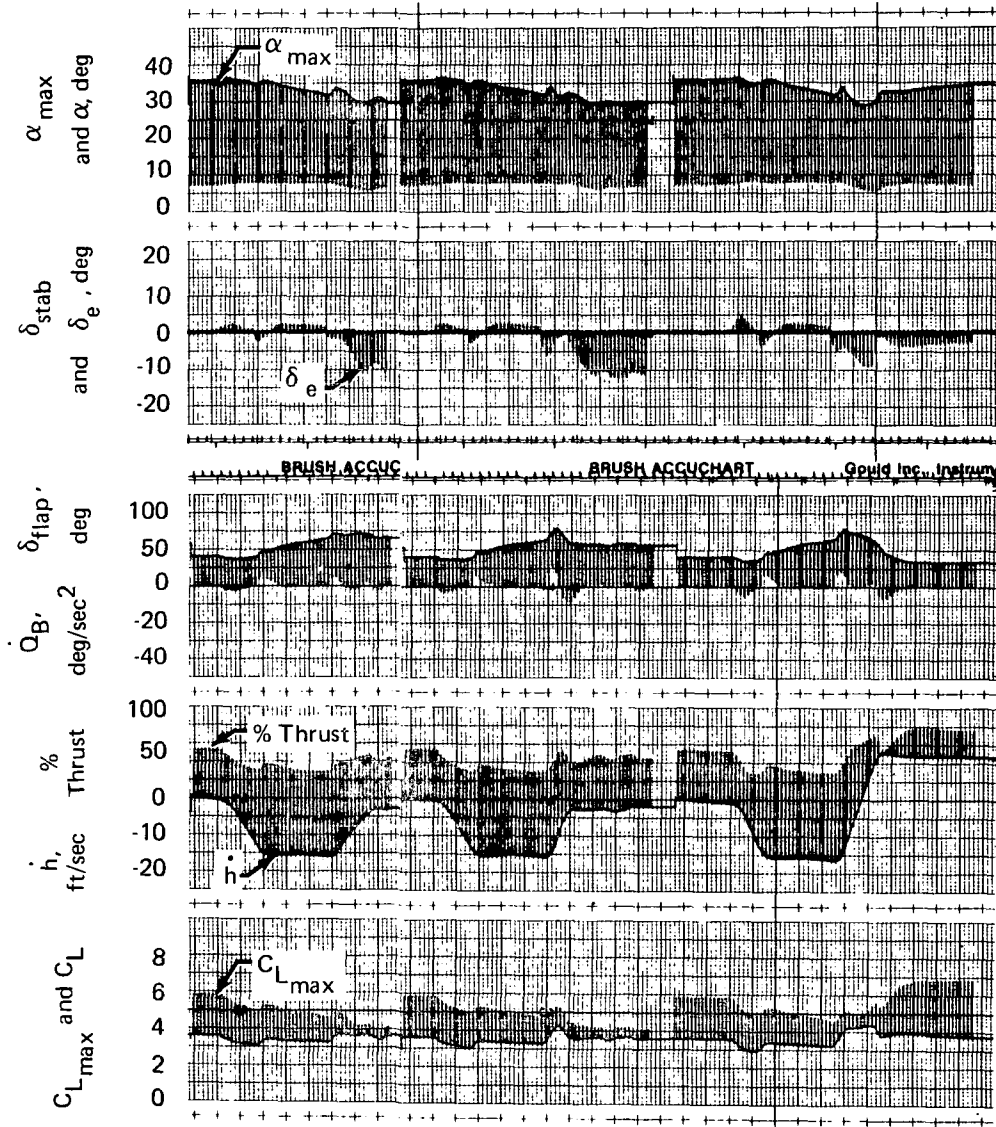


FIGURE 17.—CONCLUDED

The second trace on figure 17 shows the same flare maneuver performed at a 0.2 g pullup load factor level. Again the flare and touchdown are satisfactory, requiring only simple column inputs. It should be noted that adequate stall margins are maintained throughout the duration of these maneuvers. In the reference 6 study, the pilots rated the flare characteristics of this system in the “good” category, as noted in table 2A.

These 0.1 and 0.2 g flare maneuvers produce air distances that bracket the requirements for 2000-ft field length.

As is characteristic of this STOL control system, the power increases that accompany pullup maneuvers also produce increased lift capability (a characteristic of powered-lift aerodynamics), and stall margins are maintained throughout all maneuvers. Criteria 3 and 5 are satisfied.

The third trace on figure 17 shows a go-around maneuver initiated from the 500-ft flare height. Even from this low altitude (chosen for convenience), a successful go-around is easily made with column input alone. The altitude loss is approximately 30 ft, and adequate stall margins are maintained throughout the maneuver. Criteria 3 and 5 of section 5.3.1 are satisfied.

Figure 17 also shows how the STOL control system automatically retracts the flaps to approximately 35° and advances power to 80% during the go-around. This same system operation would occur in the case of an engine-out go-around except that the maximum power available would be limited to 75% and there would be a drag penalty due to lateral-directional trim. The control concept is compatible with the engine-out situation, however, and achievement of an adequate climb rate is simply a conventional matter of proper engine sizing.

5.3.5 Steep Path Capability

During this study, a variety of methods were considered for increasing the negative flightpath capability of the aircraft. These methods included hot thrust vectoring to 90°, hot thrust spoiling, and addition of a drag increment to the aircraft. This latter effect might represent induced drag increase due to stepped flap deflection and tapered blowing similar to the “transparency” effect of the Breguet 940 (ref. 3). These methods were all successful and were automated in several ways, including:

- As a programmed function of trailing-edge flap deflection
- As a function of flightpath angle and power setting combined in an “or” gate function

The significant point is that all these schemes are quite satisfactory from a control system performance point of view. This STOL control system performs equally well on -6° or -12° flightpaths, provided the appropriate L/D can be provided to permit operation at reasonable power and flap settings. This is in agreement with the statement in reference 7 that the dynamic behavior of flightpath response can be treated as an increment from the trim flightpath, and that this behavior is essentially independent of the trim flightpath angle magnitude. Thus, the steep slope capability of the STOL control system can be predicted from the design map (fig. 10) by adjusting the flightpath angle scale with the addition of an appropriate drag increment ($\Delta\gamma \cong -\Delta C_D/C_L$). The proper drag increment is selected to allow operation in a portion of the design map (fig. 8) where the flightpath capability will satisfy criterion 1 of section 5.3.1. The determination of methods for producing the necessary aircraft drag increments are beyond the scope of this study.

Questions regarding system behavior when a limit is exceeded remain to be answered. In cases where the flightpath commanded exceeds system capabilities and flap or engine saturation occurs, the pilot would experience a system discontinuity. Future studies should determine pilot reaction to this situation. If the condition were found to be objectionable, a warning system might be required.

5.3.6 Root Locus

Figure 18 shows the root locations for the STOL control system with a technique 1 pilot closure ($h, \theta \rightarrow \delta_{CO1}$) using a pure gain pilot representation for the inner (θ) and outer loops (h).

Figure 18A shows the pitch attitude closure ($\theta \rightarrow \delta_{CO1}$) and identifies the pilot gain level for a crossover frequency of 1.0 rad/sec. All roots are well damped without pilot compensation.

Figure 18B shows the outer-loop closure ($h \rightarrow \delta_{CO1}$) with the inner-loop gain set for a 1.0 rad/sec crossover frequency. An outer-loop gain of 0.1 deg/ft is identified; this is believed to be a representative upper limit. It is apparent that all roots are well damped and that a large gain margin is available in the altitude closure. These characteristics are reflected in the favorable pilot ratings of the reference 6 study summarized in table 2A.

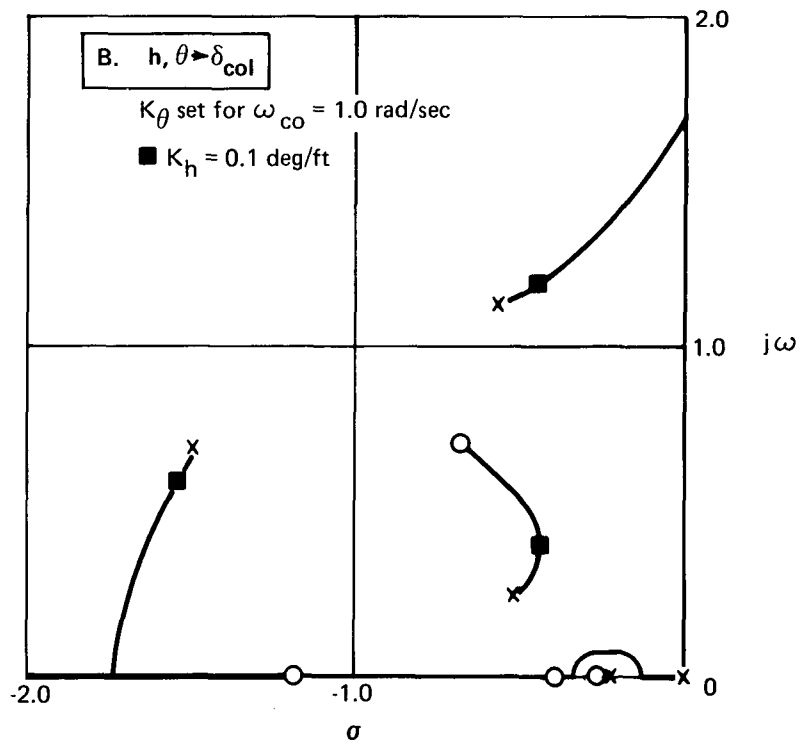
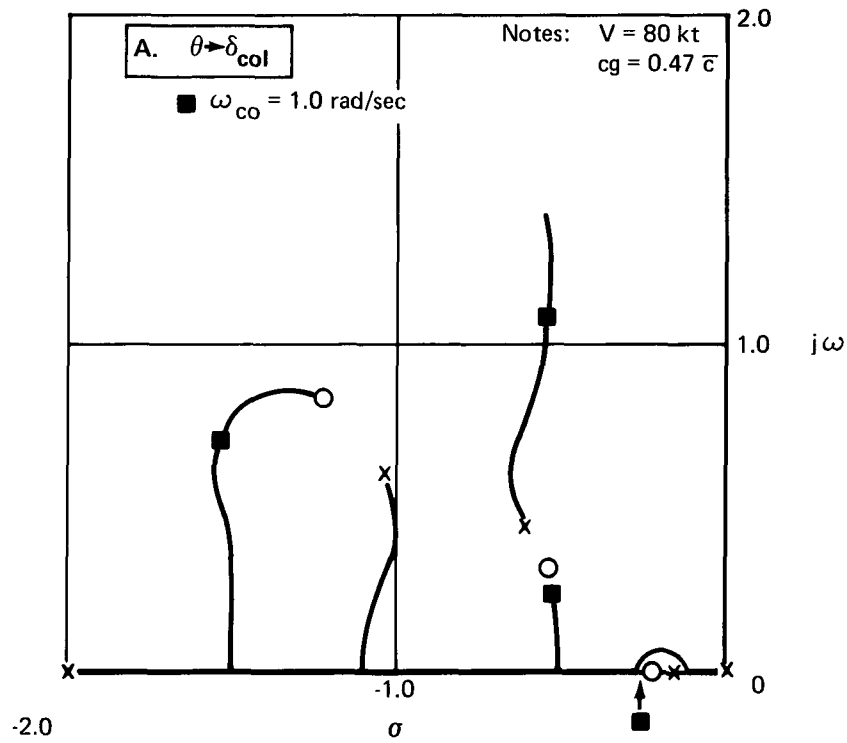


FIGURE 18.—PILOT CLOSURES WITH FULL AUGMENTATION

6.0 NOISE PROFILES

An initial study goal was to investigate the effect of single- and two-slope approaches to determine if any significant noise gains could be made. In performing these calculations, it was assumed that the glideslope capture altitude for single-slope approaches, or the transition altitude between first and second segments for two-slope approaches, would be greater than 500 ft. Final segment flightpath angles shallower than 6° were not of interest because the emphasis was on steep approach.

Noise profiles were computed from flightpath capture and track time histories that were developed using the pilot model described in section 5.3.3 and appendix A.4. These noise profile calculations indicated that first-segment flightpath angles steeper than the assumed 6° , second-segment slope have no significant effect on the 80-PNdB or higher contour closure points.

Approach maneuvers above 500-ft altitude will not affect the 80-, 83-, 89-, 95-, or 101-PNdB footprints. With the aircraft on a -6° glideslope at 500-ft altitude, the required engine power setting is such that the wing nozzle pressure ratio is 1.5, and the required flap setting is 50° to 60° . Under these conditions, the 80-PNdB closure point is approximately 5300 ft from the threshold, the 83-PNdB closure point is 3900 ft, the 89-PNdB closure point is 2000 ft, the 95-PNdB closure point is 1000 ft, and the 101-PNdB closure point is 500 ft from threshold (see fig. 19). The altitude of the aircraft at which the 95-PNdB level first touches the ground is 160 ft. These estimates assume that the other noise sources (inlet, aft fan, tailpipe, and aerodynamic noise) are suppressed and the augmentor wing noise dominates the footprint (see ref. 12).

For the augmentor wing configuration, there is no significant noise gain to be made by going to two-slope approaches.

Figure 20 shows the takeoff footprints for this aircraft for the 89-, 95-, and 101-PNdB contours. The maximum level on the 500-ft sideline during takeoff is 95.6 PNdB. The area enclosed within the 95-PNdB takeoff contour, for example, is significantly larger than the area enclosed within the 95-PNdB approach contour. Therefore, the community noise pattern about an airport serviced by this aircraft would be determined by the takeoff footprints.

ELEVATION VIEW

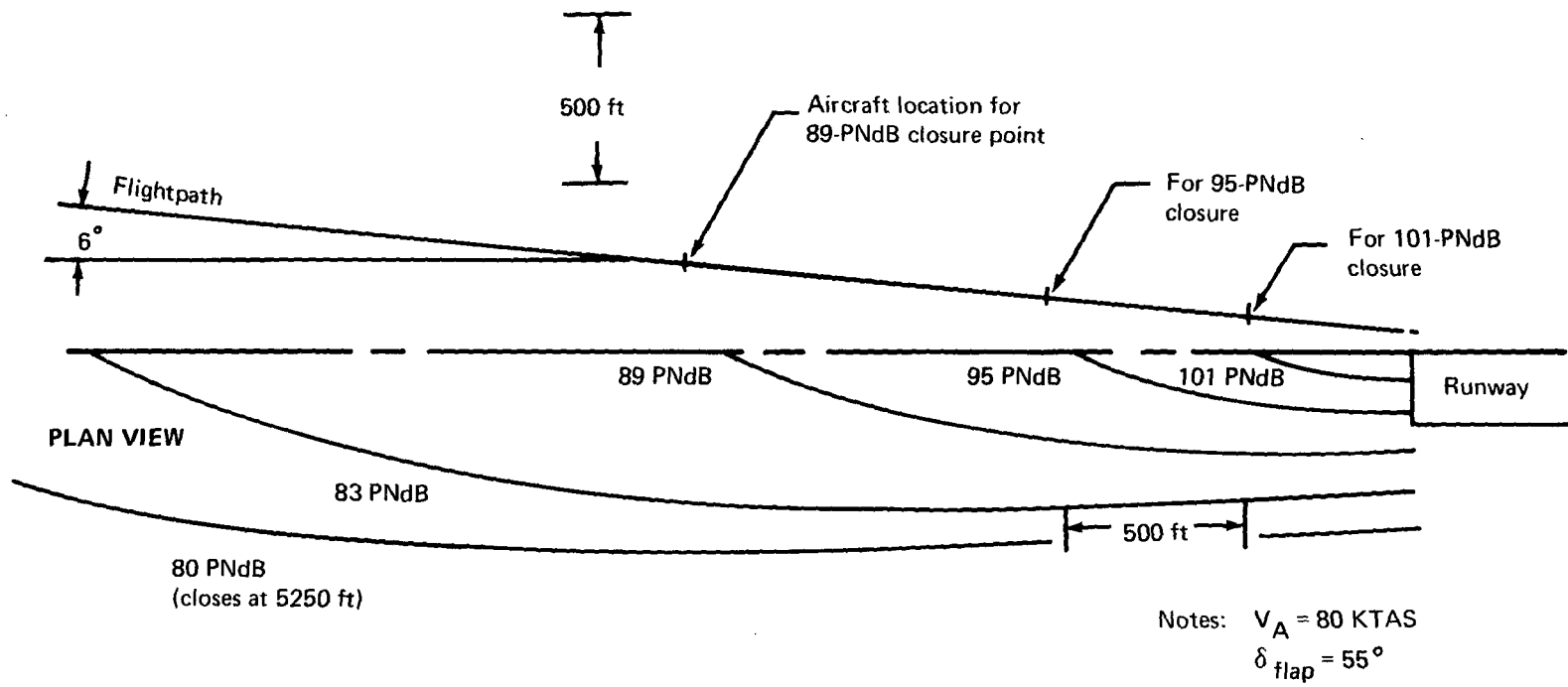


FIGURE 19.—APPROACH FOOTPRINTS

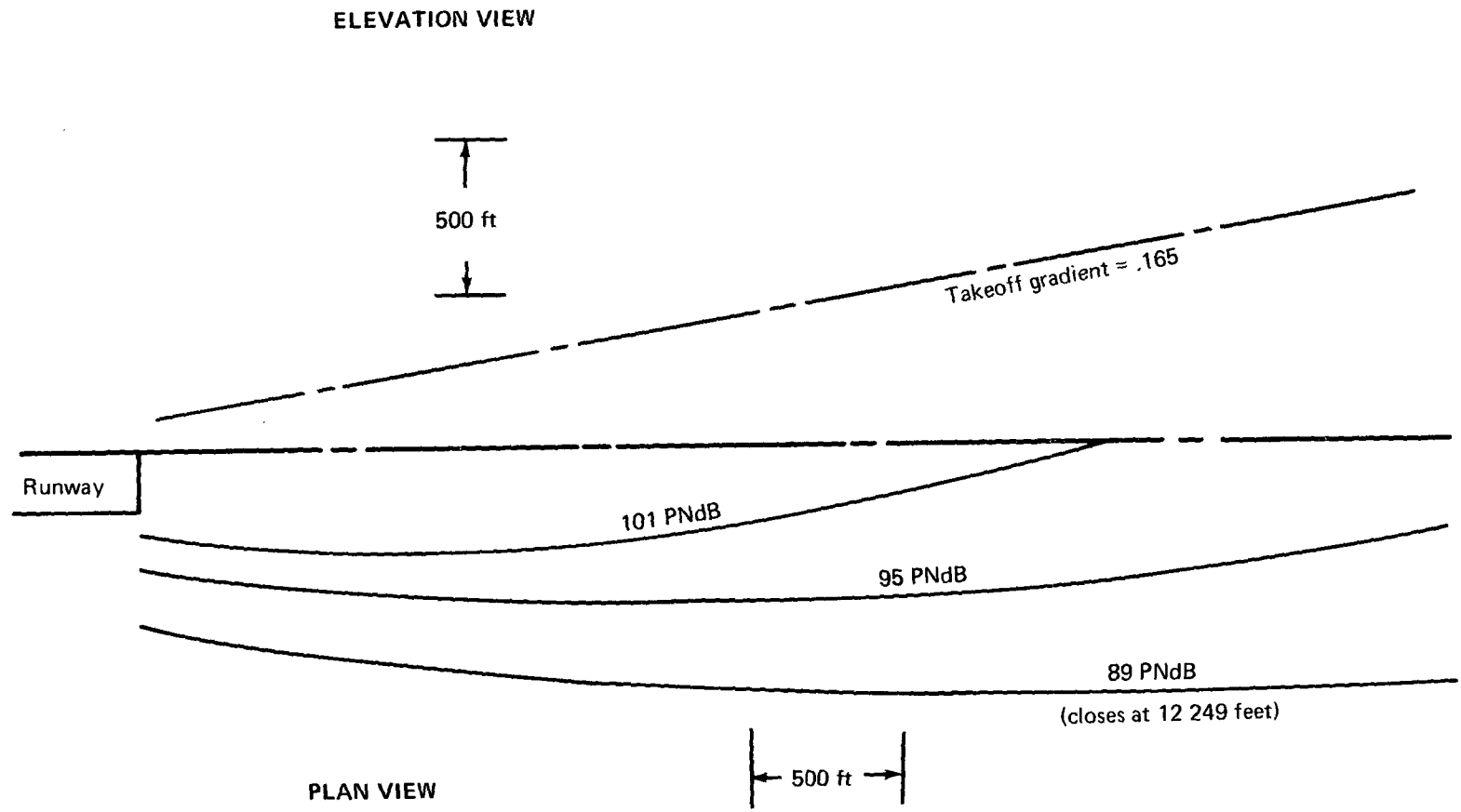


FIGURE 20.- TAKEOFF FOOTPRINTS

7.0 CONCLUSIONS

1. The recommended active-flap STOL control system concept offers potential for pilot handling qualities ratings at least as good as those of contemporary jet transport aircraft in all terminal area operation phases.
2. The active-flap control system requires trailing-edge flap rate capability of 10 to 15 deg/sec. The thrust response dynamics of present-day turbojet engines are adequate.
3. The recommended STOL control system concept is applicable to all powered-lift STOL configurations with suitable adjustment of gains and choice of the appropriate trailing-edge flap element.
4. The sensor requirements can be satisfied with conventional equipment, including barometric altitude-rate sensor, pitot airspeed sensor, vertical and horizontal accelerometers, vertical gyro, and pitch rate gyro.
5. The proposed control system offers significant potential for improvement of ride qualities in turbulence.
6. The proposed STOL control system has no inherent dynamic limitation for steep flightpaths, provided the appropriate aircraft L/D can be incorporated to permit operation at acceptable power and flap settings.
7. Results of noise calculations indicate that for the augmentor wing configuration there is no apparent noise gain to be made by going to two-slope, steep approaches. This conclusion is based on analysis of 80-PNdB and higher noise profiles, and on the assumptions that the basic aircraft noise levels are attenuated to 89 PNdB at 500-ft sideline and that the transition maneuvers are made at altitudes of 500 ft or higher.

Boeing Commercial Airplane Company
P.O. Box 3707
Seattle, Washington 98124
April 1973

APPENDIX

SIMULATION DETAILS

The augmentor wing simulation used in this study is basically the one used in the reference 6 piloted simulation study. Modifications have been made to incorporate nonlinear flap characteristics and engine dynamic response representative of current turbojet engines. Turbulence filtering circuits were added to the control system, and a pilot model was developed to allow unpiloted glideslope capture and tracking studies to be made.

The simulation was implemented on a digital computer with suitable digital-to-analog conversion for chart recorders, x-y plotter, and auxiliary sidarm controller interfaces. The mathematical details of the simulation are straightforward and will not be repeated here. This appendix presents a summary of the aerodynamic data for convenience, as well as descriptions of the pilot model and engine dynamic model that have not been reported elsewhere.

A.1 AUGMENTOR WING AIRCRAFT DEFINITION

Figure A-1 shows the augmentor wing transport configuration that was used as a baseline for the development of the STOL control system concept presented in this document. The configuration constants are presented in table A-1.

TABLE A-1.—CONFIGURATION CONSTANTS

Wingspan, b 119.5 ft
Wing area, S_w 2620 sq ft
Wing aspect ratio, AR 6.5
Wing incidence 2°
Horizontal stabilizer area, S_H 817 sq ft
Horizontal stabilizer, \bar{V} 1.225
Mean aerodynamic chord, C 20.2 ft
Center of gravity $0.344 \bar{c}$ to $0.47 \bar{c}$
Landing weight 203 000 lb
Pitch inertia, I_{yy} 6.55×10^6 slug-ft ²

	<u>Wing</u>	<u>Horiz</u>
Area, sq ft	2620	817
AR	6.5	4.0
Sweep, deg	25	30
\bar{V}	—	1.23

Engines:

2-stream, bypass 2.6, 21 500-lb SLST
 Passengers: 150 @ 6 abreast
 TOGW STOL: 206 000 lb

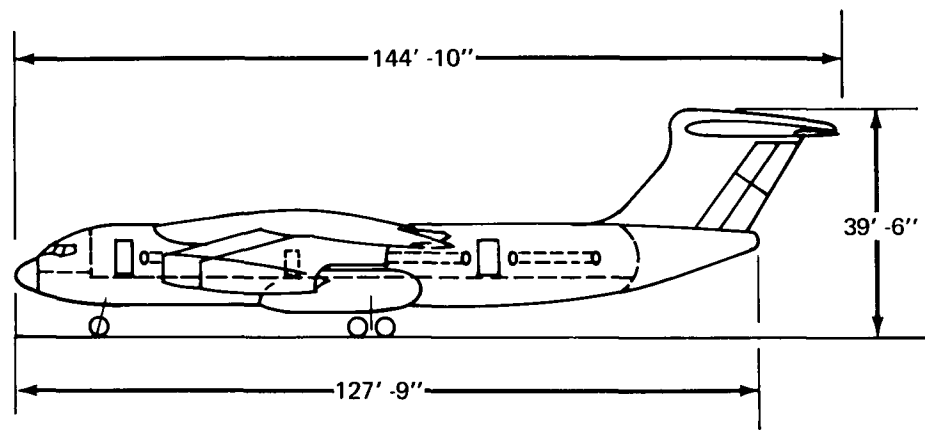
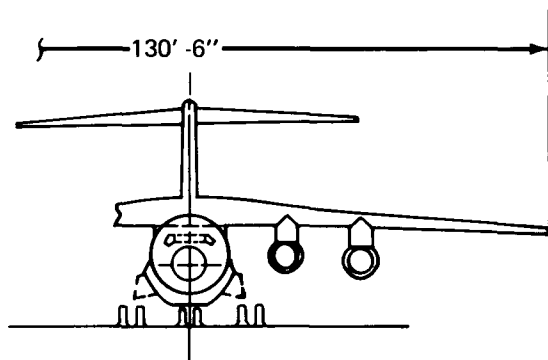
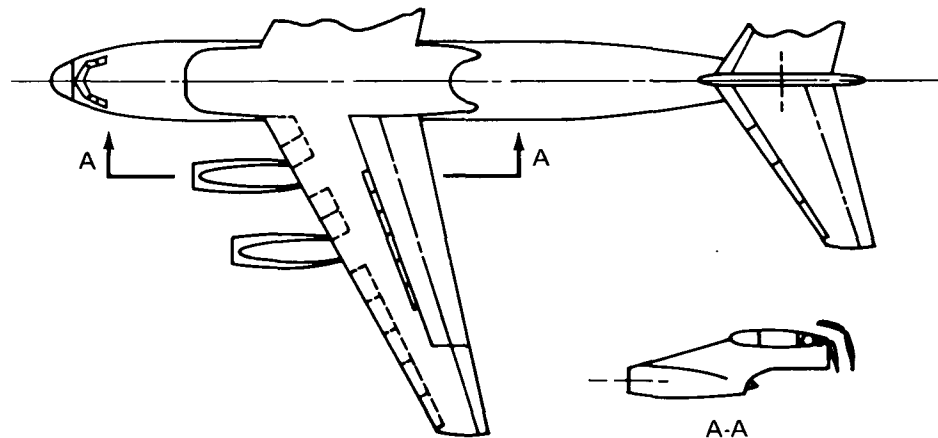


FIGURE A-1.—MODEL 751-103C AUGMENTOR WING TRANSPORT

The untrimmed longitudinal characteristics of the aircraft are presented in figures A-2 to A-12. These characteristics are based on the NASA/DHC, Ames, phase VI swept wing tests. The phase VI data were modified to account for leading-edge blowing, flap chord ratios, and wing planform differences. The estimated maximum lift capabilities of the augmentor concept are summarized in figures A-11 and A-12.

Figures A-2 through A-7 show the wing-body lift, drag, and pitching moment characteristics for trailing-edge flap settings of 40° and 70°. The data were input as a function of angle of attack, α , and thrust coefficient, C_J for each flap deflection. Data for other flap settings were interpolated or extrapolated using the flap angle cross-plots of figures A-8, A-9, and A-10. These figures are based on Ames phase VI data faired and extrapolated to 90° flap angles. This nonlinear interpolation technique allows a wide range of flap angles to be represented and retains the important data nonlinearities without requiring an excessively large number of data tables. The interpolation figures are derived for an angle of attack of 10° but are valid for the range of α covered in this study.

Figure A-13 shows the horizontal tail lift coefficient as a function of tail angle of attack. The downwash at the tail was calculated from a theoretical downwash model. The tail moment arm was calculated using the angle of attack and cg location. Elevator effectiveness is computed from a derivative buildup using $C_{L_{\delta_e}} = 0.03 \text{ deg}^{-1}$.

The effects of pitch rate and angle-of-attack rate were included by defining the appropriate angle-of-attack increment and downwash lag at the tail.

A generalized mathematical downwash model was used to calculate the augmentor wing downwash contours (figs. A-14 and A-15). The downwash model has successfully correlated test data points over a wide range of α and C_J for both AW and EBF lift systems. For simplicity, the bound vortex is represented by a linear vortex at a fixed percentage of the wing semispan. The trailing-vortex system consists of two semi-infinite vortices that originate at the wing trailing edge and are parallel to the freestream velocity. These vortices are located at a fixed percentage of the theoretical two-dimensional wake distance below the trailing edge. Theoretical two-dimensional wake locations are obtained from jet flap theory as a function of distance behind the wing, trailing edge, jet efflux angle, and trailing-edge momentum coefficient (c_μ).

The tail plane location with respect to the vortex system is a function of geometry and wing angle of attack. Velocities are computed by the Biot-Savart law. For in-ground effect calculations, a conventional image system is employed.

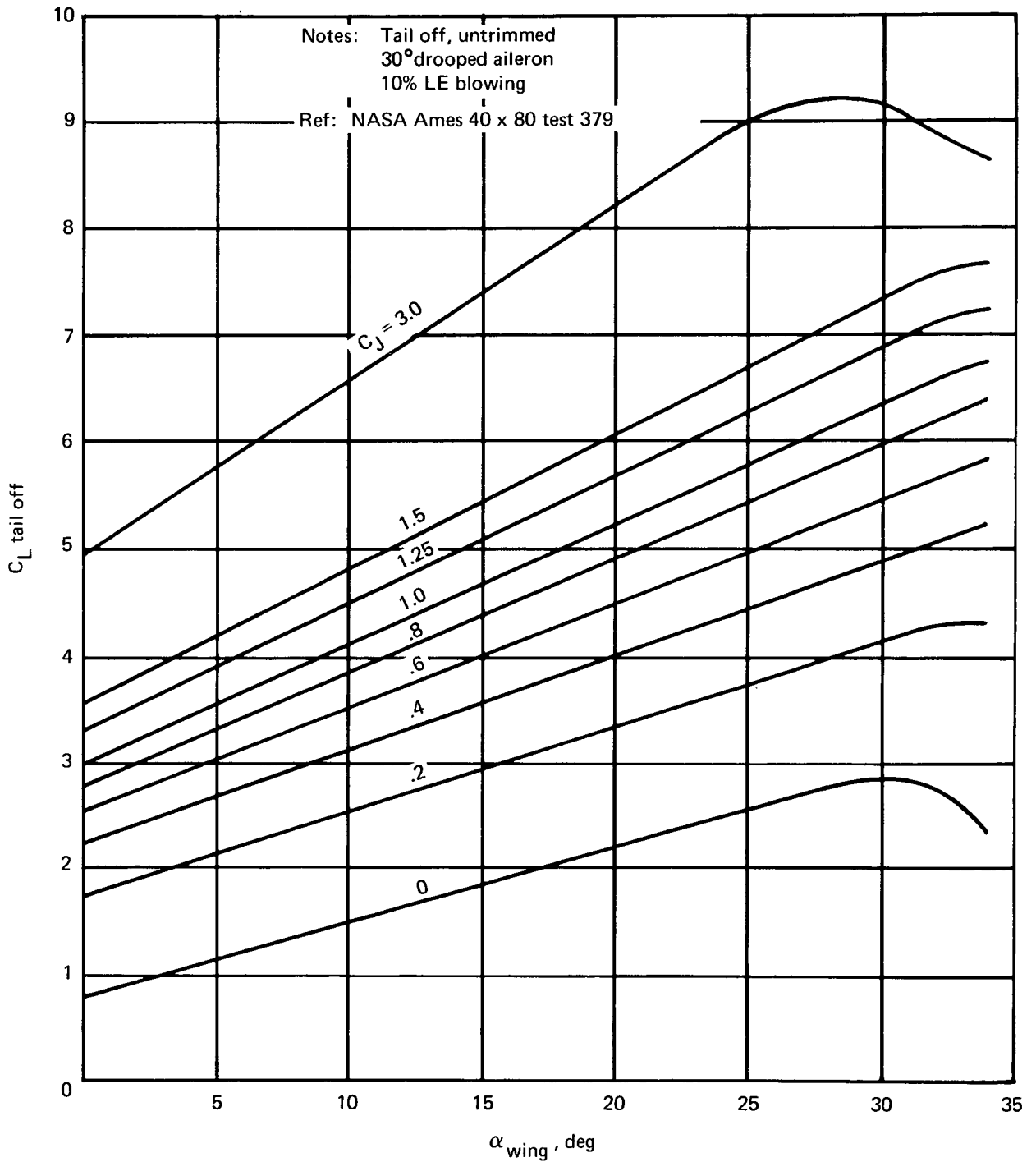


FIGURE A-2.—LIFT CURVES, TAIL OFF ($\delta_{flap} = 40^\circ$)

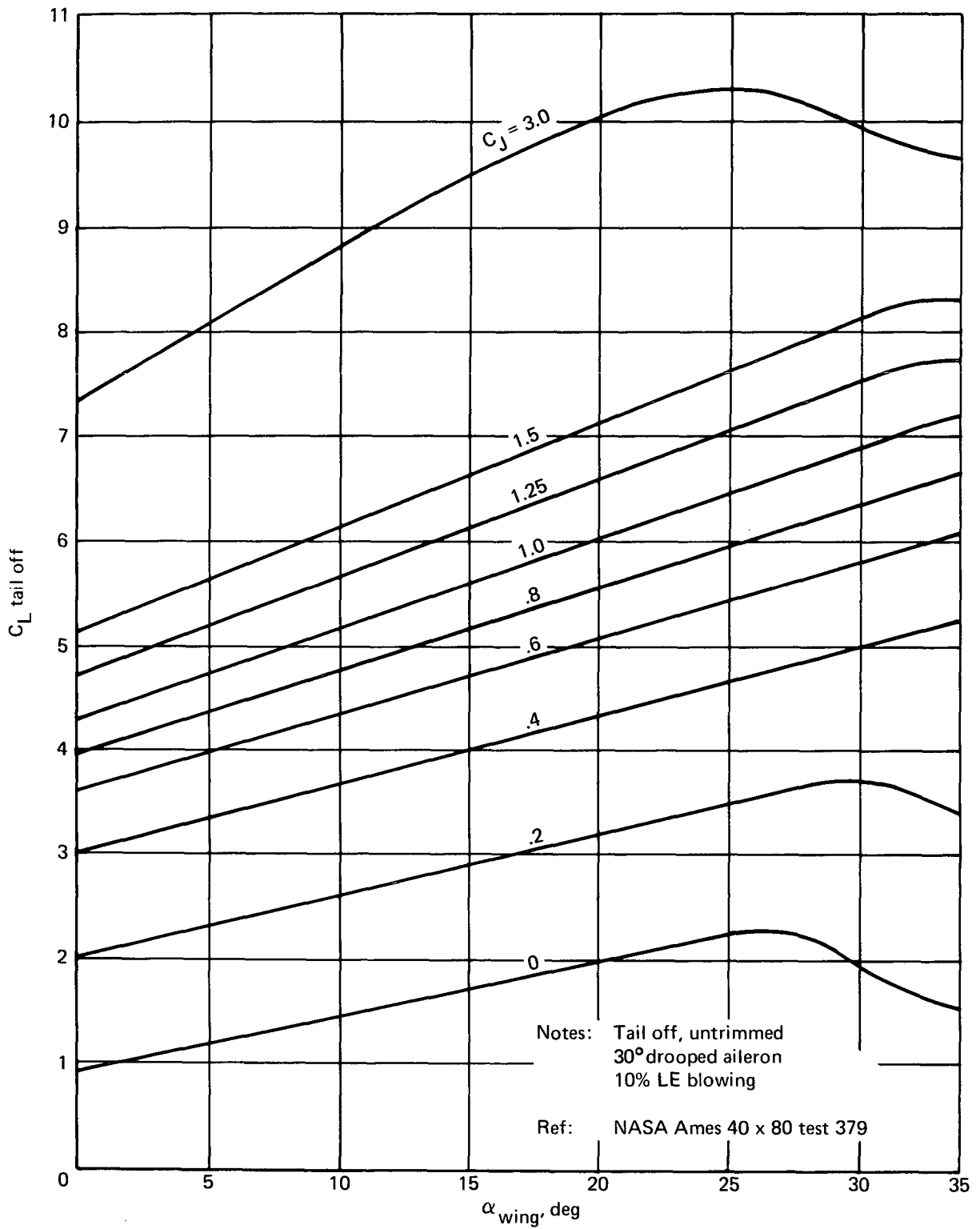


FIGURE A-3.—LIFT CURVES, TAIL OFF ($\delta_{flap} = 70^\circ$)

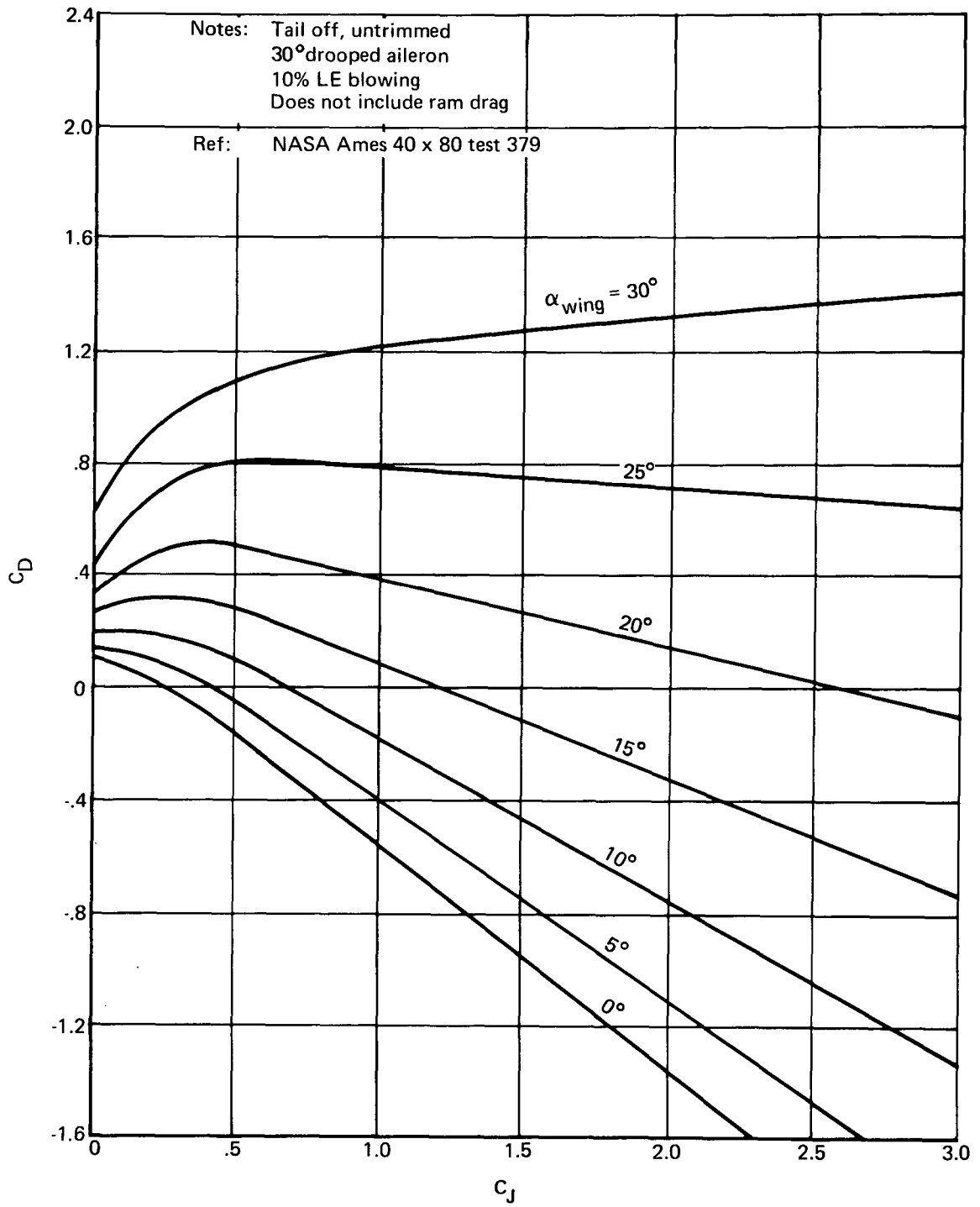


FIGURE A-4.—DRAG CHARACTERISTICS, TAIL OFF ($\delta_{flap} = 40^\circ$)

Notes: Tail off, untrimmed
 30° drooped aileron
 10% LE blowing
 Does not include ram drag
 Ref: NASA Ames 40 x 80 test 379

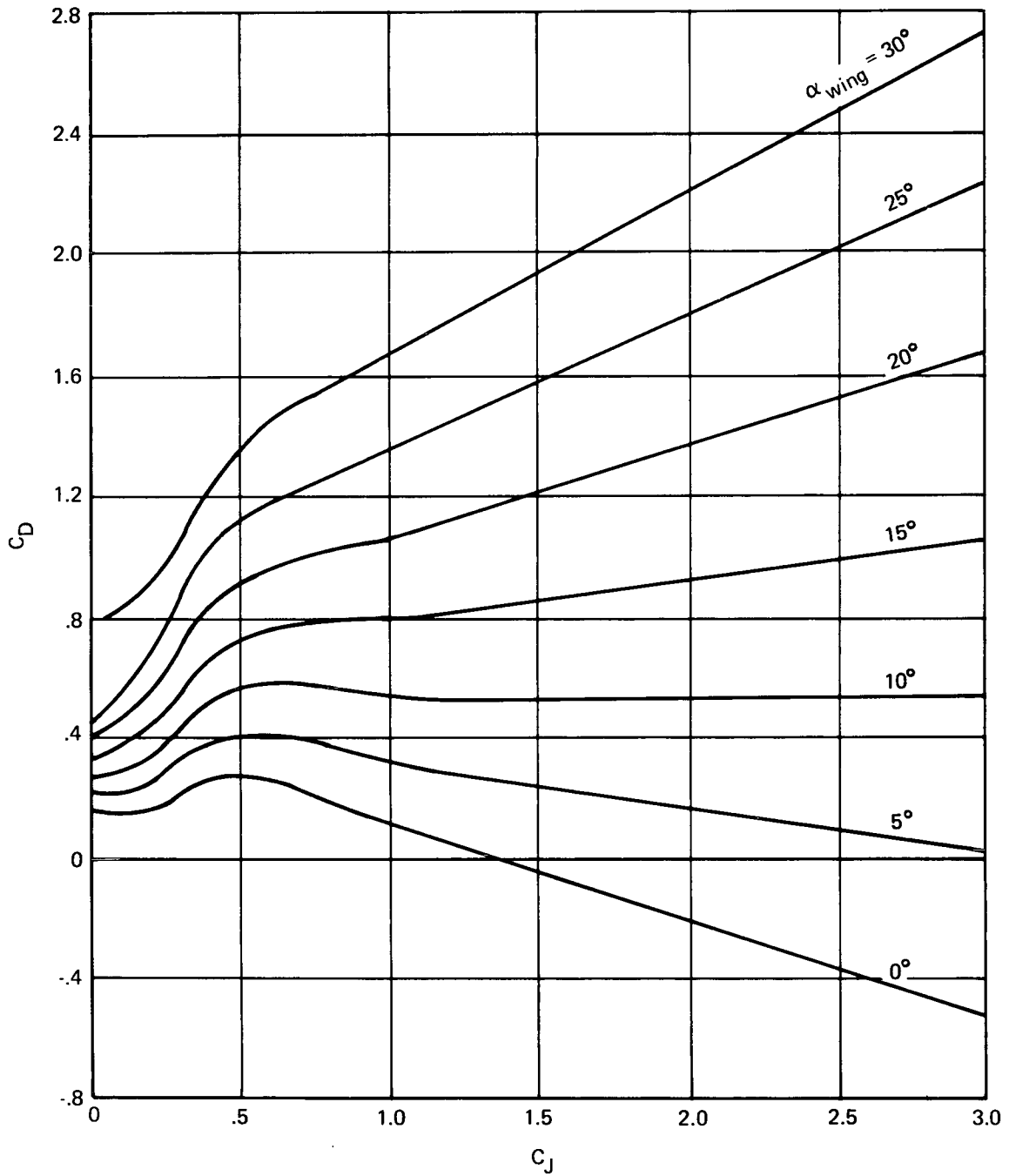


FIGURE A-5.—DRAG CHARACTERISTICS, TAIL OFF ($\delta_{flap} = 70^\circ$)

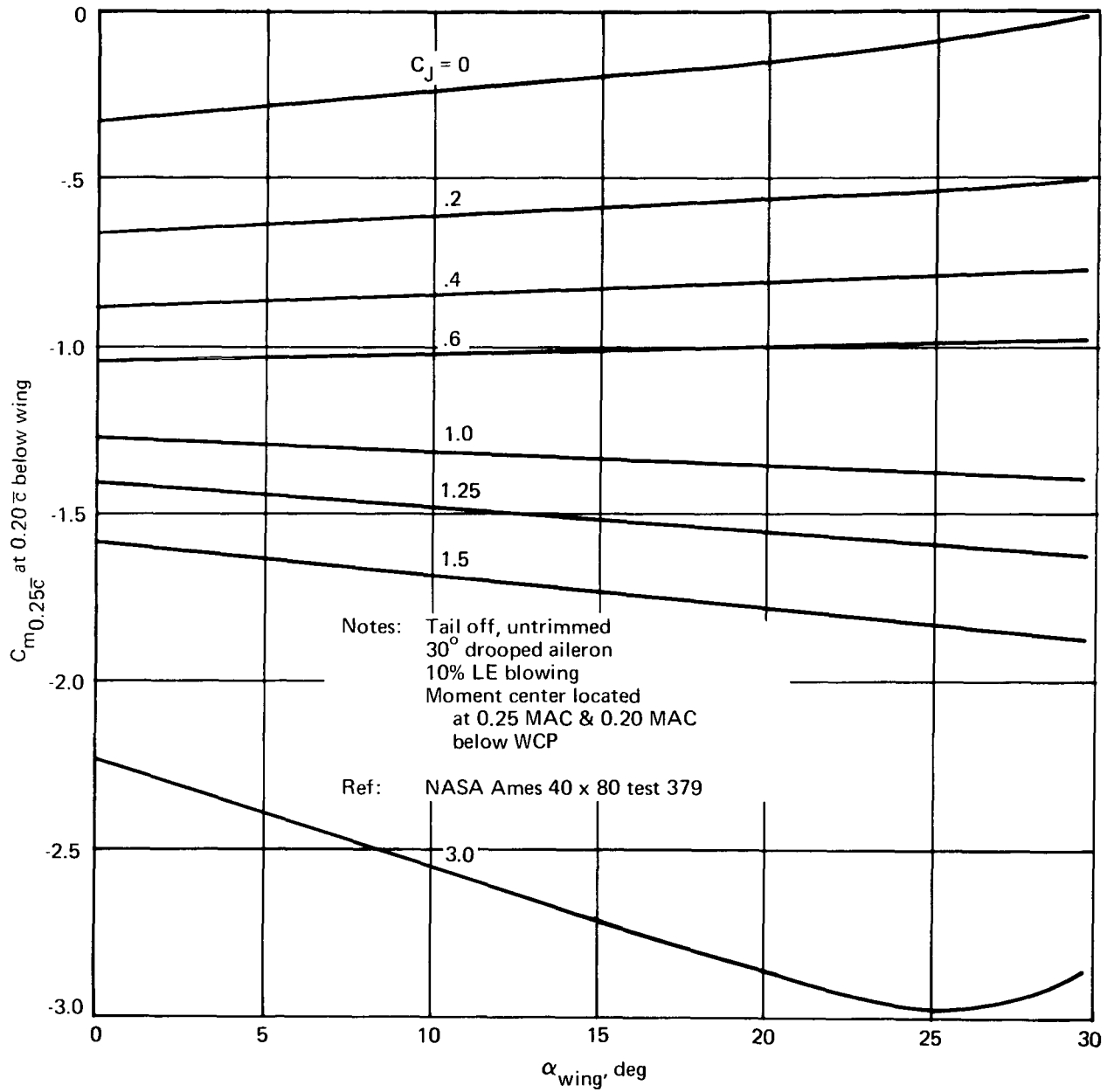


FIGURE A-6.—PITCHING MOMENT, TAIL OFF ($\delta_{flap} = 40^\circ$)

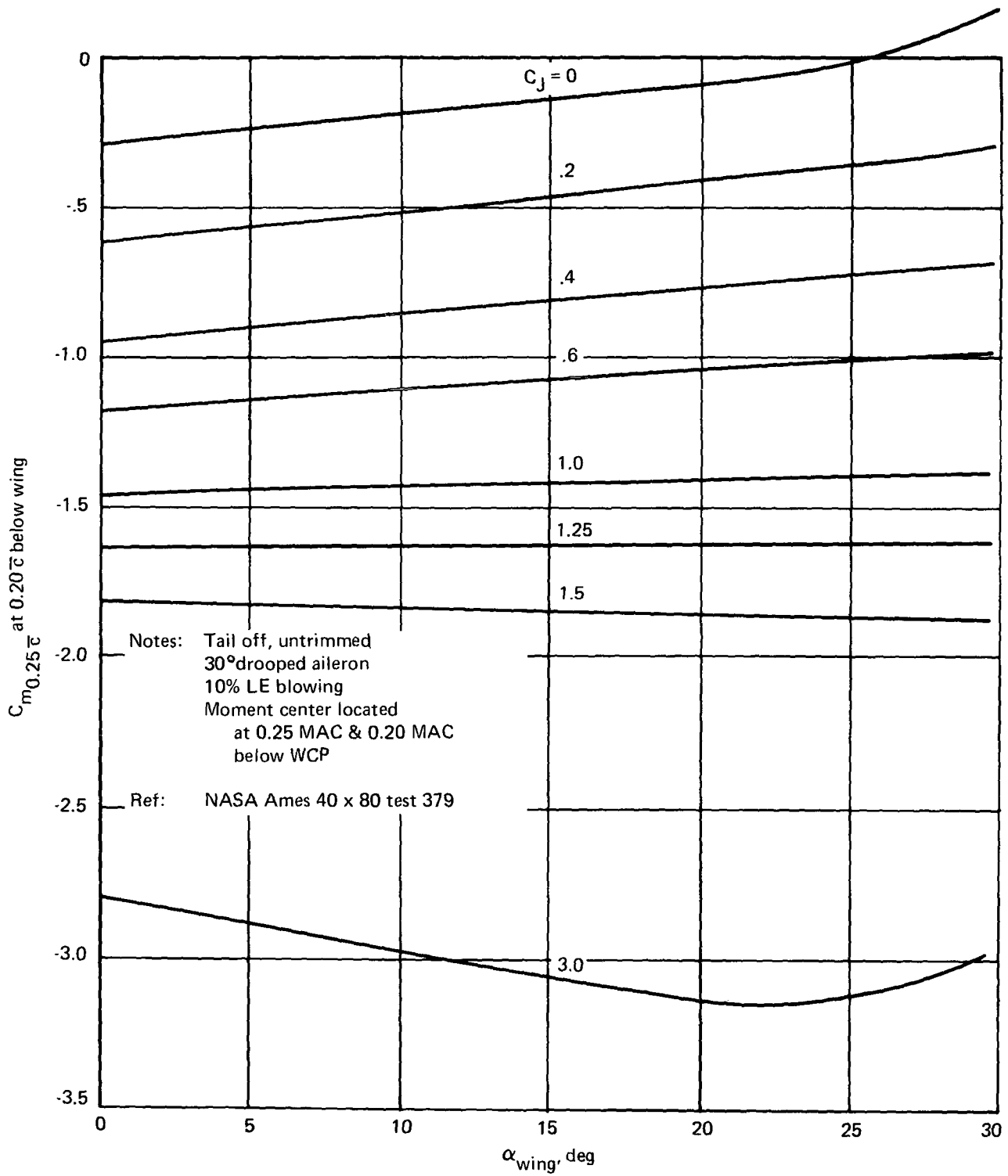


FIGURE A-7.—PITCHING MOMENT, TAIL OFF ($\delta_{flap} = 70^\circ$)

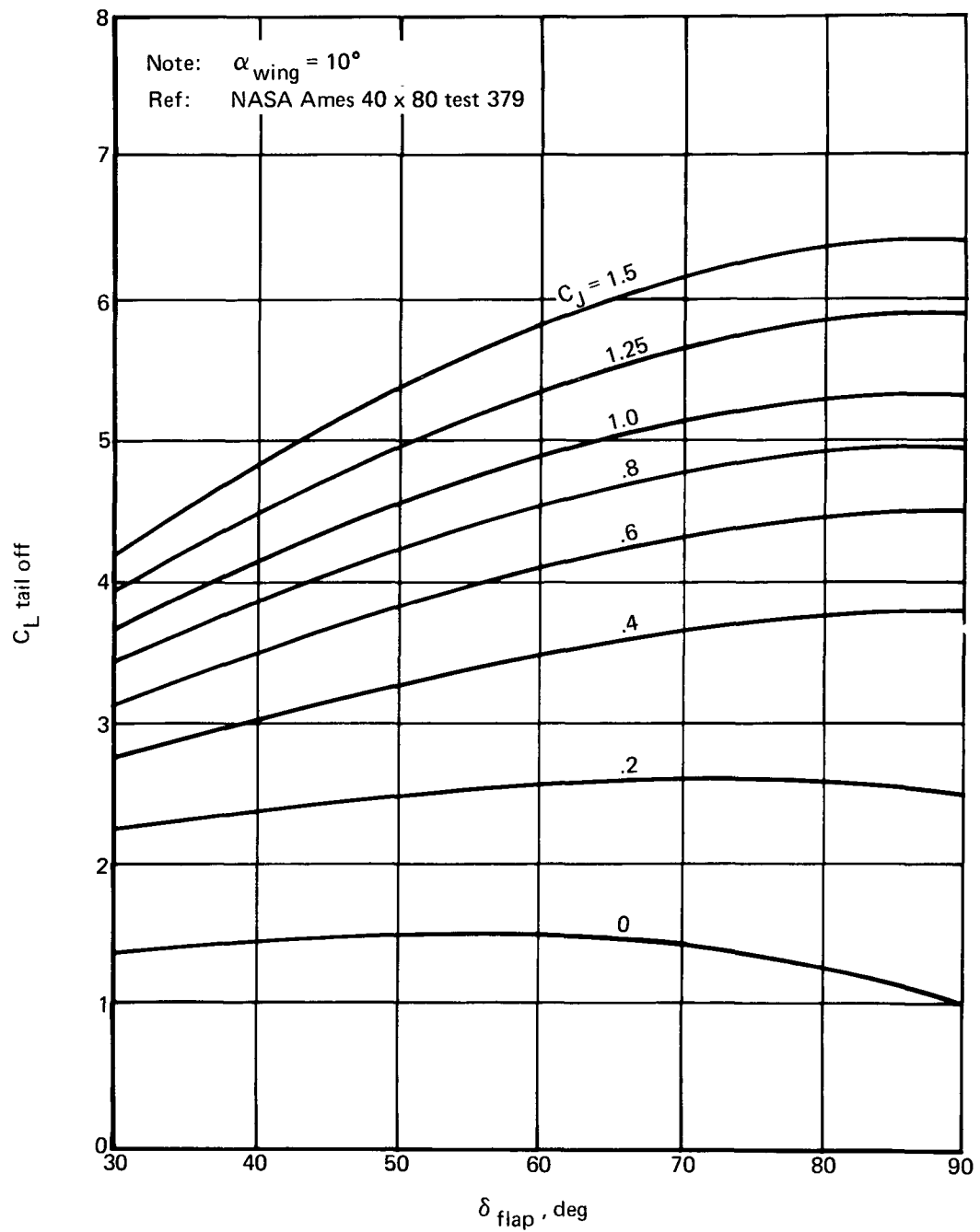


FIGURE A-8.—EFFECT OF FLAP DEFLECTION ON LIFT

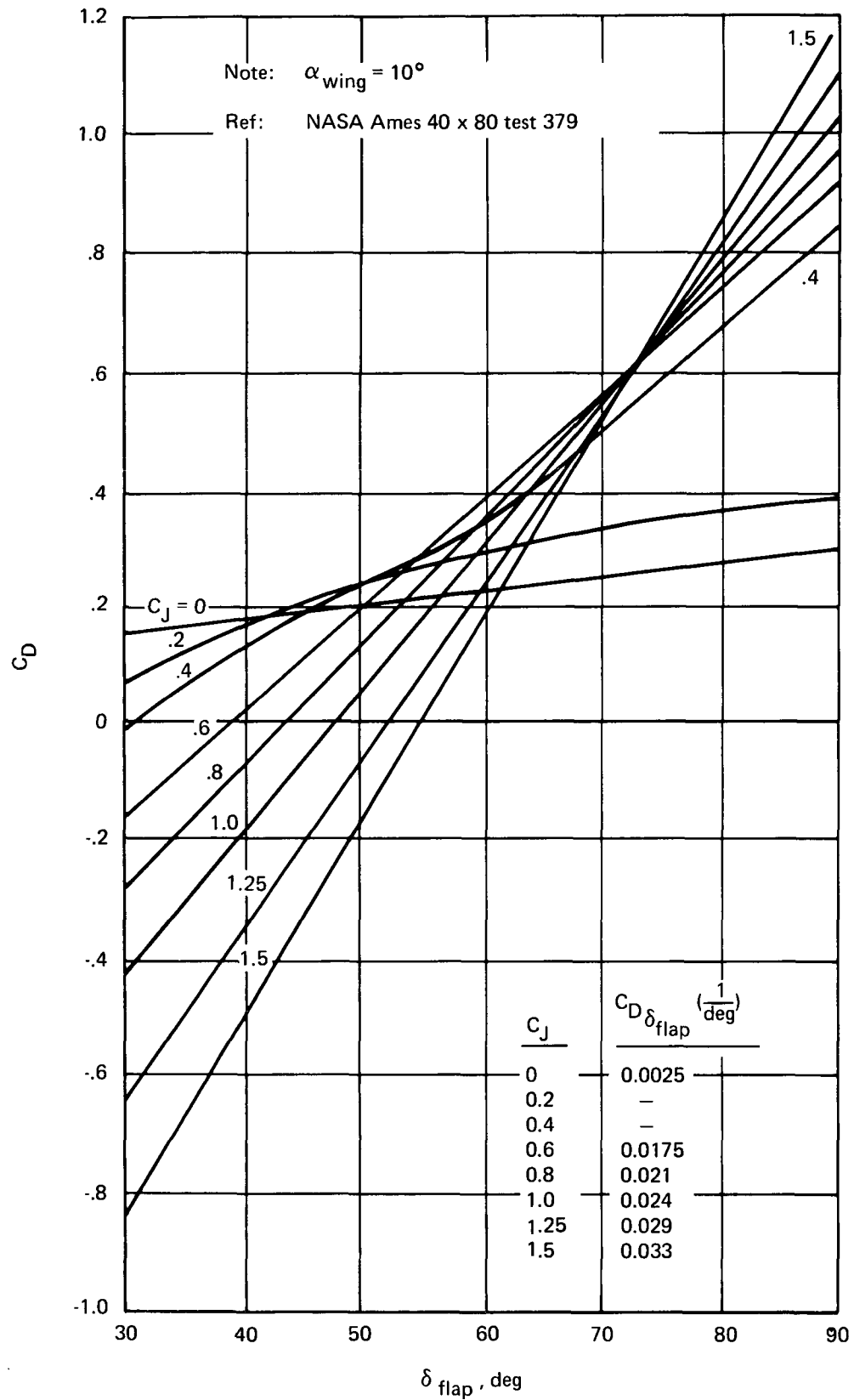


FIGURE A-9.—EFFECT OF FLAP DEFLECTION ON DRAG

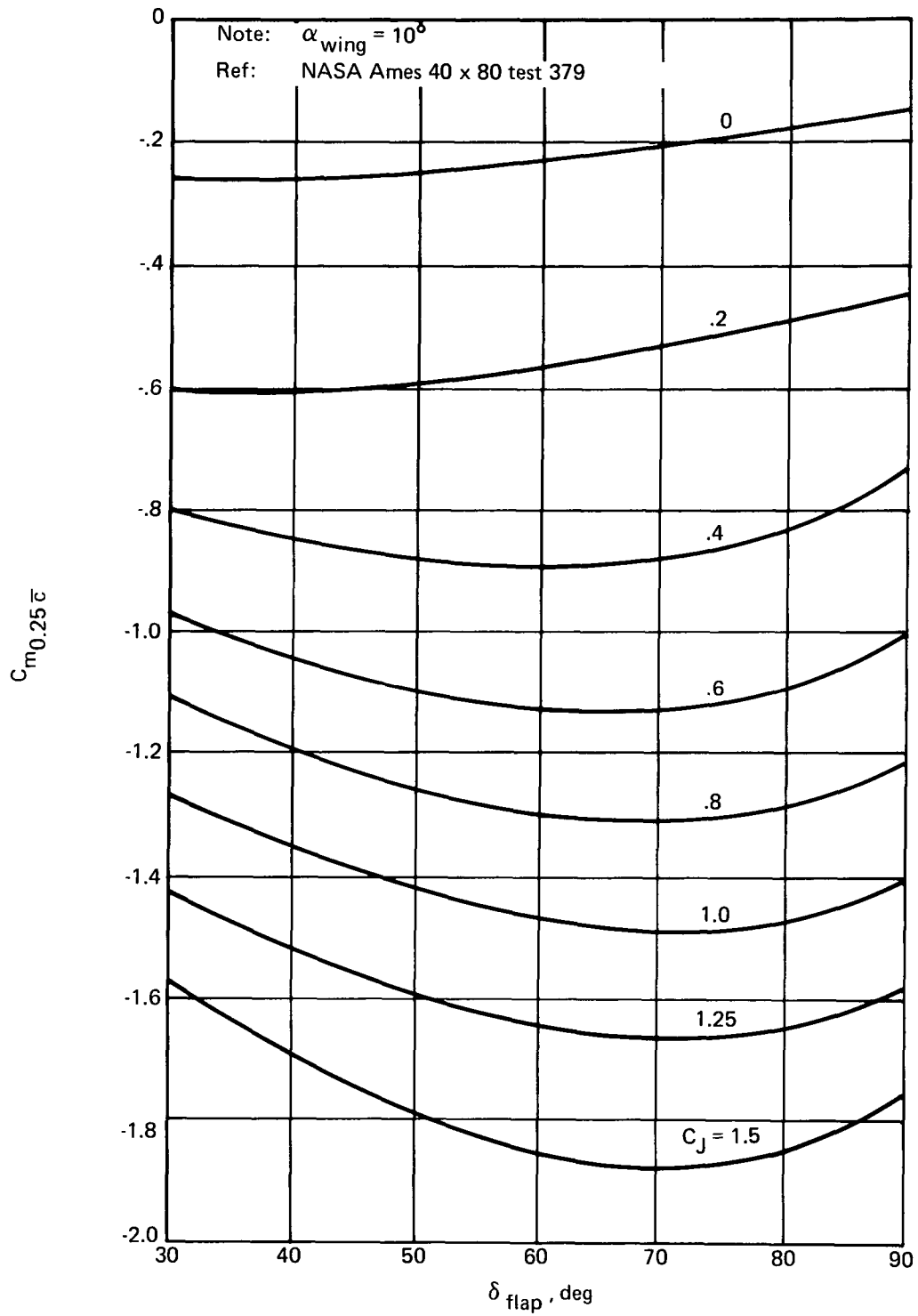


FIGURE A-10.—EFFECT OF FLAP DEFLECTION ON PITCHING MOMENT

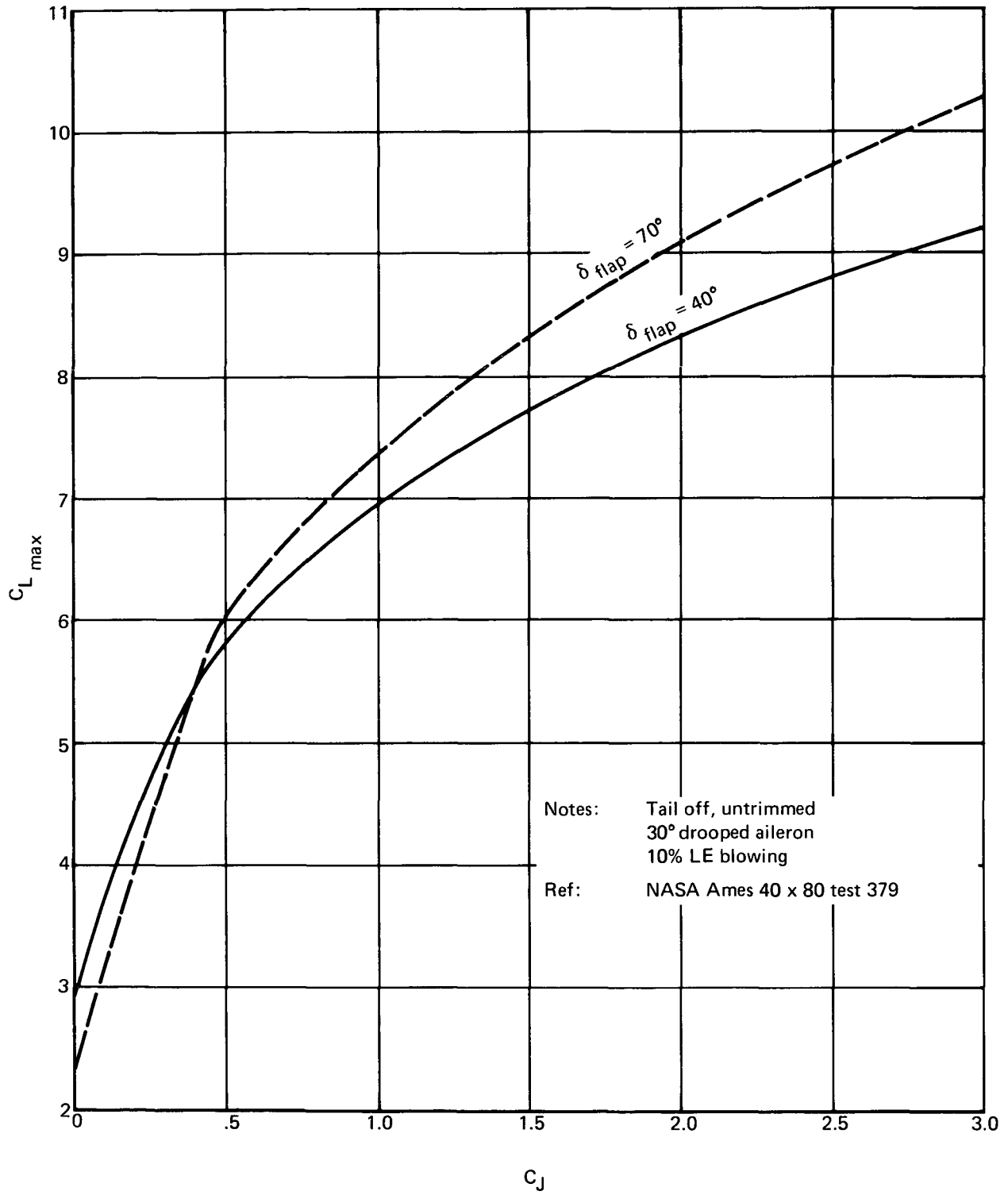


FIGURE A-11.— $C_{L_{max}}$ ($\delta_{flap} = 40^\circ$ and 70°)

Notes: Tail off, untrimmed
30° drooped aileron
10% LE blowing
Ref: NASA Ames 40 x 80 test 379

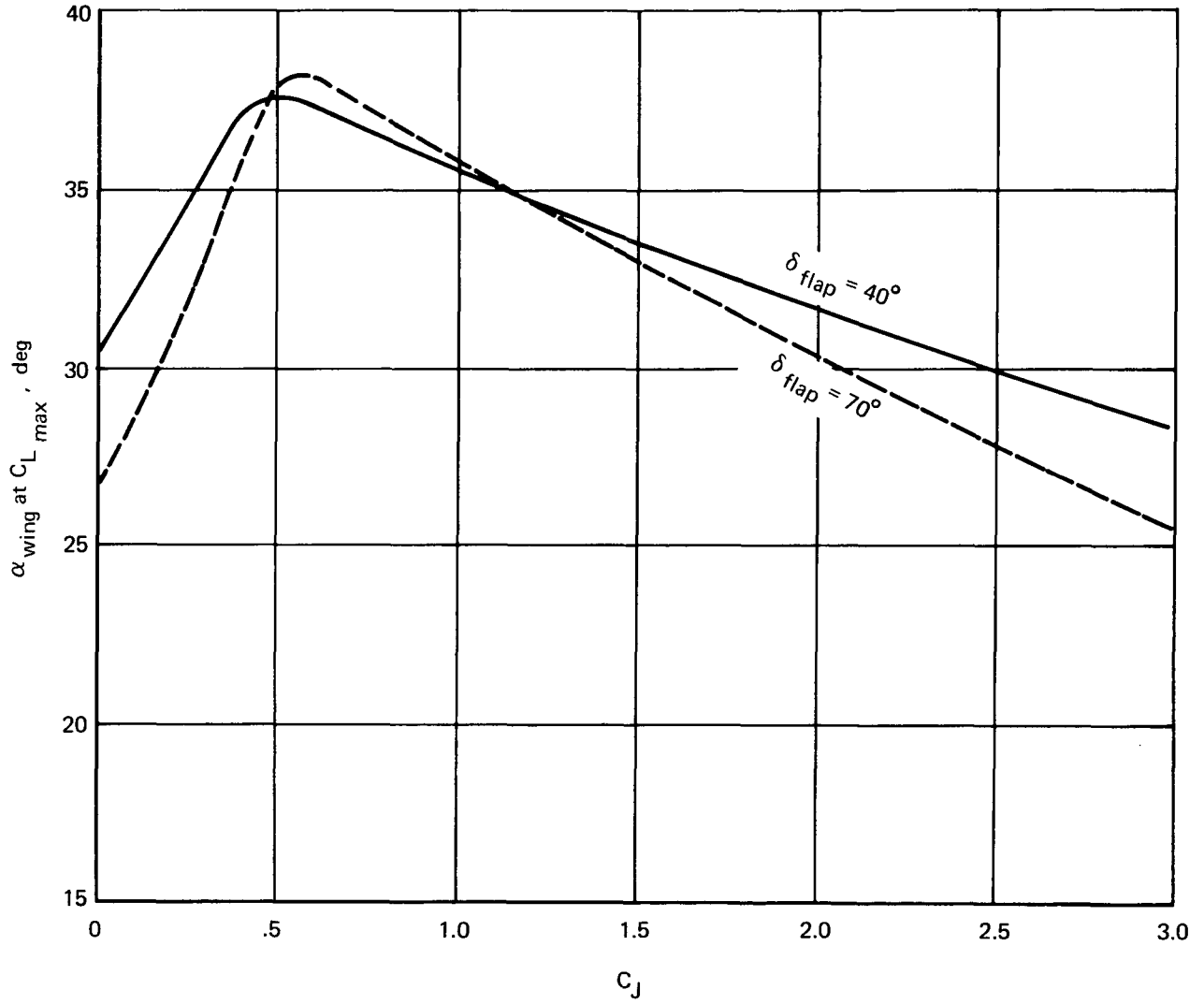


FIGURE A-12.— α_{wing} AT $C_{L_{max}}$ ($\delta_{flap} = 40^\circ$ AND 70°)

Notes: $\delta_e = 0^\circ$
 $C_{L_{\delta_e}} = 0.03 \frac{1}{\text{deg}}$
Horizontal AR = 4.0, $\Lambda_c/4 = 30^\circ$, $\lambda = 0.40$
Krueger LE device
Symmetrical section

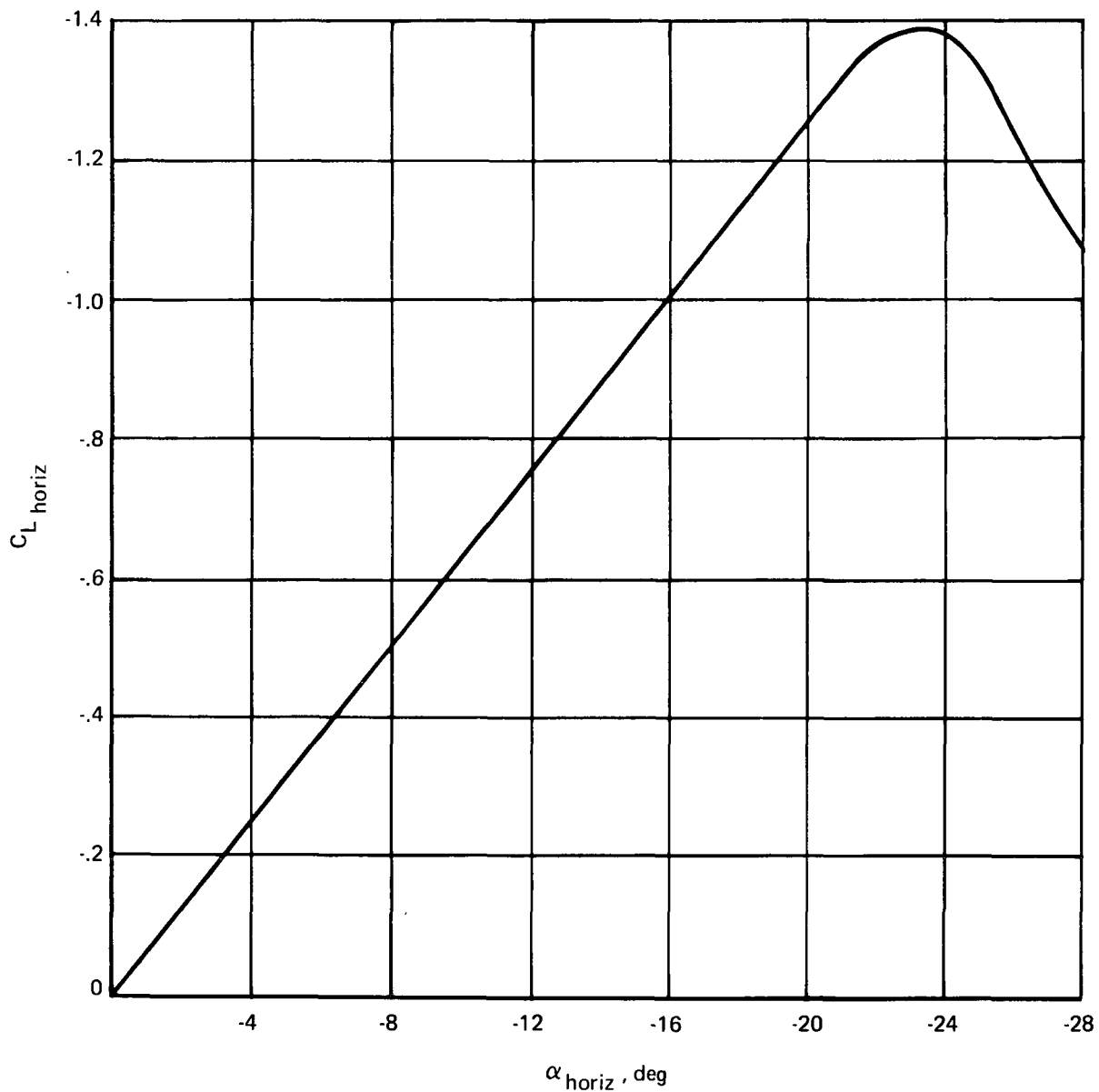


FIGURE A-13.—HORIZONTAL LIFT CURVE

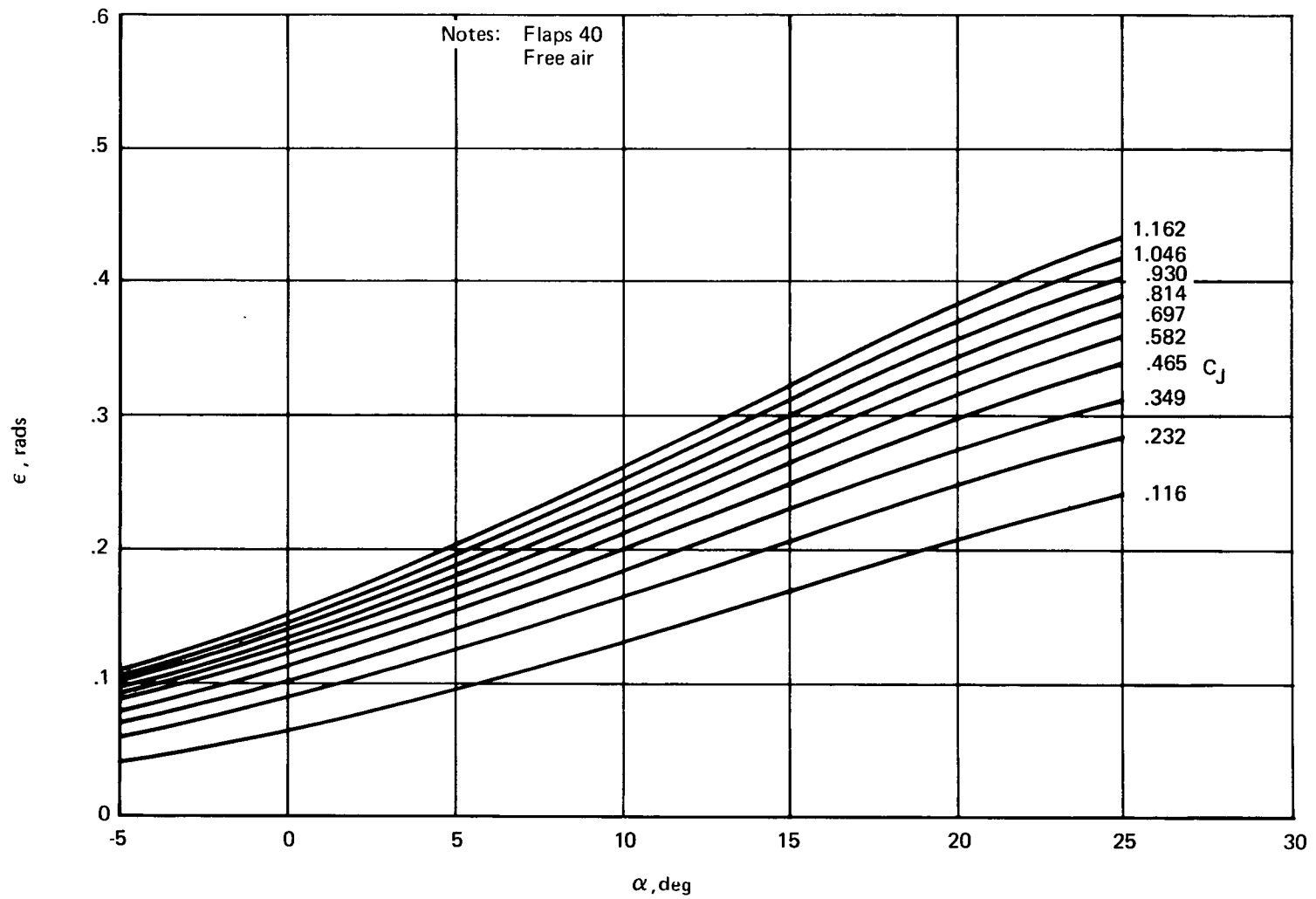


FIGURE A-14.—DOWNWASH—AUGMENTOR WING ($\delta_{flap} = 40^\circ$)

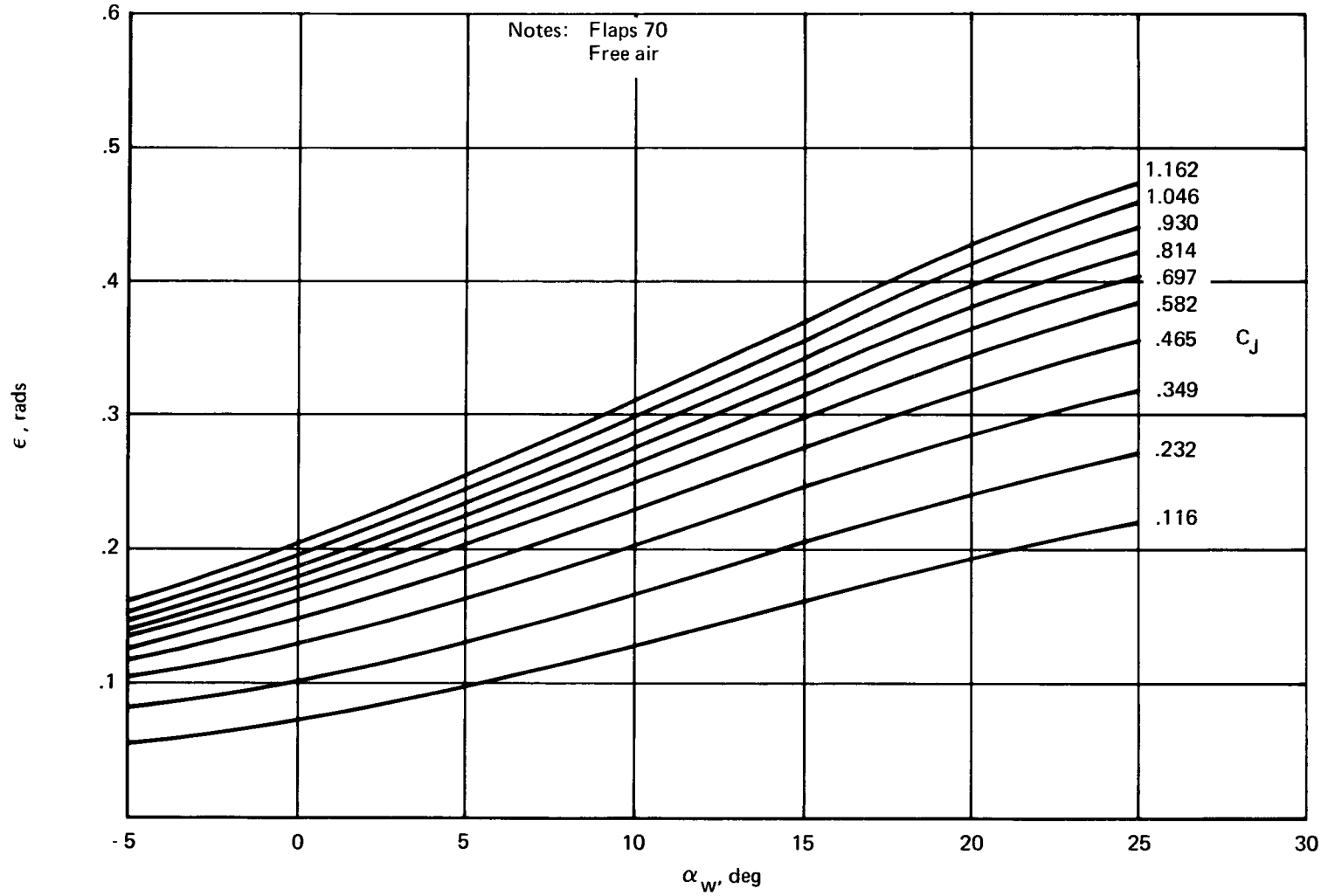
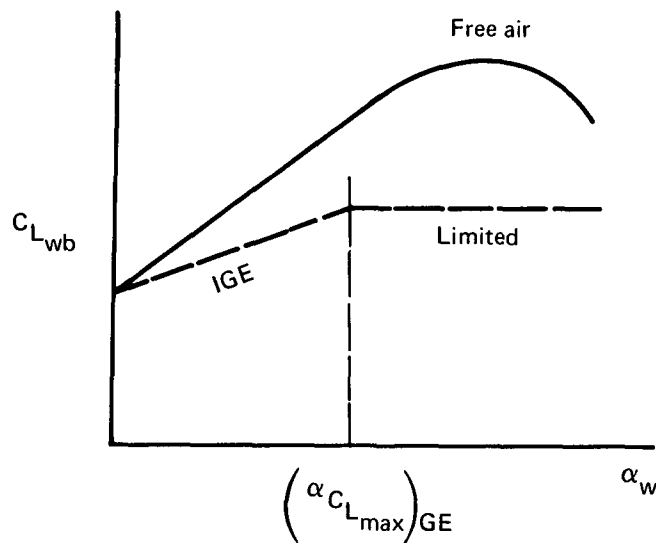


FIGURE A-15.—DOWNWASH—AUGMENTOR WING ($\delta_{flap} = 70^\circ$)

A GROUND EFFECT ON WING-BODY LIFT, DRAG, AND PITCHING MOMENT

A theoretical method was used to calculate the effects of proximity to the ground on wing-body lift, drag, and pitching moment. The additional effects due to changes in downwash when the aircraft is near the ground are calculated in the downwash model and are used in calculating the horizontal tail lift and pitching moment characteristics. The theoretical methods used agree well with Boeing wind tunnel data. In general, the ground effect model predicts a moderate lift loss for the augmentor wing configuration at gear contact height, and is probably slightly conservative.

The three variables used in the ground effect calculations are thrust coefficient, C_J , wing angle of attack, α_w , and height of the quarter chord of the mean aerodynamic chord above the ground, H_w . The theoretical method used allows the angle of attack for maximum lift in ground effect, $(\alpha_{C_{L_{max}}})_{GE}$, to be calculated as a function of C_J , H_w , and α_w . $(\alpha_{C_{L_{max}}})_{GE}$ is compared with the current α_w and is used to limit the lift coefficient as shown in the sketch below.



The calculation of lift in ground effect is based on the following considerations:

1. A correction for induced upwash, $\alpha_{GE} = \alpha_{\infty} - \Delta\alpha$

$$\frac{\Delta\alpha}{C_L} = \frac{1}{2\pi AR \left[1 + 16 \left(\frac{H_w}{CAR} \right)^2 \right]}$$

2. A reduction in the local velocity across the lifting system due to the constraint of the ground

$$\frac{q}{q_{\infty}} = \left[\frac{1}{1 + \left(\frac{C_{L\infty}}{8\pi \frac{H_w}{C}} \right) \left(\frac{1}{\sqrt{1 + 16 \left(\frac{H_w}{CAR} \right)^2}} \right)} \right]^2$$

3. An effective increase in the thrust coefficient, C_J due to the reduction in local dynamic pressure, $C_J' = \frac{C_J}{q/q_{\infty}}$

This yields:

$$C_{LGE} = \left(\frac{1}{1 - \frac{\Delta\alpha}{C_L} C_{L\alpha}} \right) \left[C_{Lwb\infty} \frac{q}{q_{\infty}} + \left(1 - \frac{q}{q_{\infty}} \right) C_{LC_J} C_J \right]$$

Similar considerations were used to estimate the ground effect on drag:

1. A reduction in induced drag at constant circulation due to the reduction in downwash
2. A reduction in drag due to the reduction in dynamic pressure
3. A reduction in force in the drag direction due to the increase in effective C

$$C_{DwbGE} = \left[C_{Dwb\infty} - C_{Lwb\infty}^2 \frac{\Delta\alpha}{C_L} \right] \frac{q}{q_{\infty}} + \left(1 - \frac{q}{q_{\infty}} \right) \frac{\partial L_D}{\partial C_J} C_J$$

The wing-body pitching moment calculation consists of corrections for the reduced dynamic pressure, the induced upwash, and the change in C_J due to ground effect.

$$\Delta C_{mwbGE} = \left(\frac{q}{q_{\infty}} - 1 \right) C_{mwb\infty} + C_{m\alpha} \frac{\Delta\alpha}{C_L} C_{LGE} + \frac{\partial C_m}{\partial C_J} \left(1 - \frac{q}{q_{\infty}} \right) C_J$$

A.3 PROPULSION MODEL

The propulsion model described in this section was developed for the augmentor wing simulation. The model was matched to the dynamic response of a current turbofan engine and was checked against the responses of several high bypass ratio engines as well. It was found to be representative of this class of engines.

Figure A-16 shows the engine model spin-up and spin-down response for several throttle steps. The responses show the effect of fuel control lag and governor topping for both full and part throttle bursts. The rapid spin-down is also shown.

At present it is not known to what extent, if any, the characteristics of the augmentor wing installation might differ from those shown in figure A-16. It is thought that the spin-up characteristics will be essentially unchanged, but the spin-down rate may possibly be slightly high.

The effects of duct volume on engine backpressure have been noted in augmentor wing Buffalo static rig testing, but no general conclusions can presently be drawn. Figure A-16 is believed to be sufficiently representative of the propulsion system dynamics to validate the proposed STOL control system concept. The propulsion dynamics of figure A-16 were not critical for the control system.

It is worth noting that because of the difference between spin-up and spin-down rates, the engine model functions as a rectifier-integrator circuit for any high-frequency throttle command inputs. In designing an autothrottle control system, it is important to provide adequate filtering of high-frequency turbulence components in the sensor paths if negative thrust ramps are to be avoided. If adequate sensor filtering could not be achieved, this effect could be eliminated by incorporating a nonlinear rate limit ahead of the engine that is in inverse of the engine characteristics.

Figure A-17 shows the block diagram of the engine model. This algorithm develops commanded thrust output percentage as a function of percent thrust command. The actual engine characteristics are obtained from figure A-18 as a function of percent thrust output. The hot thrust, blowing thrust (including duct pressure loss), and mass flow rate (for ram drag calculation) are given. This figure includes speed lapse effects for 80 kt. For small speed excursions around 80 kt, the incremental lapse rate effects are assumed to be negligible.

Figure A-17 shows the several logic switches and rate limits. This is the simplest arrangement that could produce the characteristics difference between spin-up and spin-down, the effect of separate fuel control and governor topping effect, and the proper part-power step response.

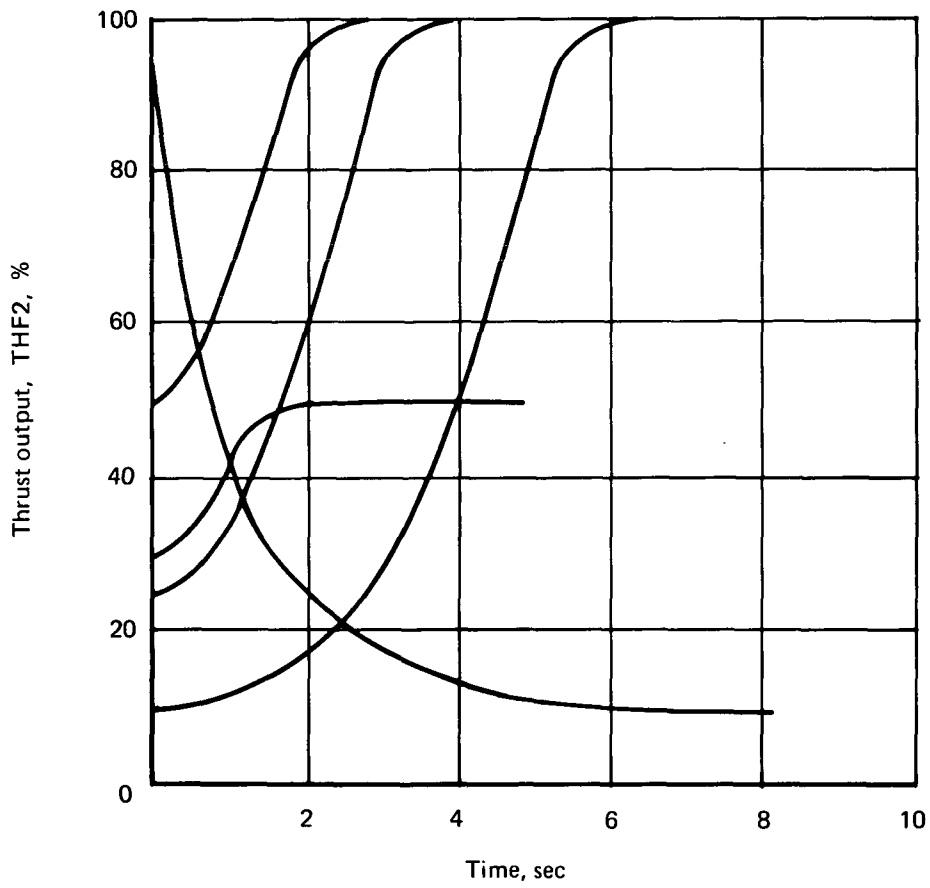
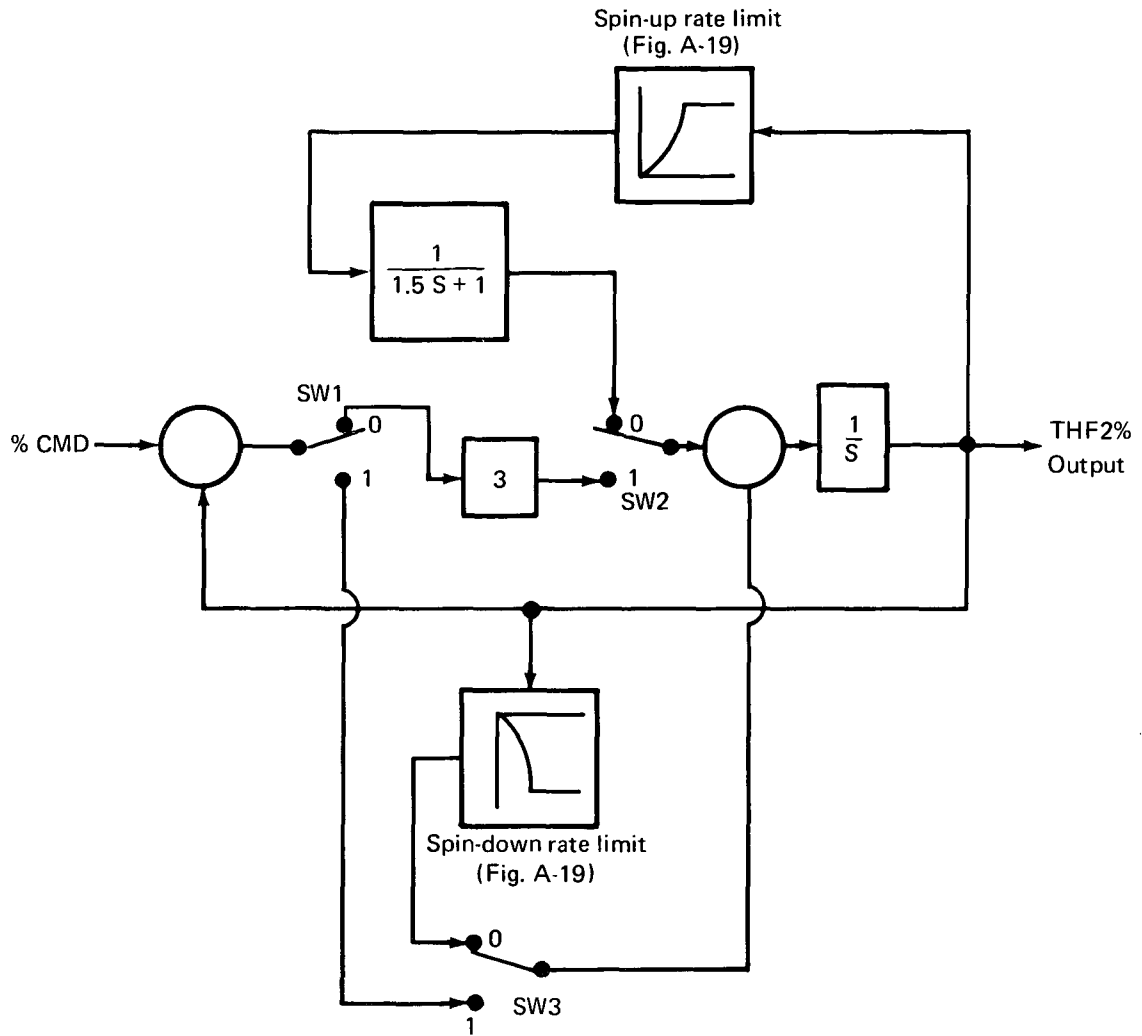


FIGURE A-16.—ENGINE MODEL STEP RESPONSE



Switch logic:

SW1	0	Error +
	1	Error -
SW2	Pick smallest value	
SW3	Pick smallest absolute value	

FIGURE A-17.—ENGINE MODEL SCHEMATIC

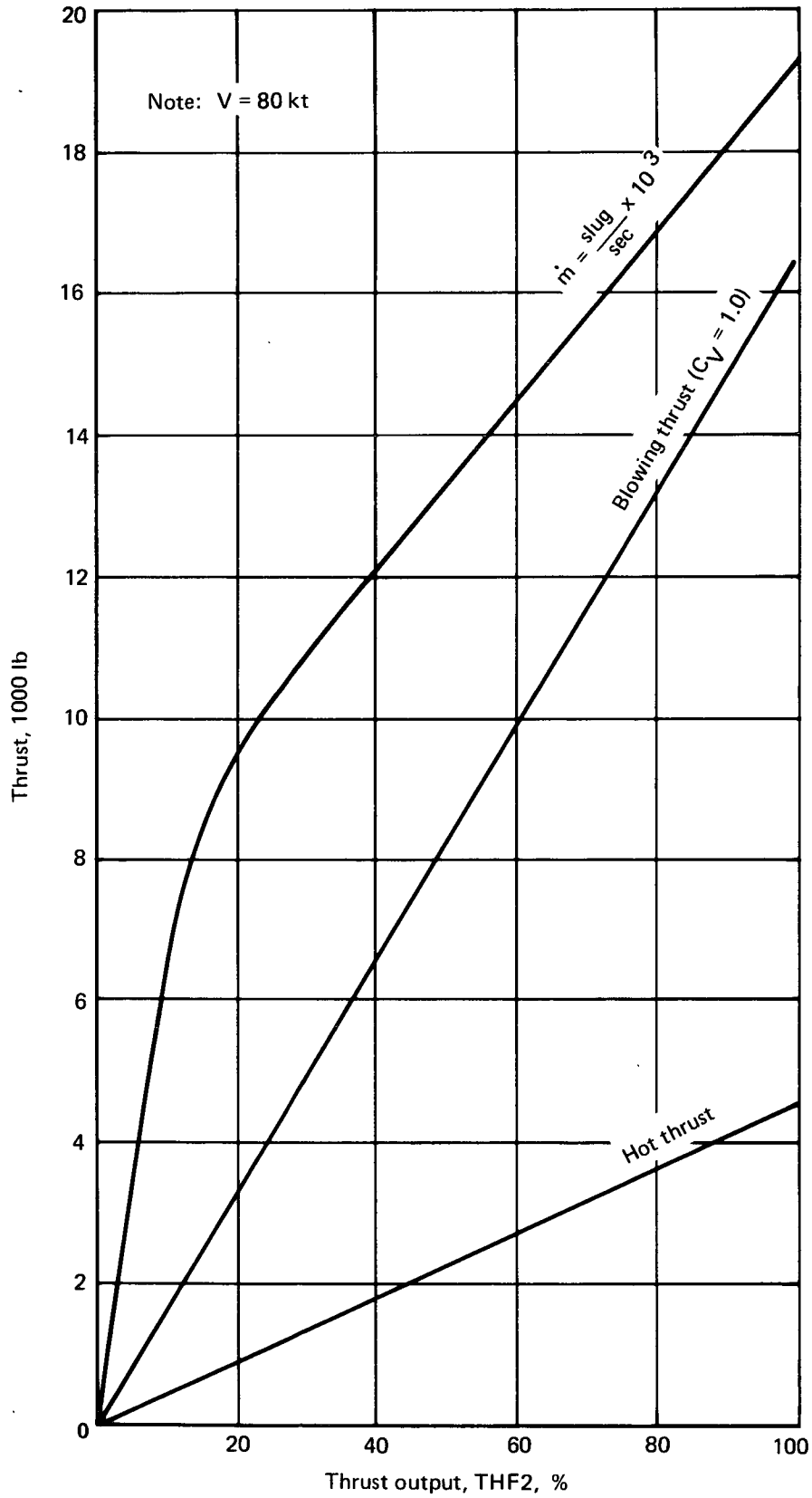


FIGURE A-18.—ENGINE CHARACTERISTICS

Switch SW1 tests the sign of the error signal and selects either the spin-up or spin-down logic path. For spin-up, SW2 selects the fuel control rate limit or the governor capture characteristic by picking the smallest value. For the spin-down path, SW3 selects the smallest absolute value of error signal or spin-down rate limit.

Figure A-19 shows the rate limit functions that were chosen to match the class of turbofan engines represented in this study. Other classes of engines can be represented by adjustment of figures A-18 and A-19.

For the augmentor wing aircraft, the momentum coefficient, C_J , is computed from the blowing thrust of figure A-18 by:

$$C_J = \frac{4(\text{blowing thrust})}{qS}$$

A.4 PILOT MODEL

A pilot model was developed that would provide a reasonable representation of flightpath capture and tracking maneuvers of the augmented airplane. This model provides repeatable performance that can be used in parametric studies of noise contours, and effects of flap system rate limits, turbulence filtering techniques, etc. The model was developed to permit tracking two-slope approaches although with suitable selection of input parameters it will represent capture and track of a single slope.

The approach is divided into the five segments shown in figure A-20.

1. Altitude hold. This function is held until the aircraft comes within distance HE1C of the first slope, at which time level 2 is selected.
2. Timed pushover. A constant pitch rate pushover is maintained for TCAP1 seconds and then level 3 is selected.
3. First-segment track. This function is held until the aircraft comes within distance HE2C of the second slope, at which time level 4 is selected.
4. Timed pullup. A constant pitch rate pullup is maintained for TCAP2 seconds and then level 5 is selected.

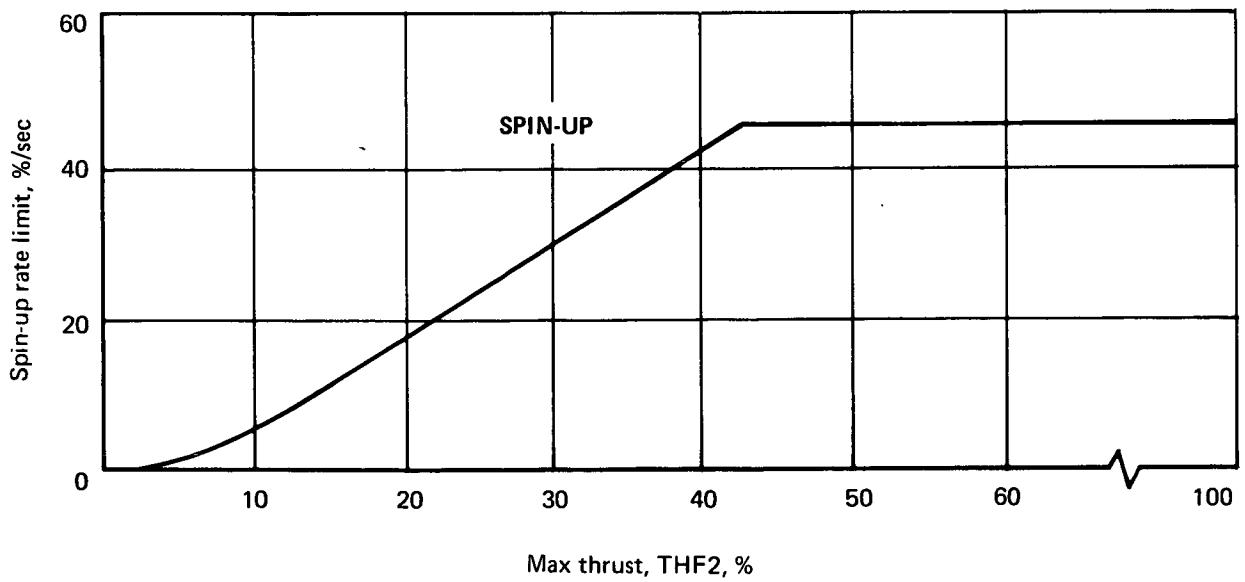
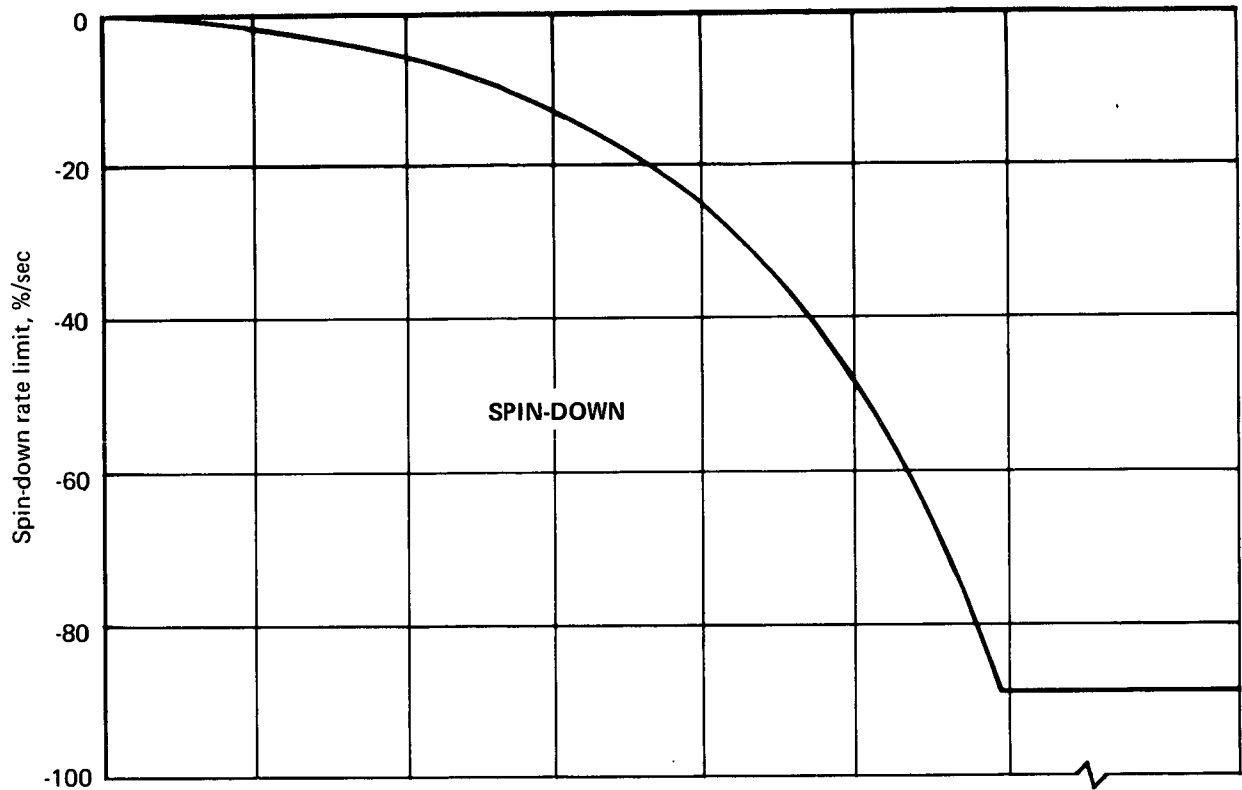
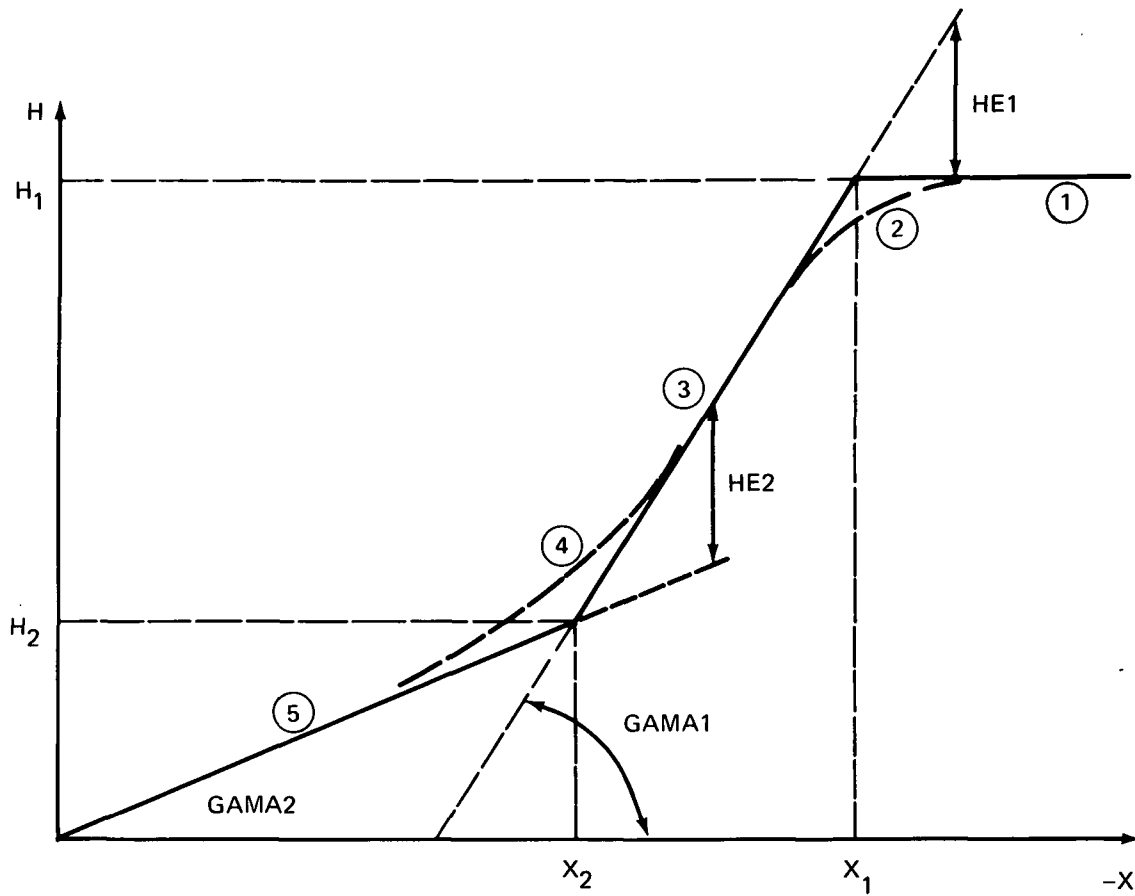


FIGURE A-19.—ENGINE MODEL RATE LIMITS



LOGIC EQUATIONS

- SW1 = (HE1 < HE1C) + SW1, OPRATE
- SW4 = SW1 DELAYED TCAP1 SECONDS
- SW2 = ((HE2 < HE2C), SW1 + SW2), OPRATE
- SW5 = SW2 DELAYED TCAP2 SECONDS

FIGURE A-20.—PILOT MODEL LOGIC

5. Second-segment track. This function is maintained until ground contact, at which time the problem is automatically terminated.

Figure A-20 also shows the logic level equations that identify the various path segments.

Figure A-21 shows the feedback paths that develop the appropriate column inputs for the maneuver. The switching progression is also identified. Basically, flightpath altitude error position and rate signals are combined through suitable gains. For flightpath tracking, the altitude rate signal is biased by $V \sin \gamma$ to adjust for the steady-state sink rate. A small integral feedback of altitude error is provided to improve tracking precision.

This model is used in combination with the augmented aircraft, and only column inputs are required because the airspeed is held by the autospeed function. The model provides close capture and tracking of flightpath in both still air and heavy turbulence.

A.5 TURBULENCE GENERATION

Investigations using continuous simulations for determining control system performance employed a simulator model of an atmospheric turbulence power spectrum.

Three separate white noise generators were used with the following filter models:

$$G_u(s) = \frac{\sigma_u \sqrt{\frac{2 L_u}{V_P \Delta t}}}{1 + \frac{L_u}{V_P} S} \quad G_v(s) = \frac{\sigma_v \sqrt{\frac{L_v}{V_P \Delta t}}}{1 + \frac{L_v}{2V_P} S} \quad G_w(s) = \frac{\sigma_w \sqrt{\frac{L_w}{V_P \Delta t}}}{1 + \frac{L_w}{2V_P} S}$$

where:

σ	=	input RMS value ($\sigma_w = \sigma_v = \sigma_u$)
L_u, L_v, L_w	=	characteristic length, ft
V_P	=	true airspeed, ft/sec
Δt	=	simulation integration time, sec

Outputs of these filters were considered wind axes components of turbulence, u_w , v_w , and w_w , respectively.

Segment	H command	Name
1	H_1	HCOM1
3	$H_2 + [X_2 - X] \tan \gamma_1$	HCOM2
5	$-X \tan \gamma_2$	HCOM3

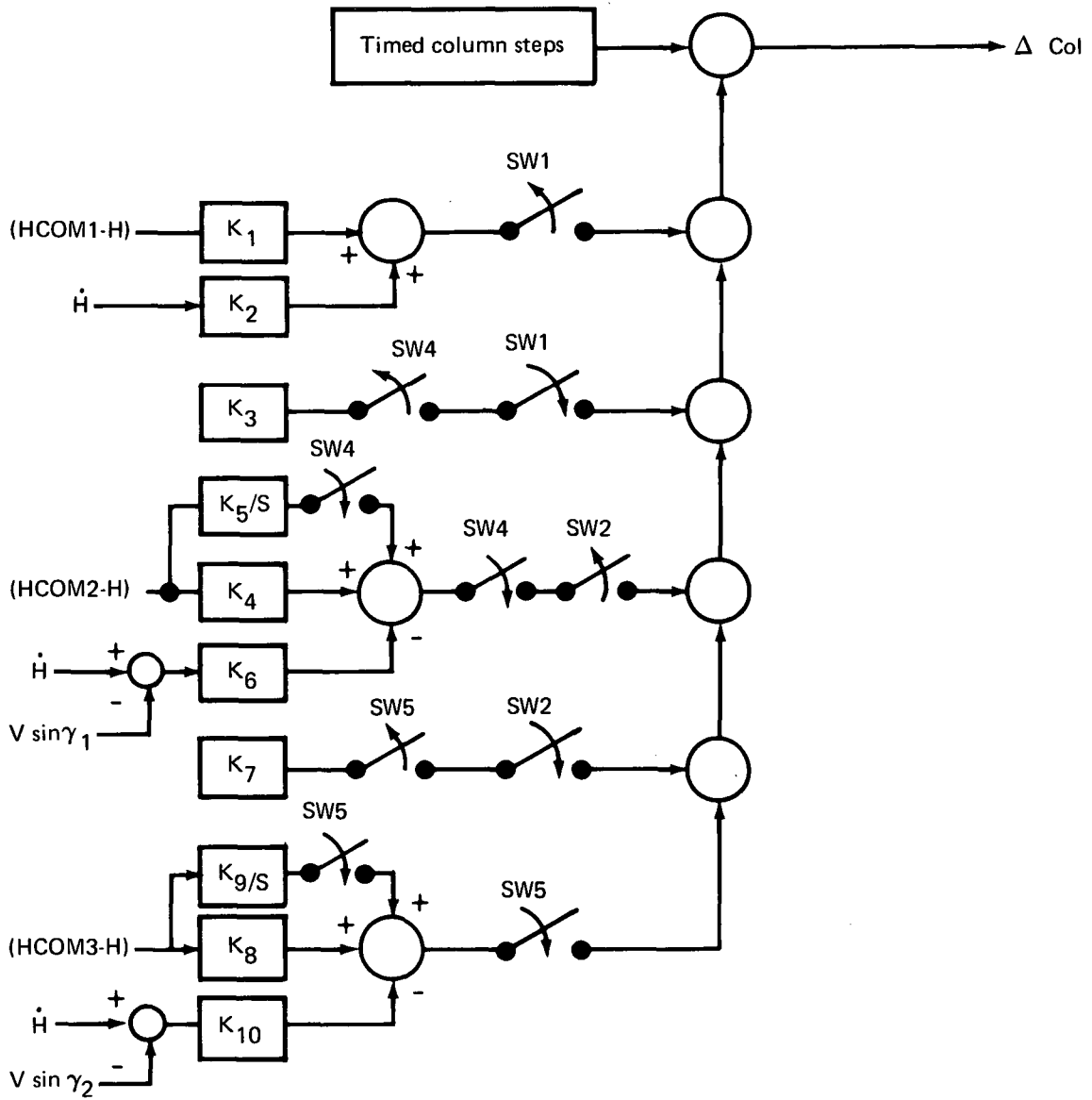


FIGURE A-21.—PILOT MODEL BLOCK DIAGRAM

The characteristic lengths L_u , L_v , and L_w were defined as functions of altitude as:

$$L_w = \begin{cases} h & h < 2500 \text{ ft} \\ 2500 & h \geq 2500 \text{ ft} \end{cases}$$
$$L_u = L_v = \begin{cases} 184 h^{1/3} & h < 2500 \text{ ft} \\ 2500 & h \geq 2500 \text{ ft} \end{cases}$$

REFERENCES

1. Spitzer, R. E.; Rumsey, P. C.; and Quigley, H. C.: Use of the Flight Simulator in the Design of a STOL Research Aircraft. AIAA Paper 72-762, August 1972.
2. Anon: Inter-Metropolitan STOL Evaluation (Phase X)—Final Report. American Airlines Development Engineering Report 5, January 1970.
3. Quigley, H. C.; Innis, R. C.; and Holzhauser, C. A.: A Flight Investigation of the Performance, Handling Qualities, and Operational Characteristics of a Deflected Slipstream STOL Transport Airplane Having Four Interconnected Propellers. NASA TND-2231, March 1964.
4. Franklin, J. A.; and Innis, R. C.: Pitch Attitude, Flight Path, and Airspeed Control During Approach and Landing of a Powered Lift STOL Aircraft. NASA TMX-62, 203, December 1972.
5. Ashkenas, I. L.; and Craig, S. J.: Multiloop Piloting Aspects of Longitudinal Approach Path Control. ICAS Paper 72-46, 1972.
6. Allison, R. L.; Mack, M.; and Rumsey, P. C.: Design Evaluation Criteria for Commercial STOL Transports. NASA CR-114454, June 1972.
7. Grantham, W. D.; Nguyen, L. T.; Patton, J. M., Jr.; Deal, P. D.; Champine, R. A.; and Carter C. R.: Fixed Base Simulator Study of an Externally Blown Flap STOL Transport Airplane During Approach and Landing. Langley Working Paper LWP-1049, May 15, 1972.
8. Melvin, W. W.: Effects of Wind Shear on Approach With Associate Faults of Approach Couplers and Flight Directors. AIAA Paper 69-796, July 1969.
9. Ashkenas, I. L.; and Durand, T. S.: Simulator and Analytical Studies of Fundamental Longitudinal Control Problems for Carrier Approach. AIAA Simulation for Aerospace Flight Conference (Columbus, Ohio), August 1963.
10. Franklin, J. A.; and Innis, R. C.: Longitudinal Handling Qualities During Approach and Landing of a Powered Lift STOL Aircraft. NASA TMX-62, 144, March 1972.
11. Innis, R. C.; Holzhauser, C. A.; and Quigley, H. C.: Airworthiness Considerations for STOL Aircraft. NASA TND-5594, January 1970.
12. Campbell, J. M.; and Bosch, J. C.: Noise Estimates for a Family of Four-Engine Augmentor-Wing STOL Aircraft. Boeing Document D6-41180 (in preparation).